**Title**
Mitochondrial Functionality and Mammalian Sperm Quality: Implications for Fertility



**Author**
Bulkeley, Evelyn Anne

**Publication Date**
2022

Peer reviewed|Thesis/dissertation

**Mitochondrial Functionality and Mammalian Sperm Quality: Implications for Fertility**

By

EVELYN ANNE BULKELEY
DISSERTATION

Submitted in partial satisfaction of the requirements for the degree of

DOCTOR OF PHILOSOPHY

in

Integrative Pathobiology

in the

OFFICE OF GRADUATE STUDIES

of the

UNIVERSITY OF CALIFORNIA

DAVIS

Approved:

_____

Stuart Meyers

_____

Jon Ramsey

_____

Gary Cherr

Committee in Charge

2022

## Table of Contents

**Acknowledgements**

A special thanks is owed to all of the collaborators that made the work in this dissertation possible. This includes extended thanks to our collaborators at Texas A&M University, Dr. Dickson Varner and Sheila Teague, for their support and provision of equine sperm samples. Special thanks are also owed to Dr. Brett McNabb for allowing this project to expand species and include investigation into bovine sperm physiology. I would also like to thank our collaborators from Guide Dogs for the Blind, Dr. Kris Gonzales and Heather Power, for allowing the opportunity to contribute to clinically applicable research in canine reproduction.

Stuart, thank you for allowing me the opportunity to be your student, and for the relentless support and encouragement you have given me. I have learned so much from you, both research and life-based, and will be forever grateful. To Alejandro de la Fuente, Momoe Kato, Tawny Scanlan, Azarene Foutouhi, and Amie Romney, thank you for being excellent lab mates and a wonderful 'work family.' All of your curiosity, intelligence and kindness never ceases to impress me.

To my family and friends, thank you for supporting me and my 'education habit.' The right words do not exist to express what the love and support of my husband, Jacob Arntzen, has meant for me throughout this process, so I will leave it at a simple 'thanks.'

## Preface

The requirements for the Doctor of Philosophy in Integrative Pathobiology, with a designated emphasis in Reproductive Biology, in the office of Graduate Studies of the University of California, Davis (UCD) are fulfilled by this dissertation, and the research from which it is composed. This work was completed within the Department of Anatomy, Physiology, and Cell Biology of the School of Veterinary Medicine (SVM) from 2016 to 2022 and was made possible by funding support from the Center for Equine Health (CEH; UCD SVM), Center for Food Animal Health (CFAH; UCD SVM), the ARCS® Foundation, the NIH STAR and YEAR programs, as well support from the UCD Graduate Student Support Program (GSSP), the Graduate Group of Integrative Pathobiology (UCD SVM) and the Veterinary Scientist Training Program (VSTP; UCD SVM).

**Dissertation Abstract**

Mammalian sperm quality is often clinically investigated by assessing parameters such as sperm motility and morphology as indicators of sperm health and male fertility. Though commonly assessed, the physiology and pathophysiology underlying sperm quality parameters remains to be fully elucidated. This knowledge gap limits the clinical and scientific knowledge of male fertility across mammalian species. Study of mammalian sperm physiology is complicated by interspecies variation, which has left differing knowledge gaps between species. The interspecies variation also challenges efforts to advance the field of human male fertility, for which more appropriate models than the commonly used rodent models are needed. The overall objective of this dissertation research was to investigate the physiology and pathophysiology of mammalian sperm quality parameters frequently assessed in the clinical setting, specifically morphology and motility. This dissertation includes assessment of bull, stallion and canine sperm to address specific knowledge gaps in sperm physiology and pathophysiology of said species. I aimed to further explore the physiologic significance of sperm quality parameters by investigating their relationship with mitochondrial functionality and oxidative metabolism in multiple mammalian species. This was accomplished in four chapters. Chapter 1, *Mammalian sperm quality and oxidative metabolism- a review*, provides a review of the literature pertaining to mammalian sperm quality and oxidative metabolism, emphasizing knowledge gaps, disagreements in existing literature, and implications for male fertility. In Chapter 2, *Effects from disruption of mitochondrial electron transport chain function on bull sperm motility*, I investigate the relationship between mitochondrial function and motility in bull sperm by simultaneously measuring motility parameters and mitochondrial oxygen consumption in the presence of several mitochondrial effector drug treatments. The bull was chosen as the model for

this chapter due to conflicting results in the literature regarding the role of mitochondria in fueling bull sperm motility. Motility parameters were only observed to differ significantly from the vehicle with antimycin (inhibitor of complex III of the electron transport chain) treatment, for which significant decreases in numerous parameters, including total motility ($p$=0.007), progressive motility ($p$=0.01), and velocity parameters, such as VAP and VSL ($p$<0.05), were identified. These results indicate that bovine sperm motility is impacted by mitochondrial functionality. In Chapter 3, the novel use of imaging flow cytometry was employed to investigate the relationship between sperm morphology and reactive oxygen species generation in fresh and cool-stored stallion sperm. The stallion was used as the model in this chapter in part due to literature associating the percentage of morphologically abnormal sperm with elevated ROS and decreased fertility, but limited information regarding ROS generation of specific morphologic abnormalities. Compared to morphologically normal sperm, ROS production was significantly higher in cells with abnormal heads, proximal droplets and abnormal midpieces in both fresh and cooled semen. These results indicate that excessive oxidative stress contributes to the pathophysiology of morphologic abnormalities, which may contribute to findings previously reported in the literature linking certain morphologic abnormalities to decreased fertility in stallions. In Chapter 4, we evaluated the repeatability and accuracy of the tablet-based Canine iSperm® instrument compared to computer-assisted sperm analysis (CASA) for assessment of motility (total and progressive) in fresh and frozen-thawed canine sperm. This tablet-based system is available for both stallion and canine sperm, but prior to our study, published validation was only available for stallion sperm. Correlational analysis revealed significant positive correlations between CASA and iSperm® assessment for both fresh and frozen-thawed samples. These results indicate the iSperm® system offers an accurate alternative to CASA for

measurement of canine sperm motility. This tablet-based system for motility assessment is substantially more affordable to veterinary practitioners than conventional CASA systems and could allow for more clinical data collection of canine sperm motility, which would be invaluable to future research efforts to expand knowledge of canine sperm physiology. The multispecies work in this dissertation reports findings in sperm quality, physiology and bioenergetics. The results of this work directly contribute to current clinical knowledge by improving the diagnostic power of commonly employed sperm quality measures and by elucidating some of the underlying pathophysiology of sperm morphologic abnormalities and sperm motility. Further, the findings from this dissertation research informs future research efforts, with potential applications in advancement and improvement of mammalian male fertility, sperm preservation techniques, species conservation efforts and mitochondrial physiology.

## Dissertation Introduction and Outline

The mammalian sperm is a fascinating cell and the focus of this dissertation. The male gamete is the smallest cell in the mammalian body and, in its mature form, possesses minimal intracellular organelles compared to somatic cells. Despite this, the sperm is a motile and remarkably complex cell, capable of traversing the female reproductive tract and achieving fertilization. This ability to accomplish a wide range of cellular functions despite limited intracellular machinery is unique to sperm, and many fundamental mechanistic questions pertaining to sperm physiology and function, such as mechanisms underlying motility regulation, remain to be fully elucidated.

The necessity of sperm in species survival and evolution is apparent, and it is not surprising that significant interspecies differences in sperm form and function exist, further complicating the understanding of mammalian sperm function. There is more anatomic and pathologic interspecies variation in the reproductive system than in any other organ system[1]. Better understanding of both the similarities and differences between species will provide mechanistic understanding to improve and study fertility of not only domestic species, but also exotics, wildlife, endangered species, and humans. Though sperm are commonly assessed for a variety of microscopic and biochemical endpoints, much is unknown regarding the pathophysiology of semen quality parameters like sperm motility and sperm morphology. Further study of these parameters and the underlying pathophysiology will inform efforts to improve male fertility both in humans and domestic species, and that information can be applied to benefit conservation efforts in exotic and endangered species.

The overall objective of this dissertation research was to investigate the physiology and pathophysiology of mammalian sperm quality parameters frequently assessed in the clinical setting, specifically morphology and motility. I aimed to further explore the physiologic significance of those parameters and address knowledge gaps in sperm pathophysiology by investigating their relationship with mitochondrial functionality in multiple mammalian species. This was accomplished by the research reported in the following chapters:

Chapter 1 provides a review of the literature pertaining to mammalian sperm quality and oxidative metabolism.

In Chapter 2, we investigated the relationship between mitochondrial function and sperm motility in fresh bovine sperm through simultaneous measurement of mitochondrial oxygen consumption and motility parameters. The bull was chosen as the model for this chapter due to conflicting results in the literature regarding the role of mitochondria in fueling bull sperm motility

In Chapter 3, a novel use of imaging flow cytometry is utilized to investigate ROS production in specific sperm morphologies in both fresh and cooled stallion semen. The stallion was used as the model in this chapter in part due to literature associating the percentage of morphologically abnormal sperm with elevated ROS and decreased fertility, but limited information regarding ROS generation of specific morphologic abnormalities. Additionally, there has been debate in the literature as to whether elevated ROS production is present in more robust, fertile stallion sperm or if it is more indicative of poor-quality semen.

In Chapter 4, we validated a new, portable device for the assessment of canine sperm motility that is more feasibly accessible for data acquisition in the general practice clinical setting. This

tablet-based system is available for both stallion and canine sperm, but prior to our study, published validation was only available for stallion sperm.

This dissertation includes the following publications:

Bulkeley EA, Foutouhi A, Wigney K, Santistevan AC, Collins C, McNabb B, Meyers SA. Effects from disruption of mitochondrial electron transport chain function on bull sperm motility. Theriogenology 2021;176:63–72. https://doi.org/10.1016/j.theriogenology.2021.09.015.

Bulkeley EA, Collins C, Foutouhi A, Gonzales K, Power H, and Meyers SA. Assessment of an iPad-based sperm motility analyzer for determination of canine sperm motility. Translational Animal Science 2021; 5(2): 1-7. 10.1093/tas/txab066

**References**

1. Jubb KVF, Kennedy PC, Palmer NC. *Jubb, Kennedy, and Palmer's Pathology of Domestic Animals*. 5th ed. (Maxie MG, ed.). Elsevier Saunders Ltd; 2007. https://linkinghub.elsevier.com/retrieve/pii/B9780702028236500439

# Chapter 1: Mammalian Sperm Quality and Oxidative Metabolism- A Review

Evelyn A. Bulkeley[1]

Department of Anatomy, Physiology, and Cell Biology, School of Veterinary Medicine, University of California, Davis, CA[1]

## Introduction

The mammalian sperm is a fascinating cell that has been the subject of scientists' study, bewilderment and awe for hundreds of years. The tadpole-like structure of mammalian sperm was first described by Leeuwenhoek in 1677, who hypothesized the cell's conformation contributed to fertilization[1,2]. Leeuwenhoek's findings were met with intrigue and fueled further investigation, though it was not until the development of more advanced experimental techniques and modalities in the mid-20$^{th}$ century, such as electron microscopy, that large advancements were made in elucidating sperm form and function[2]. Despite the advancement of scientific understanding of mammalian sperm, much remains to be elucidated regarding sperm function, and in turn, male fertility. Though sperm are commonly assessed for a variety of microscopic and biochemical endpoints, much is unknown regarding the pathophysiology of semen quality parameters like sperm motility and sperm morphology. Further study of these parameters and the underlying pathophysiology will inform efforts to improve male fertility both in humans and domestic species, and that information can also be applied to benefit conservation efforts of exotic and endangered species. Additionally, unique aspects of the mature sperm, such as the limited intracellular organelles, make the sperm an interesting research subject that may harbor mechanistic insight of cellular biology and bioenergetics for extrapolation and further study in somatic cells.

The aim of this review chapter is to provide a brief overview of the literature regarding mammalian sperm quality and function, and what is known regarding sperm quality parameters and male fertility. We begin with a brief review of sperm structure, relevant anatomic components and cellular metabolism. Then, an overview of mammalian sperm quality

components, and current knowledge of each component and relevance to male fertility is discussed.

**The Mammalian Sperm- A Structural Review**

The mature form of the sperm comes to be through the complex process of spermatogenesis, spermiogenesis and post-testicular maturation. During spermatogenesis, diploid spermatogonia undergo meiosis, maturation and morphologic changes into haploid sperm. These sperm are then released into the rete testis from the seminiferous tubular epithelium of the testes in the process known as spermiogenesis and travel through the epididymis on the path to eventual ejaculation. During travel through the epididymis, final biochemical and morphologic maturation occurs resulting in a population containing mature functional sperm. Sperm morphology and motility will be discussed later in this review, but it is worth noting that morphologic defects and motility deficits have been linked to abnormal spermatogenesis and maturation stages [3]. Additionally, aberrant spermatogenesis has also been linked to age-related declines in male sperm quality and fertility[4].

Leeuwenhoek's discovery of the tadpole-like structure of sperm was greatly expanded upon with the introduction of electron microscopes in the mid-20$^{th}$century which facilitated study of sperm ultrastructure [2]. Early, thorough descriptions of bovine sperm ultrastructure were provided in a series of two publications by Saacke and Almquist in 1964[5,6]. Additionally, an excellent review of mammalian sperm ultrastructure was also provided by Fawcett in 1975[7] which is considered a classic writing in the field. Here, I summarize sperm morphology and relevant cellular features. The fundamental structure of the mammalian sperm is depicted in

Figure 1.1. The basic cellular structure consists of a head and flagellum, each of which can be further anatomically subdivided (Figure 1.1).

The sperm head is commonly anatomically subdivided into the acrosomal region, the equatorial segment, the post-acrosomal region, which includes the nucleus, and the posterior ring, which delineates the convergence of the head and the flagellum[2]. The nucleus takes up the majority of the space in the head and contains the paternal genetic material, which includes either an X or a Y chromosome and a haploid number of somatic chromosomes. DNA and the associated proteins are referred to as chromatin, and an important distinction between sperm and somatic cells is that chromatin in mature sperm is highly condensed during the latter stages of spermatogenesis, collectively known as spermiogenesis.

The flagellum can be anatomically subdivided into the connecting piece, the midpiece (or middle piece), the principal piece, and the end piece (Fig 1.1). Sperm mitochondria primarily, though not exclusively, reside in the midpiece region. Fawcett (1970) noted that one or two flattened mitochondria are typically situated on the dorsal and ventral aspect of the midpiece region: one or two flattened mitochondria are typically on the dorsal and ventral aspects of the neck[8]. Interestingly, Fawcett (1970) went on to note that such mitochondria occasionally sent projections into the connecting piece, which they hypothesized implicated energy-requiring processes in the non-motile portion of the spermatozoon[8]. When discussing the existing literature regarding mammalian sperm ultrastructure, it is worth noting that many studies investigating mammalian sperm ultrastructure utilized a detergent to remove the plasma membrane and mitochondrial sheath[9], which disappointingly limits obtainable knowledge of sperm mitochondrial anatomy and anatomic associations. The sperm flagellum consists of the basic 9 + 2 axonemal arrangement of microtubules, more specifically 9 outer doublets surrounding 2

single central microtubules, commonly referred to as the central pair (CP) that is typical of most cilia and flagella, with some modifications due to substantial additional accessory structural components[10]. The outer doublets have two rows of projections composed of dynein motor proteins, which provide the motive force that bends the flagellum, a feature essential for motility. Ultimately, sperm motility is fueled by ATP, which is utilized by axonemal dynein ATPases within the sperm flagellum[11], but the cellular pathways by which mammalian sperm predominantly produce ATP has been debated for decades and appears to be subject to significant interspecies variation[12–17].

**Sperm Metabolism**

Like somatic cells, sperm have been demonstrated to utilize both anaerobic metabolism (glycolysis) and aerobic metabolism (oxidative phosphorylation) for energy production. Study of sperm metabolism is complicated by apparent interspecies variation in metabolic preferences. An overview of metabolism and its consequences, in the form of reactive oxygen species (ROS generation), is provided below.

*Glycolysis*

Anaerobic metabolism is most classically accomplished by glycolysis, which occurs within the cytosol. During glycolysis, glucose is converted into pyruvate, producing energy in the form of ATP. Hydrogen ions (protons, $H^+$) are also generated during glycolysis, which can contribute to extracellular acidification[18]. There are three potential fates of pyruvate generated during glycolysis: 1. Conversion of pyruvate into ethanol occurs during anaerobic conditions in some microorganisms[18] but is not important for purposes of this review. 2. Conversion of pyruvate into

lactate occurs during anaerobic conditions and is catalyzed by lactate dehydrogenase (LDH); lactate then undergoes lactic acid fermentation, regenerating $NAD^+$ and producing a small amount of ATP. 3. The last fate of pyruvate occurs during aerobic conditions, when it is shuttled into the mitochondrial matrix by the pyruvate carrier protein (PYC), wherein pyruvate dehydrogenase (PDH) catalyzes its decarboxylation into acetyl-CoA[19] .

*Oxidative phosphorylation (OXPHOS) and the Electron Transport Chain (ETC)*

In addition to glycolysis, sperm production of energy in the form of ATP can also occur within the midpiece-associated sperm mitochondria. The structure of a mitochondrion is depicted in Figure 1.2. Mitochondria are highly specialized subcelluar organelles with a specific, organized structure composed of four sub-compartments: an outer mitochondrial membrane (OMM), intermembrane space (IMS), inner mitochondrial membrane (IMM), and mitochondrial matrix (Figure 1.2). The IMM and IMS house the majority of mitochondrial proteins for the wide array of cell functions mitochondria take part in, including calcium homeostasis, apoptosis, and lipid and amino acid metabolism[20,21], but their most important role is as "powerhouse of the cell," producing energy in the form of ATP via oxidative phosphorylation (OXPHOS).

Within the mitochondrial matrix, acetyl-CoA enters the citric acid cycle (Krebs cycle), which consists of a series of oxidizing reactions, culminating in the reduction of $NAD^+$, generating NADH. NADH is a high-energy electron carrier, which delivers electrons ($e^-s$) to protein complex I of the electron transport chain (ETC). Another high-energy electron carrier, $FADH_2$, also transfers electrons through Complex II. Within the ETC is where the process of OXPHOS occurs with reductive transfer of $e^-s$ through protein complexes (I, II, III, & IV) that is coupled to proton pumps, allowing protons (hydrogen ions; $H^+$) to travel against their concentration gradient into the

mitochondrial IMS (Figures 1.2 and 1.3). Specifically, proton pumping occurs at complexes I, III, and IV. The net accumulation of $H^+$ within the IMS creates an electrochemical proton gradient. As $H^+$ begin to flow through ATP synthase (V), down their electrochemical gradient and back into the mitochondrial matrix, ATP synthase harnesses the energy (the electrochemical proton motive force; Δp) to generate ATP[18,22].

It is important to note that during ETC activity, a basal, small amount of electron leakage occurs from complex I or III. The leaked $e^-s$ then incompletely reduce oxygen ($O_2$), resulting in the formation of ETC reactive oxygen species (ROS), specifically superoxide anion ($O_2^{\bullet-}$). ROS are oxygen species that are more reactive than ground state oxygen. Specific types of ROS, called free radicals, possess an unpaired electron that makes them highly reactive and capable of inflicting catastrophic cellular damage to phospholipid membranes, proteins, lipids and DNA. Upon formation, $O_2^{\bullet-}$ then rapidly dismutates, spontaneously or catalyzed by mitochondrial superoxide dismutase (mSOD), into hydrogen peroxide ($H_2O_2$), which, unlike $O_2^{\bullet-}$, is capable of passing through cellular membranes and can therefore diffuse out of the mitochondria to inflict further cellular damage.

*Reactive Oxygen Species (ROS) and Sperm*

Low levels of ROS play an important physiologic role in many sperm cell functions, including signaling events controlling capacitation[23,24], acrosome reaction[23,24], hyperactivation[24,25] and sperm-oocyte fusion[13,26]; however, excessive ROS production that overwhelms intrinsic antioxidant defense and repair mechanisms results in a wide array of cellular damage and compromised function. Excessive ROS production has been observed in defective sperm[27–29] and as a result of cryopreservation[30–34]. Currently, there are two known mechanisms in sperm capable

of generating ROS: ROS-derived from cytosolic sources, such as the enzymatic activity of NADPH oxidase, and through electron leakage from the electron transport chain (ETC). However, although NADPH oxidases that are capable of ROS production have been identified in human and equine sperm, more evidence that these enzymes significantly contribute to sperm ROS-generation needs to be provided[35–37]. The generation of ROS during ETC function is well-documented and considered the primary means of ROS generation in mammalian sperm[20,26,38–40].

There are numerous negative consequences of ROS on sperm cells, but the mechanistic pathway behind sperm cell damage that has been receiving the most attention recently[39,41–43] is that of ROS resulting in lipid peroxidation and the subsequent production of toxic aldehyde adducts, notably 4-hydroxynonenal (4-HNE)[44]. Such adducts can result in dephosphorylation of protein kinase B, activating Caspase 3 and the intrinsic apoptotic pathway, ultimately leading to cell death[30,39]. Attempts to classify the increased susceptibility of mammalian sperm to oxidative damage compared to somatic cells are in strong agreement on two sperm cell characteristics: diminished enzymatic defense and repair mechanisms and cell and mitochondrial membrane characteristics.

1) *Low levels of cytoplasmic defense and repair enzymes.* As the mammalian sperm develops and matures, it sheds the majority of intracellular organelles and excess cytoplasm, adopting a highly specialized architecture. As a direct result of decreased cytosolic content, compared to somatic cells, sperm have diminished cytoplasmic enzyme content, which has long been attributed to the increased risk of free-radical damage[14,27,45–47] due to decreased availability of cytoplasmic enzymes, including those involved in the intrinsic cellular defense system against ROS[27,45,46]. In light of this, it is not surprising that a large amount of research aiming to improve sperm cryopreservation techniques have investigated the cytoplasmic content of antioxidant enzymes,

including glutathione peroxidase (GPX)[47–51], superoxide dismutase (SOD)[52,53], and catalase (CAT)[48,52]. The sperm cell's lack of defense against oxidative damage is further compounded by reduced activity of cellular repair enzymes, including exonucleases, endonucleases, glycosidases, and polymerases, to reverse inflicted oxidative damage[14,27,47]. *2) Sperm membranes are rich in polyunsaturated fatty acids (PUFAs).* The sperm membrane has a high level of PUFAs when compared to somatic cells[54]. This unique membrane composition and structure allows flexibility, a requirement for certain sperm functions. However, increased flexibility does not come without cost- providing increased substrate for free radical attack[27]. The relationship between ROS membrane and lipid peroxidation and sperm motility is well established[55,56]. In fact, sperm membrane peroxidation, and its involvement in male infertility, has been studied for decades[28,40,57]. Interestingly, the mitochondrial membrane is even more PUFA-rich than the cellular membrane, which when combined with local ROS production by the ETC, has catastrophic potential. This propensity of sperm membranes, particularly the mitochondrial membrane, to undergo lipid peroxidation led many researchers to prematurely conclude that OXPHOS is less than optimal for ATP production to fuel mammalian sperm motility. Ultimately, the metabolic pathway mammalian sperm utilize as a primary energy source remains highly contested and appears subject to significant interspecies variation[58]. For example, it has been demonstrated stallion sperm rely almost exclusively on mitochondria-produced ATP to fuel active motility[33], while the glycolytic pathway has been shown to be the primary energy source for human sperm motility[59]. Active motility in bull sperm was previously believed to function independent of mitochondrial function[60], though a more recent study in bull sperm contradicts those findings[61]. In chapter 2 of this dissertation, we investigate this discrepancy in the literature by determining the effects from disruption of ETC function on bull sperm motility[62]. It is clear that interspecies variation exists in

the metabolic pathways used to fuel motility, but more research is needed to classify these differences and identify their pathophysiologic significance.

**Mammalian Sperm Quality**

Several parameters are routinely assessed to determine mammalian sperm quality in the clinical environment, most commonly including total sperm numbers and viability, sperm morphology, and sperm motility. These parameters have been correlated with significantly higher fertility in mammalian species, including humans [63,64], bulls[65], dogs[66] and horses[67]. In this section, we briefly review fundamental sperm quality assessment techniques and their relationship to male fertility.

*Total Sperm Numbers and Viability*

Measurement of semen volume and sperm concentration in ejaculates to calculate total sperm numbers is a cornerstone to semen evaluation and has been associated with increased male fertility across mammalian species[63,65,68]. Higher sperm concentrations and total sperm numbers have been associated with shortened time to pregnancy in humans[64]. Critical evaluation of studies, particularly those with smaller sample size, is necessary as there have been documented inaccuracies in the measurement of semen volume, most notably with pipetting or decanting for cylindrical volumetric measurements demonstrating significantly underestimated semen volume compared to measurements calculated based on ejaculate weight[69]. Sperm concentration can be determined by manual assessment utilizing a hemocytometer; though this modality is prone to variation and inaccuracy, a benefit is that it can be performed with a simple light microscope, which is available to most general practitioners. Alternatively, sperm concentration can be

determined by lysing cell membranes and utilizing a nuclear fluorescent dye, such as propidium iodide (PI), which allows total cell numbers to be determined by an automated cell counter, such as a NucleoCounter® (ChemoMetec, Allerød, Denmark). These cell counters can assess sperm viability, by analyzing a non-lysed semen sample, since propidium iodide does not permeate intact cell membranes. This modality is more accurate than hemocytometer concentration measures and has the added value of providing viability data, though the equipment and reagents can be costly. It is worth noting that sperm viability has been correlated with superior fertility in mammalian species, including bulls[65] and stallions[70].

*Morphology*

Percentage of morphologically normal sperm is one of the most commonly employed morphologic parameters for sperm quality assessment, and sperm morphology assessment is arguably the only test commonly available to assess intrinsic sperm quality. There are numerous techniques and preparation methods for sperm morphologic assessment typically at 60-100X under oil or water immersion microscope objectives. In general, assessment involves evaluation of fixed sperm samples stained with a cellular stain such as Wright's or Giemsa, or a background stain, such as eosin-nigrosin, the so-called "Theriogenology" stain all of which utilize light microscopy for manual morphologic assessment[68]. Additionally, light microscopic methods such as phase contrast, reverse phase contrast, and differential interference microscopy (DIC, Nomarski) have been used for greater optical precision for determining sperm morphologic variations in unstained specimens. In addition to determining the percentage of morphologically normal sperm, quantification of specific morphologic abnormalities is also beneficial in breeding soundness examinations, as it can aid in diagnosis of certain conditions. For example, elevated

numbers of detached heads is indicative of conditions causing sperm accumulation or other spermatogenic defects, while other defects, such as increased numbers of abnormal heads, are more often associated with testicular spermatogenic dysfunction[68].

Percentage of morphologically normal sperm have been associated with positive functional parameters, such as zona-induced acrosome reaction and DNA integrity, in humans[71]. The proportion of morphologically normal sperm has also been associated with shortened time to pregnancy in humans[64]. In stallions, the percentage of morphologically normal sperm has been positively correlated with pregnancy rates, while a negative correlation between pregnancy rates and certain morphologic abnormalities, such as midpiece and tail defects, has been observed [72,73]. Another study confirmed a positive link between percentage of normal sperm and fertility in stallions with an increased percent pregnant/cycle and percent pregnant/first cycle[67] . Interestingly, no correlation was found specifically between abnormal sperm heads and fertility in the same study.

Several studies have linked morphologic abnormalities in mammalian sperm to increased oxidative stress. For example, sperm head defects and oxidative DNA damage have been linked to infertility in humans[74]. Similarly, reactive oxygen species production has been linked to infertility and subfertility in humans and has also been associative with sperm morphologic defects and an elevated sperm deformity index[75,76]. These findings do not appear exclusive to human sperm, as abnormal head morphology and oxidative DNA damage have also been negatively correlated with fertility in bulls[77]. Study of ROS production in sperm can be accomplished by several methods, with fluorescent indicator dyes, such as dihydroethidium (DHE), and flow cytometry being the most commonly employed method[78,79]. Though technically these stains would allow for concurrent evaluation of ROS and morphologic abnormalities by

employing fluorescence and light microscopy, low throughput and long analysis times limit the feasibility of this approach. In Chapter 3 of this dissertation, we employ the novel use of imaging flow cytometry to concurrently evaluate ROS generation and morphologic abnormalities on an individual cell level in stallion sperm.

*Motility*

Sperm motility assessment is a cornerstone of sperm quality analysis across mammalian species, and sperm motility has been positively associated with fertility in numerous species, including bulls[65] and stallions[67]. Before discussing motility assessment in semen analysis, it necessary to review some fundamental concepts pertaining to sperm motility.

There are two types of physiological mammalian sperm motility: (1) activated motility, often simply referred to as "motility," and (2) hyperactivated motility. Activated motility is the pattern typically seen in freshly ejaculated sperm and is important for the linear propulsion of sperm through the female reproductive tract [80]. Activated motility is characterized by a symmetrical, low-amplitude flagellar waveform that results in sperm moving in a relatively straight line, or minor arc, in non-viscous media[80]. Hyperactive motility is a rapid, non-linear, high amplitude motility pattern activated during final maturation events near the site of fertilization in the female reproductive tract. Hyperactive motility aids the sperm in navigating the viscous mucus and cumulus cells that surround the oocyte that allows sperm access to the oocyte, as well as assisting in penetration of the zona pellucida[81–83]. Hyperactive motility is a rapid, whip like movement of the flagellum, often producing a non-linear star-like or circular motility pattern [84]. The focus of my discussion in this dissertation, will predominantly be on active motility.

Several methods employing microscopy for sperm motility assessment exist. Visual assessment of total and progressively motile sperm using a light microscope is commonly employed in clinical practice and is denoted as a percentage of sperm demonstrating each mode of motility. A benefit to this modality is it requires minimal specialized equipment, as it can be performed with only a simple light microscope. Most laboratories employ phase-, reverse phase-, or differential interference contrast (DIC) optics to allow precision and clarity of individual sperm. However, visual analysis is inherently subjective and prone to human error, which limits the accuracy and repeatability of the motility assessment performed. More objective and accurate assessment of sperm motility can be accomplished through the use of microscopy in combination with computer-assisted sperm analysis (CASA) systems, though this assessment modality requires costly, specialized equipment. CASA systems also allow additional motility parameters to be reliably quantified, beyond total motility, including progressive motility (sperm moving forward) and various motion and velocity parameters.

Recently developed technology, the iSperm® instrument, is a tablet-based method for motility assessment and is much less costly than traditional CASA systems. This technology has been confirmed to be reliable for basic sperm motility assessment in stallions[85] and is also validated in dogs in Chapter 4 of this dissertation[86].

Sperm motility has been associated with fertility and pregnancy rates in mammalian species [65,67]. Sperm motility has been shown to discriminate between subfertile stallions and stallions with higher fertility than average[67]. In bulls, *in vivo* fertility has been correlated with sperm motility and straight-line velocity[65]. It is worth noting that fertility rates are also known to decrease if insemination is performed with cryopreserved sperm[87] which has been noted to have up to a 50% loss of motility[88]. There are many devastating consequences of cryopreservation-

induced sperm damage[89], including increased oxidative stress[30], elevated intracellular calcium ($Ca^{2+}_i$) levels[90], and increased apoptosis[91].

**Summary**

Mammalian sperm quality is assessed by a variety of parameters, with sperm motility and morphology commonly evaluated as cornerstones of semen analysis. Although these semen parameters have been linked to fertility in mammalian species, their pathophysiology remains to be completely elucidated. It is well-established that oxidative stress has severe detrimental consequences on sperm[27–29], and mature sperm have diminished capabilities to combat excess ROS and oxidative damage [27,45,46]. Oxidative damage has been associated with irreversible DNA damage and decreases in fertility across mammalian species[92]. Though assessment of oxidative status can be performed by specialty laboratories for semen analysis, the majority of practitioners do not have access to such assays and rely on the more traditional sperm quality parameters, such as sperm morphology assessment and visual assessment of sperm motility using a light microscope. Current knowledge suggests a relationship exists between oxidative stress and sperm quality parameters, but ultimately the pathophysiology remains unclear and debated in the literature.

Sperm morphology is one of the most commonly assessed semen quality parameters and can be used as an intrinsic marker of sperm quality[68]. Sperm morphologic abnormalities have been linked to decreased fertility and increased oxidative damage in mammalian species[64,71–73,75–77]. However, the studies investigating the relationship between morphologic abnormalities and oxidative stress have limitations including that they predominantly assess sperm quality at a population level rather than examining individual cell characteristics and ROS production. The

pathophysiology of sperm morphologic abnormalities and consequences on male fertility remain to be fully elucidated. The study in Chapter three of this dissertation was designed to address some of these shortcomings by evaluation of sperm morphologic subpopulations and ROS generation using imaging flow cytometry.

Although much has been discovered regarding mechanisms of sperm motility (for more thorough review, see Turner, 2006 [80] and Pereira and colleagues, 2015 [93]), many of the mechanisms underlying sperm motility regulation remain to be elucidated. Specifically, there is much disagreement in the literature regarding the preferred metabolic pathway to fuel sperm motility [94]. This debate is complicated by interspecies variation and the likelihood that sperm possess the metabolic flexibility to adjust to a given environment, substrate availability and physiologic need. As discussed, oxidative stress has been a central focus of the debate regarding the pathway of cellular metabolism predominantly utilized to fuel sperm motility due to the production of ROS secondary to mitochondrial metabolism. Current evidence suggests that some species, such as horses, rely primarily on mitochondrial metabolism to fuel activated motility [33], while other species, such as bovine sperm, are more heavily reliant on anaerobic metabolism to fuel activated motility [60], though these dogmas are subject to debate and disagreement exists in the literature [58,61,94]. Further research is needed to investigate the role of mitochondrial metabolism in motility regulation of mammalian species. In Chapter 2 of this dissertation, I demonstrate that perturbation of mitochondrial ETC activity in bovine sperm significantly reduces motility, contrary to historical findings[60] and in agreement with a more recent report in the literature[61]. Advancement of research on sperm motility and male fertility has been limited by the high cost of CASA systems, which prevents general practitioners from gathering objective data in a clinical setting. In Chapter 4 of this dissertation, I address this need by validating a

more affordable, portable tablet-based system for sperm motility analysis in dogs[86]. This tablet-based system is currently manufactured and advertised for assessment of both equine and canine sperm, but prior to our study, published validation had only been performed in equine sperm[85,95].

Sperm motility and morphology are two commonly assessed parameters to gauge sperm quality and breeding soundness mammalian species. Both sperm motility and morphologic abnormalities have been linked to increased oxidative stress and decreased male fertility, but ultimately, it is subject to debate in the literature and the pathophysiologic significance of these findings has not been fully elucidated. Further research is needed to investigate the physiology and pathophysiology of sperm quality parameters, such as motility and morphology. Such research will not only advance current knowledge of male fertility but will also improve diagnostic power of sperm quality assessment performed by the general practitioner. This dissertation includes studies on bull, stallion and canine sperm to address specific knowledge gaps within each species.

## Figures

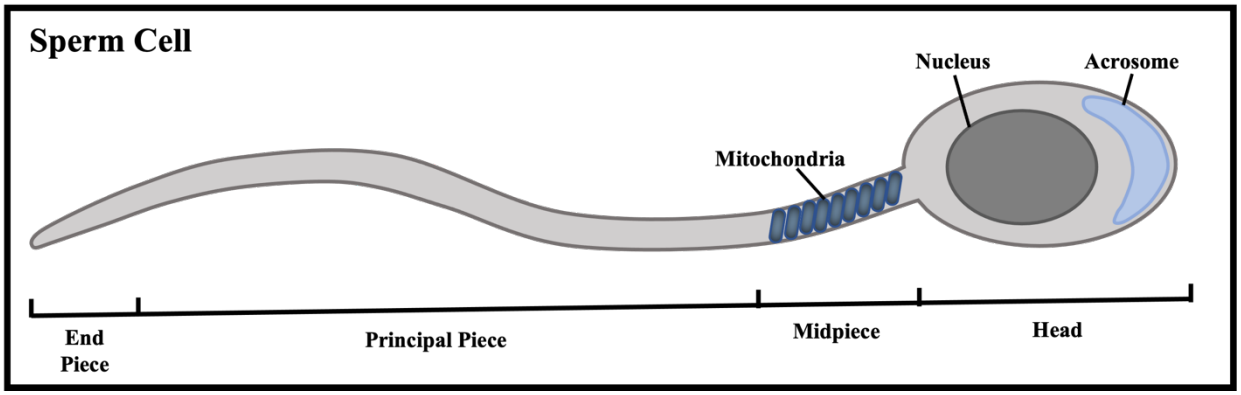


**Figure 1.1**. ***The anatomical structure of mammalian sperm.*** The mammalian sperm cell primarily consists of a head and a flagellum. The head contains the nucleus and, at the most proximal portion, the acrosome. The flagellum provides motility, and can be further subdivided into the midpiece, principal piece and end piece. Sperm mitochondria are helically arranged and reside exclusively within the midpiece of the flagellum.

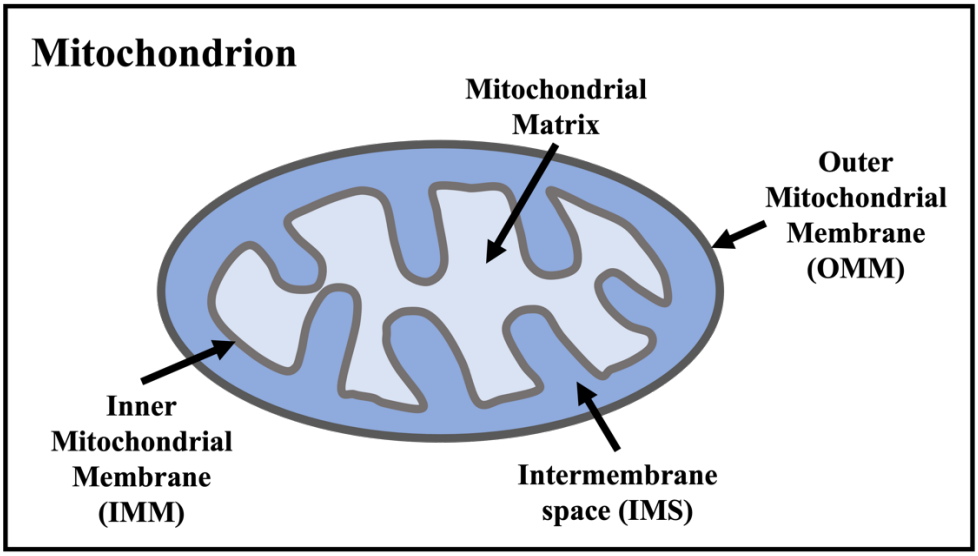


**Figure 1.2:** ***Structure of a Mitochondrion.*** Mitochondria are highly specialized organelles composed of four sub-compartments: an outer mitochondrial membrane (OMM), intermembrane space (IMS), inner mitochondrial membrane (IMM), and mitochondrial matrix. The latter two are the house the majority of mitochondrial proteins and enzymatic activities.

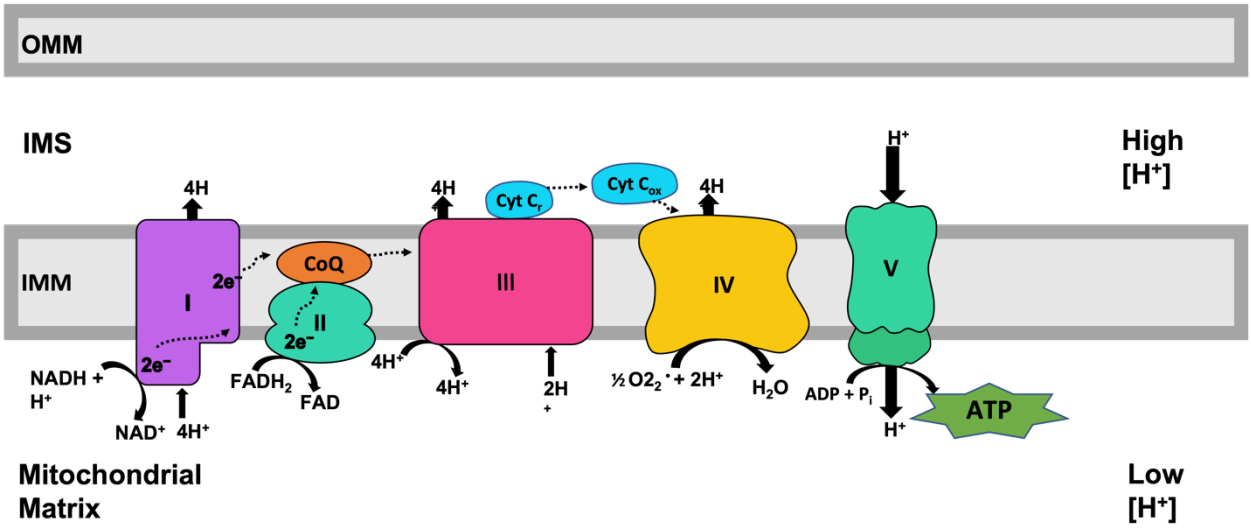


**Figure 1.2**. ***Movement of electrons through the Electron Transport Chain (ETC).*** Electrons are delivered to Complex I of the ETC by NADH and to Complex II by $FADH_2$. Reductive transfer of $e^-s$ through protein complexes (I, II, III, & IV) is coupled to proton pumps (Complexes I, III and IV), allowing protons (hydrogen ions; $H^+$) to travel against their electrochemical gradient into the IMS. Ultimately, the protons flow back down their electrochemical gradient and into the mitochondrial matrix, during which time, complex V (ATP synthase) harnesses the energy of the electrochemical gradient pulling the protons into the matrix (the proton motive force, $\Delta p$) to power the generation of ATP.

**References**


1. Ruestow EG. Images and ideas: Leeuwenhoek's perception of the spermatozoa. *J Hist Biol*. 1983;16(2):185-224. doi:10.1007/BF00124698
2. Varner DD, Johnson L, Green EM. From a sperm's eye view-revisiting our perception of this intriguing cell. *Proc Annu Conv AAEP - Orlando, Florida, 2007*. 2007;53:104-177. http://www.cabdirect.org/abstracts/20083097814.html
3. Lehti MS, Sironen A. Formation and function of sperm tail structures in association with sperm motility defects†. *Biol Reprod*. 2017;97(4):522-536. doi:10.1093/biolre/iox096
4. Santiago J, Silva J V, Alves MG, Oliveira PF, Fardilha M. Testicular aging: an overview of ultrastructural, cellular and molecular alterations. *J Gerontol A Biol Sci Med Sci*. 2018;00(00):1-12. doi:10.1093/gerona/gly082
5. Saacke RG, Almquist JO. Ultrastructure of bovine spermatozoa. I. The head of normal, ejaculated sperm. *Am J Anat*. 1964;115(1):143-161. doi:10.1002/aja.1001150109
6. Saacke RG, Almquist JO. Ultrastructure of bovine spermatozoa. II. The neck and tail of normal, ejaculated sperm. *Am J Anat*. 1964;115(1):163-183. doi:10.1002/aja.1001150110
7. Fawcett DW. The mammalian spermatozoon. *Dev Biol*. 1975;44(2):394-436. doi:10.1016/0012-1606(75)90411-X
8. Fawcett DW. A Comparative View of Sperm Ultrastructure. *Biol Reprod*. 1970;(suppl_2):90-127. doi:10.1095/biolreprod2.Supplement_2.90
9. Ounjai P, Kim KD, Lishko P V., Downing KH. Three-dimensional structure of the bovine sperm connecting piece revealed by electron cryotomography. *Biol Reprod*. 2012;87(3):1-9. doi:10.1095/biolreprod.112.101980
10. Lindemann CB, Lesich KA. Functional anatomy of the mammalian sperm flagellum.

*Cytoskeleton*. 2016;73(11):652-669. doi:10.1002/cm.21338

11. Freitas M, Vijayaraghavan S, Fardilha M. Signaling mechanisms in mammalian sperm motility. *Biol Reprod*. 2016;bio 144337(1):2-12. doi:10.1095/biolreprod.116.144337
12. Kim YH, Haidl G, Schaefer M, Egner U, Mandal A, Herr JC. Compartmentalization of a unique ADP/ATP carrier protein SFEC (Sperm Flagellar Energy Carrier, AAC4) with glycolytic enzymes in the fibrous sheath of the human sperm flagellar principal piece. *Dev Biol*. 2007;302(2):463-476. doi:10.1016/j.ydbio.2006.10.004
13. Twigg JP, Irvine DS, Aitken RJ. Oxidative damage to DNA in human spermatozoa does not preclude pronucleus formation at intracytoplasmic sperm injection. *Hum Reprod*. 1998;13(7):1864-1871. doi:10.1093/humrep/13.7.1864
14. Aitken RJ, Buckingham D, Harkiss D. Use of a xanthine oxidase free radical generating system to investigate the cytotoxic effects of reactive oxygen species on human spermatozoa. *J Reprod Fertil*. 1993;97(April):441-450. doi:10.1530/jrf.0.0970441
15. Tourmente M, Villar-Moya P, Rial E, Roldan ERS. Differences in ATP generation via glycolysis and oxidative phosphorylation and relationships with sperm motility in mouse species. *J Biol Chem*. 2015;290(33):20613-20626. doi:10.1074/jbc.M115.664813
16. Piomboni P, Focarelli R, Stendardi A, Ferramosca A, Zara V. The role of mitochondria in energy production for human sperm motility. *Int J Androl*. 2012;35(2):109-124. doi:10.1111/j.1365-2605.2011.01218.x
17. Luo SM, Schatten H, Sun QY. Sperm mitochondria in reproduction: Good or bad and where do they go? *J Genet Genomics*. 2013;40(11):549-556. doi:10.1016/j.jgg.2013.08.004
18. Koopman M, Michels H, Dancy BM, Kamble R, Mouchiroud L, Auwerx J, Nollen EAA,

Houtkooper RH. A screening-based platform for the assessment of cellular respiration in Caenorhabditis elegans. *Nat Protoc*. 2016;11(10):1798-1816. doi:10.1038/nprot.2016.106

19. Gunter TE, Yule DI, Gunter KK, Eliseev RA, Salter JD. Calcium and mitochondria. *FEBS Lett*. 2004;567(1):96-102. doi:10.1016/j.febslet.2004.03.071

20. Koppers AJ, De Iuliis GN, Finnie JM, McLaughlin EA, Aitken RJ. Significance of mitochondrial reactive oxygen species in the generation of oxidative stress in spermatozoa. *J Clin Endocrinol Metab*. 2008;93(8):3199-3207. doi:10.1210/jc.2007-2616

21. Rodríguez-Gil JE, Bonet S. Current knowledge on boar sperm metabolism: Comparison with other mammalian species. *Theriogenology*. 2016;85(1):4-11. doi:10.1016/j.theriogenology.2015.05.005

22. Gottlieb E, Armour SM, Harris MH, Thompson CB. Mitochondrial membrane potential regulates matrix configuration and cytochrome c release during apoptosis. *Cell Death Differ*. 2003;10(6):709-717. doi:10.1038/sj.cdd.4401231

23. de Lamirande E, Gagnon C. Capacitation-associated production of superoxide anion by human spermatozoa. *Free Radic Biol Med*. 1995;18(3):487-495. doi:10.1016/0891-5849(94)00169-K

24. de Lamirande E, Gagnon C. Reactive oxygen species and human spermatozoa. II. Depletion of adenosine triphosphate plays an important role in the inhibition of sperm motility. *J Androl*. 1992;13(5):379-386.

25. Chang H, Suarez SS. Rethinking the Relationship Between Hyperactivation and Chemotaxis in Mammalian Sperm1. *Biol Reprod*. 2010;83(4):507-513. doi:10.1095/biolreprod.109.083113

26. Aitken RJ, Fisher HM, Fulton N, Gomez E, Knox W, Lewis B, Irvine S. Reactive oxygen

species generation by human spermatozoa is induced by exogenous NADPH and inhibited by the flavoprotein inhibitors diphenylene iodonium and quinacrine. *Mol Reprod Dev*. 1997;47(4):468-482. doi:10.1002/(SICI)1098-2795(199708)47:4<468::AID-MRD14>3.0.CO;2-S

27. Aitken R. Generation of reactive oxygen species, lipid peroxidation, and human sperm function. *Biol Reprod*. 1989;41(1):183-197. doi:10.1095/biolreprod41.1.183

28. Aitken RJ. Pathophysiology of human spermatozoa. *Curr Opin Obstet Gynecol*. 1994;6(2):128-135.

29. Iwasaki A, Gagnon C. Formation of reactive oxygen species in spermatozoa of infertile patients. *Fertil Steril*. 1992;57(2):409-416. http://www.ncbi.nlm.nih.gov/pubmed/1735495

30. Martin Munoz P, Ferrusola CO, Vizuete G, Davila MP, Martinez HR, Pena FJ. Depletion of Intracellular Thiols and Increased Production of 4-Hydroxynonenal that Occur During Cryopreservation of Stallion Spermatozoa Lead to Caspase Activation, Loss of Motility, and Cell Death. *Biol Reprod*. 2015;93(6):143-143. doi:10.1095/biolreprod.115.132878

31. Baumber J, Ball BA, Linfor JJ, Meyers SA. Reactive Oxygen Species and Cryopreservation Promote DNA Fragmentation in Equine Spermatozoa. *J Androl*. 2003;24(4):621-628. doi:10.1002/j.1939-4640.2003.tb02714.x

32. Yeste M, Estrada E, Casas I, Bonet S, Rodríguez-Gil JE. Good and bad freezability boar ejaculates differ in the integrity of nucleoprotein structure after freeze-thawing but not in ROS levels. *Theriogenology*. 2013;79(6):929-939. doi:10.1016/j.theriogenology.2013.01.008

33. Darr CR, Cortopassi GA, Datta S, Varner DD, Meyers SA. Mitochondrial oxygen consumption is a unique indicator of stallion spermatozoal health and varies with

cryopreservation media. *Theriogenology*. 2016;86(5):1382-1392. doi:10.1016/j.theriogenology.2016.04.082

34. Gadea J, Molla M, Selles E, Marco MA, Garcia-Vazquez FA, Gardon JC. Reduced glutathione content in human sperm is decreased after cryopreservation: Effect of the addition of reduced glutathione to the freezing and thawing extenders. *Cryobiology*. 2011;62(1):40-46. doi:10.1016/j.cryobiol.2010.12.001

35. Sabeur K, Ball BA. Characterization of NADPH oxidase 5 in equine testis and spermatozoa. *Reproduction*. 2007;134(2):263-270. doi:10.1530/REP-06-0120

36. Musset B, Clark R a, DeCoursey TE, Petheo GL, Geiszt M, Chen Y, Cornell JE, Eddy C a, Brzyski RG, El Jamali A. NOX5 in human spermatozoa: expression, function, and regulation. *J Biol Chem*. 2012;287(12):9376-9388. doi:10.1074/jbc.M111.314955

37. Ghani E, Keshtgar S, Habibagahi M, Ghannadi A, Kazeroni M. Expression of NOX5 in human teratozoospermia compared to normozoospermia. *Andrologia*. 2013;45(5):351-356. doi:10.1111/and.12023

38. Cassina A, Silveira P, Cantu L, Montes JM, Radi R SR. Defective Human Sperm Cells Are Associated with Mitochondrial Dysfunction and Oxidant Production. *Biol Reprod*. 2015;93((5)):119. doi:10.1095/biolreprod.115.130989

39. Muñoz PM, Ferrusola CO, Lopez LA, Del Petre C, Garcia MA, de Paz Cabello P, Anel L, Peña FJ. Caspase 3 Activity and Lipoperoxidative Status in Raw Semen Predict the Outcome of Cryopreservation of Stallion Spermatozoa. *Biol Reprod*. 2016;95(3):53. doi:10.1095/biolreprod.116.139444

40. Thomson LK, Fleming SD, Aitken RJ, De Iuliis GN, Zieschang JA, Clark AM. Cryopreservation-induced human sperm DNA damage is predominantly mediated by

oxidative stress rather than apoptosis. *Hum Reprod*. 2009;24(9):2061-2070. doi:10.1093/humrep/dep214

41. Gibb Z, Lambourne SR, Aitken RJ. The paradoxical relationship between stallion fertility and oxidative stress. *Biol Reprod*. 2014;91(3):1-10. doi:10.1095/biolreprod.114.118539

42. Gallardo Bolaños JM, Balao da Silva CM, Martín Muñoz P, Morillo Rodríguez A, Plaza Dávila M, Aparicio IM, Tapia JA, Ortega Ferrusola C, Peña FJ. Akt (protein kinase B) preserves motility in stallion sperm by inhibiting caspases 3 and 7. *J Equine Vet Sci*. 2014;34(1):66-67. doi:10.1016/j.jevs.2013.10.041

43. Gallardo Bolaños JM, Balao Da Silva CM, Martín Muñoz P, Morillo Rodríguez A, Plaza Dávila M, Rodríguez-Martínez H, Aparicio IM, Tapia JA, Ortega Ferrusola C, Peña FJ. Phosphorylated AKT preserves stallion sperm viability and motility by inhibiting caspases 3 and 7. *Reproduction*. 2014;148(2):221-235. doi:10.1530/REP-13-0191

44. Aitken RJ, Whiting S, De Iuliis GN, McClymont S, Mitchell LA, Baker MA. Electrophilic aldehydes generated by sperm metabolism activate mitochondrial reactive oxygen species generation and apoptosis by targeting succinate dehydrogenase. *J Biol Chem*. 2012;287(39):33048-33060. doi:10.1074/jbc.M112.366690

45. Alvarez JG, Touchstone JC, Blasco L, Storey BT. Spontaneous Lipid Peroxidation and Production of Hydrogen Peroxide and Superoxide in Human Spermatozoa Superoxide Dismutase as Major Enzyme Protectant Against Oxygen Toxicity. *J Androl*. 1987;8(5):338-348. doi:10.1002/j.1939-4640.1987.tb00973.x

46. Jones R, Mann T, Sherins R. Peroxidative Breakdown of Phospholipids in Human Spermatozoa, Spermicidal Properties of Fatty Acid Peroxides, and Protective Action of Seminal Plasma. *Fertil Steril*. 1979;31(5):531-537. doi:10.1016/S0015-0282(16)43999-3

47. Alvarez JG, Storey BT. Role of glutathione peroxidase in protecting mammalian spermatozoa from loss of motility caused by spontaneous lipid peroxidation. *Gamete Res*. 1989;23(1):77-90. doi:10.1002/mrd.1120230108

48. Castro LS, Hamilton TRS, Mendes CM, Nichi M, Barnabe VH, Visintin JA, Assumpção MEOA. Sperm cryodamage occurs after rapid freezing phase: flow cytometry approach and antioxidant enzymes activity at different stages of cryopreservation. *J Anim Sci Biotechnol*. 2016;7(1):17. doi:10.1186/s40104-016-0076-x

49. Zhu Z, Fan X, Lv Y, Lin Y, Wu D, Zeng W. Glutamine protects rabbit spermatozoa against oxidative stress via glutathione synthesis during cryopreservation. *Reprod Fertil Dev*. 2017;29(11):2183. doi:10.1071/RD17020

50. Mata-Campuzano M, Álvarez-Rodríguez M, Álvarez M, Tamayo-Canul J, Anel L, de Paz P, Martínez-Pastor F. Post-thawing quality and incubation resilience of cryopreserved ram spermatozoa are affected by antioxidant supplementation and choice of extender. *Theriogenology*. 2015;83(4):520-528. doi:10.1016/j.theriogenology.2014.10.018

51. Fontoura P, Mello MD, Gallo-Sá P, Erthal-Martins MC, Cardoso MCA, Ramos C. Leptin Improves Sperm Cryopreservation via Antioxidant Defense. *J Reprod Infertil*. 2017;18(1):172-178. http://www.ncbi.nlm.nih.gov/pubmed/28377896

52. Kankofer M, Kolm G, Aurich J, Aurich C. Activity of glutathione peroxidase, superoxide dismutase and catalase and lipid peroxidation intensity in stallion semen during storage at 5°C. *Theriogenology*. 2005;63(5):1354-1365. doi:10.1016/j.theriogenology.2004.07.005

53. Grant KE, De Oliveira R V., Hennington BS, Govindaraju A, Perkins A, Stokes J, Rowe D, Topper E, Kaya A, Moura A, Memili E. Sperm superoxide dismutase is associated with bull fertility. *Reprod Fertil Dev*. 2016;28(9):1405-1413. doi:10.1071/RD14399

54. Sanocka D, Kurpisz M. Reactive oxygen species and sperm cells. *Reprod Biol Endocrinol*. 2004;2(1):12. doi:10.1186/1477-7827-2-12

55. Aitken RJ, Jones KT, Robertson SA. Reactive oxygen species and sperm function - In sickness and in health. *J Androl*. 2012;33(6):1096-1106. doi:10.2164/jandrol.112.016535

56. Donnelly ET, O'Connell M, McClure N, Lewis SE. Differences in nuclear DNA fragmentation and mitochondrial integrity of semen and prepared human spermatozoa. *Hum Reprod*. 2000;15(7):1552-1561. doi:10.1093/humrep/15.7.1552

57. De Iuliis GN, Thomson LK, Mitchell LA, Finnie JM, Koppers AJ, Hedges A, Nixon B, Aitken RJ. DNA Damage in Human Spermatozoa Is Highly Correlated with the Efficiency of Chromatin Remodeling and the Formation of 8-Hydroxy-2′-Deoxyguanosine, a Marker of Oxidative Stress1. *Biol Reprod*. 2009;81(3):517-524. doi:10.1095/biolreprod.109.076836

58. Ford WCL. Glycolysis and sperm motility: does a spoonful of sugar help the flagellum go round? *Hum Reprod Update*. 2006;12(3):269-274. doi:10.1093/humupd/dmi053

59. Nascimento JM, Shi LZ, Tam J, Chandsawangbhuwana C, Durrant B, Botvinick EL, Berns MW. Comparison of glycolysis and oxidative phosphorylation as energy sources for mammalian sperm motility, using the combination of fluorescence imaging, laser tweezers, and real-time automated tracking and trapping. *J Cell Physiol*. 2008;217(3):745-751. doi:10.1002/jcp.21549

60. Krzyzosiak J, Molan P, Vishwanath R. Measurements of bovine sperm velocities under true anaerobic and aerobic conditions. *Anim Reprod Sci*. 1999;55(3-4):163-173. doi:10.1016/s0378-4320(99)00016-0

61. Magdanz V, Boryshpolets S, Ridzewski C, Eckel B, Reinhardt K. The motility-based

swim-up technique separates bull sperm based on differences in metabolic rates and tail length. Kues WA, ed. *PLoS One*. 2019;14(10):e0223576. doi:10.1371/journal.pone.0223576

62. Bulkeley EA, Foutouhi A, Wigney K, Santistevan AC, Collins C, McNabb B, Meyers S. Effects from disruption of mitochondrial electron transport chain function on bull sperm motility. *Theriogenology*. 2021;176:63-72. doi:10.1016/j.theriogenology.2021.09.015

63. Wang C, Swerdloff RS. Limitations of semen analysis as a test of male fertility and anticipated needs from newer tests. *Fertil Steril*. 2014;102(6):1502-1507. doi:10.1016/j.fertnstert.2014.10.021

64. Slama R, Eustache F, Ducot B, Jensen TK, Jørgensen N, Horte A, Irvine S, Suominen J, Andersen AG, Auger J, Vierula M, Toppari J, Andersen AN, Keiding N, Skakkebaek NE, Spira A, Jouannet P. Time to pregnancy and semen parameters: a cross-sectional study among fertile couples from four European cities. *Hum Reprod*. 2002;17(2):503-515. doi:10.1093/humrep/17.2.503

65. Gillan L, Kroetsch T, Chis Maxwell WM, Evans G. Assessment of in vitro sperm characteristics in relation to fertility in dairy bulls. *Anim Reprod Sci*. 2008;103(3-4):201-214. doi:10.1016/j.anireprosci.2006.12.010

66. Root Kustritz MV. The value of canine semen evaluation for practitioners. *Theriogenology*. 2007;68(3):329-337. doi:10.1016/j.theriogenology.2007.04.017

67. Love CC. Relationship between sperm motility, morphology and the fertility of stallions. *Theriogenology*. 2011;76(3):547-557. doi:10.1016/j.theriogenology.2011.03.007

68. Love CC. Sperm quality assays: How good are they? The horse perspective. *Anim Reprod Sci*. 2018;194(January):63-70. doi:10.1016/j.anireprosci.2018.04.077

69. Cooper TG, Brazil C, Swan SH, Overstreet JW. Ejaculate Volume Is Seriously Underestimated When Semen Is Pipetted or Decanted Into Cylinders From the Collection Vessel. *J Androl*. 2006;28(1):1-4. doi:10.2164/jandrol.106.001297

70. Melo CM, Zahn FS, Martin I, Orlandi C, Dell'Aqua JA, Alvarenga MA, Papa FO. Influence of Semen Storage and Cryoprotectant on Post-thaw Viability and Fertility of Stallion Spermatozoa. *J Equine Vet Sci*. 2007;27(4):171-175. doi:10.1016/j.jevs.2007.02.008

71. Abu Hassan Abu D, Franken DR, Hoffman B, Henkel R. Accurate sperm morphology assessment predicts sperm function. *Andrologia*. 2012;44(SUPPL.1):571-577. doi:10.1111/j.1439-0272.2011.01229.x

72. Saacke RG. Sperm morphology: Its relevance to compensable and uncompensable traits in semen. *Theriogenology*. 2008;70(3):473-478. doi:10.1016/j.theriogenology.2008.04.012

73. Love CC, Varner DD, Thompson JA. Intra- and inter-stallion variation in sperm morphology and their relationship with fertility. *J Reprod Fertil Suppl*. 2000;(56):93-100. http://www.ncbi.nlm.nih.gov/pubmed/20681120

74. Elshal MF, El-Sayed IH, Elsaied MA, El-Masry SA, Kumosani TA. Sperm head defects and disturbances in spermatozoal chromatin and DNA integrities in idiopathic infertile subjects: Association with cigarette smoking. *Clin Biochem*. 2009;42(7-8):589-594. doi:10.1016/j.clinbiochem.2008.11.012

75. Aziz N, Saleh RA, Sharma RK, Lewis-Jones I, Esfandiari N, Thomas AJ, Agarwal A. Novel association between sperm reactive oxygen species production, sperm morphological defects, and the sperm deformity index. *Fertil Steril*. 2004;81(2):349-354. doi:10.1016/j.fertnstert.2003.06.026

76. Said TM, Aziz N, Sharma RK, Lewis-Jones I, Thomas AJ, Agarwal A. Novel association between sperm deformity index and oxidative stress-induced DNA damage in infertile male patients. *Asian J Androl*. 2005;7(2):121-126. doi:10.1111/j.1745-7262.2005.00022.x

77. Sailer BL, Tost LK, Evenson DP. Bull sperm head morphometry related to abnormal chromatin structure and fertility. *Cytometry*. 1996;24(2):167-173. doi:10.1002/(SICI)1097-0320(19960601)24:2<167::AID-CYTO9>3.0.CO;2-G

78. Burnaugh L, Sabeur K, Ball BA. Generation of superoxide anion by equine spermatozoa as detected by dihydroethidium. *Theriogenology*. 2007;67(3):580-589. doi:10.1016/j.theriogenology.2006.07.021

79. Rodrigues MB. An Efficient Technique to Detect Sperm Reactive Oxygen Species: The CellRox Deep Red® Fluorescent Probe. *Biochem Physiol Open Access*. 2015;04(02):0-5. doi:10.4172/2168-9652.1000157

80. Turner RM. Moving to the beat: a review of mammalian sperm motility regulation. *Reprod Fertil Dev*. 2006;18(2):25. doi:10.1071/RD05120

81. Katz DF, Yanagimachi R. Movement Characteristics of Hamster Spermatozoa Within the Oviduct. *Biol Reprod*. 1980;22(4):759-764. doi:10.1095/biolreprod22.4.759

82. Suarez SS, Katz DF, Overstreet JW. Movement characteristics and acrosomal status of rabbit spermatozoa recovered at the site and time of fertilization. *Biol Reprod*. 1983;29(5):1277-1287. doi:6652189

83. Yanagimachi R. The movement of golden hamster spermatozoa before and after capacitation. *J Reprod Fertil*. 1970;23(1):193-196. http://www.ncbi.nlm.nih.gov/pubmed/16274254

84. Hinrichs K, Loux SC. Hyperactivated Sperm Motility: Are Equine Sperm Different? *J*

*Equine Vet Sci*. 2012;32(8):441-444. doi:10.1016/j.jevs.2012.05.070

85. Dini P, Troch L, Lemahieu I, Deblende P, Daels P. Validation of a portable device (iSperm®) for the assessment of stallion sperm motility and concentration. *Reprod Domest Anim*. 2019;54(8):1113-1120. doi:10.1111/rda.13487

86. Bulkeley E, Collins C, Foutouhi A, Gonzales K, Power H, Meyers S. Assessment of an iPad-based sperm motility analyzer for determination of canine sperm motility. *Transl Anim Sci*. 2021;5(2):1-7. doi:10.1093/tas/txab066

87. Masoudi R, Sharafi M, Zareh Shahneh A, Towhidi A, Kohram H, Esmaeili V, Shahverdi A, Davachi ND. Fertility and flow cytometry study of frozen-thawed sperm in cryopreservation medium supplemented with soybean lecithin. *Cryobiology*. 2016;73(1):69-72. doi:10.1016/j.cryobiol.2016.05.010

88. Ball BA. Oxidative stress, osmotic stress and apoptosis: Impacts on sperm function and preservation in the horse. *Anim Reprod Sci*. 2008;107(3-4):257-267. doi:10.1016/j.anireprosci.2008.04.014

89. Meyers SA. Cryostorage and Oxidative Stress in Mammalian Spermatozoa. In: Agarwal, Ashok Aitken, Robert J. Alvarez J, ed. *Studies on Men's Health and Fertility*. Humana Press, c/o Springer Science+Business Media, LLC; 2012:41-56. doi:10.1007/978-1-61779-776-7

90. Albrizio M, Moramarco AM, Nicassio M, Micera E, Zarrilli A, Lacalandra GM. Localization and functional modification of L-type voltage-gated calcium channels in equine spermatozoa from fresh and frozen semen. *Theriogenology*. 2015;83(3):421-429. doi:10.1016/j.theriogenology.2014.10.005

91. Balao CM, Bolan JMG, Tapia A, Ferrusola CO, Pen FJ. Autophagy and Apoptosis Have a

Role in the Survival or Death of Stallion Spermatozoa during Conservation in Refrigeration. 2012;7(1):1-9. doi:10.1371/journal.pone.0030688

92. Agarwal A, Said TM. Oxidative stress, DNA damage and apoptosis in male infertility: A clinical approach. *BJU Int*. 2005;95(4):503-507. doi:10.1111/j.1464-410X.2005.05328.x

93. Pereira R, Sá R, Barros A, Sousa M. Major regulatory mechanisms involved in sperm motility. *Asian J Androl*. 2015;0(0):0. doi:10.4103/1008-682X.167716

94. Storey BT. Mammalian sperm metabolism: Oxygen and sugar, friend and foe. *Int J Dev Biol*. 2008;52(5-6):427-437. doi:10.1387/ijdb.072522bs

95. Moraes CR, Runcan EE, Blawut B, Coutinho da Silva MA. Technical Note: The use of iSperm technology for on-farm measurement of equine sperm motility and concentration. *Transl Anim Sci*. 2019;3(4):1513-1520. doi:10.1093/tas/txz115

# Chapter 2: Effects from disruption of mitochondrial electron transport chain function on bull sperm motility

Evelyn A. Bulkeley[1], Azarene Foutouhi[1], Kayla Wigney[1], Anthony C. Santistevan[3], Christine Collins[1], Bret McNabb[2], Stuart Meyers[1]

[1]Department of Anatomy, Physiology, and Cell Biology, [2]Department of Population Health and Reproduction, School of Veterinary Medicine,[3]Department of Psychology, University of California, Davis

**Abstract**

Sperm mitochondrial function is essential for normal physiology and fertility, but the importance of mitochondrial activity to support specific sperm functions, such as motility, varies between species. It was previously believed that mitochondrial function was not necessary for bull sperm motility [1]; however, this theory is contradicted by recently reported findings that the upper fraction of bull sperm swim-up preparations had both high motility and elevated mitochondrial oxygen consumption rates[2]. The objective of this study was to investigate the relationship between mitochondrial function and motility in bull sperm. We hypothesized that sperm motility would be positively correlated with mitochondrial oxygen consumption (MITOX) but unaffected by pharmacological inhibition of electron transport chain (ETC) activity. This was accomplished by monitoring both mitochondrial oxygen consumption and motility parameters in the presence of mitochondrial effector drug treatments. Duplicate ejaculates were collected by electroejaculation from Black Angus bulls (n=4). Oxygen consumption, as % air saturation ($pO_2$; oxygen partial pressure), over time was monitored in the presence of 5 drug treatments: vehicle control, FCCP, Antimycin (ANTI), Oligomycin (Oligo), and FCCP+Oligomycin (FCCP+OLIGO). Duplicate aliquots were prepared for concurrent motility assessment by computer-assisted sperm analysis (CASA) at 6- and 30-min post-treatment (t6 and t30). The impact of treatments on $pO_2$ (in % air saturation) over time were assessed by generalized linear mixed effects modeling (GLMM) which was also used to test for differences in average motility across treatment conditions and time points (t6 and t30). Pearson product-moment correlation was used to investigate relationships between oxygen consumption and motility parameters. Overall, $pO_2$ differed over time between treatment conditions ($p<0.0001$). When compared to the vehicle treatment, ANTI and OLIGO significantly inhibited oxygen consumption ($p<0.05$,

adjusted), and FCCP stimulated a marked increase in oxygen consumption. No significant differences in motility over time were observed between treatments, so comparison of motility parameters between treatment conditions was performed with pooled timepoints. Motility parameters were only observed to differ significantly from the vehicle with ANTI Treatment, for which significant decreases in numerous parameters, including total motility ($p$=0.007), progressive motility ($p$=0.01), DAP ($p$=0.01), VAP ($p$=0.01) and VSL ($p$=0.02) were identified. For the vehicle treatment, correlational analysis did not reveal any significant correlations between $pO_2$ and any motility parameters at t6; however, several significant correlations were identified at t30. Mean $pO_2$ was negatively correlated with local motility ($p$<0.01) and positively correlated with DCL, DAP, and VCL (p<0.05). Results from this study suggest that bovine sperm motility is impacted by mitochondrial functionality, with ETC inhibition by ANTI causing significant reduction in motility parameters. This study also demonstrates the use of a new technology for the assessment of bovine sperm mitochondrial function. This modality for evaluation of bull sperm mitochondrial function will inform future efforts to understand bull sperm function and fertility and aid investigations into toxicological agents.

## Introduction

Energy, in the form of adenosine triphosphate (ATP), is required for many sperm functions and fertilizing events, including motility, capacitation, and acrosome reaction[3]. The highest yield of ATP is achieved by mitochondrial oxidative phosphorylation (OXPHOS), which produces a net of 36 ATP molecules from one molecule of pyruvate, while glycolysis only produces a net of 2 ATP. The electron transport chain (ETC) is a series of protein complexes located within the inner mitochondrial membrane (IMM). In OXPHOS, reduced electron carriers (NADH and $FADH_2$) deliver electrons which are then passed from one ETC complex to the next by a series of redox reactions, with oxygen acting as the terminal electron acceptor. The energy released from these reactions is used to pump protons ($H^+$) across the IMM from the mitochondrial matrix to the intermembrane space (IMS), establishing an electrochemical gradient, with high [$H^+$] in the intermembrane space and low [$H^+$] in the mitochondrial matrix. This allows for gradient-driven synthesis of ATP, wherein the protons located in the IMS flow down their gradient and back into the matrix. In order to cross the impermeable IMM, the protons pass through a pore in ATP synthase (ETC complex V), causing conformational changes that facilitate ATP production[4,5].

Although it is well-established that normal sperm mitochondrial function is essential for fertility, the role of mitochondria supporting specific sperm functions, such as motility and capacitation, has been shown to vary extensively between species. For example, stallion sperm rely almost exclusively on mitochondria-produced ATP to fuel motility[6], while the glycolytic pathway has been shown to be the primary energy source for human sperm motility[7]. The role of mitochondria in supporting bull sperm functions and motility is complex and has not been fully elucidated. Although bull sperm are dependent on OXPHOS to support capacitation[8], it has long

been thought that OXPHOS is not necessary to support bull sperm motility. In support, Krzyzosiak and colleagues (1999) reported that bull sperm can maintain motility in the presence of ETC inhibitors, if glycolytic substrates are provided in the media; in combination with experimentation of bovine sperm under aerobic and anerobic conditions, the authors concluded that active bovine sperm motility can be solely fueled by anaerobic metabolism (glycolysis) [1]. However, a recent study by Magdanz and colleagues (2019) reported that the upper fraction of bovine sperm swim-up preparations had higher motility and metabolic activity, including elevated mitochondrial oxygen consumption rates[2], raising questions about the long-accepted theory that bull sperm motility is not fueled by mitochondria-produced ATP and warranting further investigation.

The objective of this study was to investigate the relationship between mitochondrial function and motility in bull sperm by monitoring both mitochondrial oxygen consumption and motility parameters in the presence of mitochondrial effector drug treatments. Consideration of the aforementioned literature in combination with the fluid state of cellular metabolism, it is feasible that highly motile sperm likely utilize mitochondrial metabolism for higher yield of ATP, but upon ETC inhibition/disruption, a flux to anaerobic metabolism is possible to maintain active motility in bovine sperm**.** We hypothesized that sperm motility would be positively correlated with mitochondrial oxygen consumption (MITOX) but unaffected by pharmacological disruption of ETC activity, which would support the theory that bovine sperm flagellar motility is impacted by, but not dependent on, mitochondrial ETC function. To accomplish this, we adapted a fluorescence, plate-based system to monitor oxygen consumption in freely motile bull sperm. We then assessed mitochondrial oxidative function by monitoring sperm oxygen consumption in the presence of an array of mitochondrial effector drug treatments and performed

simultaneous motility evaluations to elucidate the relationship between mitochondrial OXPHOS function and bovine sperm motility. The successful development and application of this assay in bovine sperm and the information elucidated regarding bull sperm mitochondrial function will inform future efforts to understand bull sperm function and fertility and aid investigations into possible roles for toxicological and medical pharmaceutical agents to influence sperm function.

## Material and Methods

### *Chemicals and media*

All chemicals were purchased from MilliporeSigma (Burlington, MA) unless otherwise indicated. Calcium chloride (0.1M, RICCA-1760-32) was purchased from Sycamore Life Sciences (Houston, TX). NucleoCounter® SP-100™ reagents were purchased from ChemoMetec (Allerød, Denmark).

The culture medium for this experiment was a modified Tyrode's medium (TALP)[9], with slight modifications to the TALP (Sp-TALP) described previously for use in bovine sperm [10,11]. This media consisted of 1 mg/mL fatty acid-free bovine serum albumin (BSA, Fraction V), 80 mmol/L NaCl, 2.8 mmol/L KCl, 0.2645 mmol/L $KH_2PO_4$, 40 mmol/L HEPES sodium salt, 2 mmol/L $NaHCO_3$, 2 mmol/L $CaCl_2$ (0.1 M solution, Ricca), and 0.4 mmol/L $MgCl_2$ (1 M solution). Complete medium contained metabolites which consisted of 5 mmol/L D-glucose, 1 mmol/L sodium pyruvate, and 0.1862% (v/v; 21.6 mmol/L) DL-Lactic acid syrup. Medium pH was adjusted to 7.4 ± 0.02 and osmolality of 300 ± 10 mOsm/kg. The complete modified Sp-TALP medium was prepared fresh daily for experimentation and pre-warmed to 37ºC prior to semen collection.

### *Animals, semen collection and sperm processing*

Semen was collected by electroejaculation from mature Black Angus bulls (n=4) at the UC Davis Beef Feedlot and Swine Facility. Bulls were maintained on a total mixed ration comprised of forage and grain, had fresh water available *ad libitum*, and daily exercise according to Institutional Animal Care and Use Committee protocols at the University of California (UC). Two separate ejaculates were collected from each bull on separate days. Briefly, bulls were restrained in a squeeze chute for breeding soundness examination and semen collection. An electrical stimulus was delivered using a 7.5cm diameter transrectal probe (Pulsator V, Lane Manufacturing Inc., Denver, CO), using a pre-programmed cycle, to evoke an erection, protrusion and ejaculation. The sperm-rich fraction of semen was collected into a sterile collection cone and immediately evaluated. Forward progressive motility was initially evaluated by dilution of semen with 2.9% sodium citrate solution and observed using phase contrast microscopy at 400X magnification. Ejaculate volume was recorded and ejaculates were then immediately extended 1:4 (v:v) in pre-warmed (37°C) modified TALP media and transported to the lab 37°C where initial concentration, viability and motility parameters were assessed before further processing. Following initial sperm quality assessment, semen was washed twice using centrifugation (8 min at 250×*g*) and resuspension to a concentration of 70 x $10^6$ viable cells/mL.

*Sperm morphology, concentration, and viability*

Morphologic examination was achieved by preparing an aliquot of raw semen, 2.9% sodium citrate and eosin-nigrosin stain (Morphology stain, Society for Theriogenology, AL), then making an air-dried smear for evaluation. Individual sperm morphology was examined under 1000X magnification under immersion oil and all morphologic defects were recorded by a board-certified Theriogenologist to calculate the percentage of morphologically normal sperm (MN), sperm with proximal droplets (PD), abnormal midpieces (MP), head shape abnormality

(HS) and detached heads (DH) was calculated. Sperm concentration (million/mL) and viability (%) were assessed using a NucleoCounter® SP-100™ instrument (ChemoMetec; Allerød, Denmark) according to manufacturer instructions. Sperm concentration was multiplied by ejaculate volume to determine total sperm numbers (million/mL).

*Computer-assisted motility analysis (CASA)*

Sperm motility parameters were evaluated by computer-assisted sperm analysis (CASA) using SpermVision® (Minitube USA; Boulder, CO) with 200x negative phase contrast microscopy. Sample aliquots (200 µL; 30-50 M/mL) were placed on a warming plate (37°C) for 5 minutes and 3 µL was then loaded into Leja® chamber slides (Leja Products BV; Luzernestraat, The Netherlands) for motility assessment. For all samples, data were collected from 7 fields to determine average motility parameters. SpermVision® CASA Settings are listed in Table 2.1. Motility parameters assessed included summary measures, measures of distance, measures of velocity and measures of linearity. Summary measures included total motility (TM, %), progressive motility (PM, %), local motility (%), hyperactive (%), linear (%) and non-linear (%). Distance measures included distance curved line (DCL, µm), distance average path (DAP, µm) and distance straight line (DSL, µm). Velocity measures included velocity average path (VAP, µm/s), velocity curved line (VCL, µm/s), and velocity straight line (VSL, µm/s). Linearity measures included amplitude of lateral head displacement (ALH), beat cross frequency (BCF, Hz), straightness (STR), wobble (WOB) and linearity (LIN).

*Oxygen consumption and simultaneous motility assessment*

Measurement of oxygen consumption was performed using fluorescence plate reader technology and the OP96U OxoPlates® (PreSens Precision Sensing GmbH; Regensburg, Germany). With this technology, oxygen consumption is monitored by utilizing optical sensors

that are integrated into the bottom of each well. The sensor is a thin polymer film that contains two separate dyes: an indicator (platinum porphine) and a reference (sulforhodamine) dye[12]. The phosphorescence intensity of the indicator dye ($I_{indicator}$) is dependent on the oxygen content of the sample, while the fluorescence intensity of the reference dye ($I_{reference}$) is independent of the oxygen content. For internal referencing of the sensor response, these two signals are used to calculate a ratio, $I_R$ ($I_{indicator}/I_{reference}$), which corresponds to the oxygen partial pressure[13]. Measurements were taken using a Synergy™ H1 plate reader (BioTek; Winooski, VT), set in dual kinetic mode and using two filter pairs for the OxoPlate® read-out (filter pair 1, $I_{indicator}$: 540 nm Ex/ 650 nm Em; filter pair 2, $I_{reference}$ : 540 nm Ex/ 590 nm Em).

OxoPlates®, media, samples and treatments were prewarmed to 37°C prior to plating to minimize temperature-derived fluctuations in fluorescence. Prior to running experimental samples, titrations were performed to determine the number of viable cells per well necessary to produce a strong enough signal to overcome background noise, to determine the optimal concentration of all drug treatments for assessment of bovine sperm in this system, and to confirm that viability was not impacted by the optimal concentration identified (data not shown). Pilot experiments were also performed to confirm consistency in cell number requirements and signal generation between Oxoplates and Biosensor plates (BD Biosciences, San Jose, CA) (data not shown); BD Biosensor Plates have previously been demonstrated to be an accurate means for monitoring sperm mitochondrial oxygen consumption[6], but these plates have been discontinued by the manufacturer, making comprehensive comparison between the two modalities impossible. The coefficient of variation was confirmed to be <10% for Oxoplates ($I_R$). All sperm and treatment combinations were plated into 6 replicate wells. Wells containing only TALP medium were included as ambient negative controls. Two-point calibration was performed according to

Oxoplate® manufacturer recommendations[13] using oxygen-free water (cal 0) and air-saturated water (cal 100). Specifically, oxygen-free water (cal 0) was prepared with 0.2g of sodium sulfite ($Na_2SO_3$; a molecular oxygen scavenger) to 20 mL of pre-warmed $H_2O$, and air-saturated water (cal 100) was prepared by placing 20 mL of pre-warmed water into a 50 mL conical tube and shaking vigorously for 2 min, followed by slightly opening the tube and moving the liquid with a gentle swirling motion for 1 min to prevent oversaturation. Each well then received 300 μL of cal 0 (6 replicates), and the wells were immediately covered with adhesive foil and 200 μL of cal100 was plated into each replicate, leaving the wells uncovered. TALP media (100μL) was then plated in all wells designated for sperm samples or ambient controls. Next, 100μL of each sperm sample (70M viable cells/mL) was added into each allotted well, for a final total of 7M viable cells/well. Cal0 act as positive controls, since, since it eliminates molecular oxygen from the media. As a negative control, it was established during pilot experimentation established that dead sperm (flash frozen 2x in liquid nitrogen) did not generate a signal significantly different than ambient control background fluorescence.

An initial fluorescence reading was taken, and the plate was then placed in an incubator (37°C) for a 20 min equilibration period. After equilibration, another fluorescence reading was taken, and treatments were then immediately added to the wells. Antimycin A (ANTI, 1 μM), an inhibitor of electron transport chain complex III, was included to determine non-mitochondrial oxygen consumption. Oligomycin (OLIGO, 2 μM), an ATP synthase inhibitor (ETC complex V), was included to approximate the rate of ATP-linked respiration[14]. Carbonyl cyanide 4-(trifluoromethoxy)phenylhydrazone (FCCP, 1 μM), a mitochondrial uncoupler, was included for stimulation of maximal oxygen consumption and served as a positive control. For establishment of basal oxygen consumption, a vehicle control treatment (VC) DMSO and DPBS (final well 1%

DMSO, v/v) was applied. Fluorescence readings were taken for 60 minutes beginning immediately following treatment addition (t0), every 2 minutes for 10 minutes (t2, t4, t6, t8, t10), then every 5 minutes for 20 minutes (t15, t20, t25, t30), and lastly, every 10 minutes for an additional 30 minutes (t40, t50, t60). Plates were incubated at 37°C between measurements. While preparing the OxoPlates®, identical aliquots of all samples were prepared in microcentrifuge tubes for parallel motility assessment. Motility was assessed by CASA, as described above, 6 and 30 minutes after treatment addition (t6 and t30, respectively). Because preliminary experiments revealed all ejaculate oxygen consumption curves reached saturation levels within 30 minutes following FCCP treatment, motility was not assessed as t60 as evaluation with oxygen consumption data beyond that timepoint would not be as meaningful.

*Data processing and statistical analysis*

Processing of oxygen consumption data was performed according to manufacturer instructions[13]. The referenced signal $I_R$, as mentioned above, of each well was first calculated for each time point using the equation[13]:

$$I_R = I_{indicator} / I_{reference}$$

The calibration constants k100 and k0 were calculated by averaging the IR values for the wells containing cal100 and cal0, respectively. Oxygen concentration, as a percentage of air saturation ($pO_2$), was used as the oxygen consumption endpoint for all analyses. For each well and time point, $pO_2$ was then calculated with the following manufacturer provided equation:

$$pO_2 = 100 \times (k0/IR - 1)/(k0/k100 - 1)$$

Correlational statistical analysis was performed in JMP® (version 14.0.0; SAS Institute Inc., Cary, NC). Total ejaculate sperm numbers, morphology, $pO_2$ and motility parameters (t6 and t30) were assessed for normality using the Shapiro-Wilk test. To fit assumptions of

normality for analysis by Pearson's product-moment correlation, specified transformations were applied to the following parameters: local and nonlinear percentage data were transformed with arcsin of the square root. The morphological parameters PD and DH were excluded from analysis because normal distribution could not be achieved through transformation. A significance level of $p<0.05$ was used for all analyses.

All other statistical analyses were performed in R version 3.6.2 (R Core Team, 2019). Average $pO_2$ values of at each time point within each treatment were first computed and then subjected to generalized linear mixed effects modeling (GLMM) using a beta family with a logistic link function[1516], accounting for repeated measurements made on each bull. Further, overdispersion was modeled by incorporating an interaction between treatment and time in a dispersion model. Modeling the overdispersion was necessary due to overdispersion of residuals over time within the separate treatment conditions. GLMMs were also used to test for differences in average motility across treatment conditions and time points (t6 and t30), adjusting for repeated measurements made on samples from bulls. Sperm motility scores were then regressed on time and treatment condition in the GLMM described above.

## Results

### *Oxygen Concentration ($pO_2$)*

Oxygen concentration over time for each treatment condition is displayed in Figure 2.1. Overall, $pO_2$ differed over time between treatment conditions ($p<0.0001$). In the results that follow, all comparisons were Bonferroni-adjusted accounting for 130 comparisons. ANTI $pO_2$ levels were greater than vehicle across all time points after 6 minutes (all $p<0.05$, adjusted). OLIGO $pO_2$ levels were greater than vehicle across all time points (all $p<0.05$, adjusted). FCCP

and FCCP+OLIGO $pO_2$ levels were lower than vehicle across all time points (all $p<0.05$, adjusted), with the exception of the first time point for FCCP and the first and second time point for FCCP+OLIGO ($p > 0.05$). ANTI and OLIGO did not differ significantly across any time points (all $p>0.05$). FCCP+OLIGO $pO_2$ was significantly greater than FCCP alone for all time points after t10 (all $p<0.05$, adjusted).

*Motility*

Changes in motility parameters between timepoints did not differ significantly between treatments, so further analysis was performed pooling the values of the two timepoints. Adjusting for time of measurement (t=6 min or t=30 min), at least two treatment conditions differed in total motility ($p=0.001$), progressive motility ($p = 0.001$), hyperactivated motility ($p<0.0001$), linear motility ($p=0.005$), DCL ($p=0.0001$), DAP ($p<0.0001$), DSL ($p=0.0002$), VAP ($p<0.0001$), VCL ($p<0.0001$), VSL ($p=0.0001$), ALH ($p=0.007$), BCF ($p=0.005$), WOB ($p=0.001$), and LIN ($p=0.009$). No significant effects of treatment were observed for local motility ($p=0.07$), nonlinear ($p=0.08$), or STR ($p=0.152$). Inclusion of an interaction term between time and treatment condition did not reveal any differences in the effects of treatments over time (all $p>0.05$). In the results that follow, all tests are adjusted using Dunnett's method for comparing several treatment conditions to one control.

Motility parameters were only determined to differ significantly from the vehicle with ANTI treatment (Figures 2.2–2.5). Specifically, significant decreases in mean total motility (8.5 percentage units, $p=0.007$), progressive motility (10.0 percentage units, $p=0.01$), hyperactive (2.2 percentage units, $p=0.04$), linear (8.8 percentage units, $p=0.04$), DAP (4.5 μm, $p=0.01$), DSL (4.5 μm, $p=0.02$), VAP (10.4 μm/s, $p=0.01$), VSL (10.4 μm/s, $p=0.02$), WOB (0.04 units, $p=0.01$), and LIN (0.05 units, $p=0.04$) were identified. No significant evidence of treatment

effect was identified for local motile ($p$=0.07), non-linear ($p$=0.08) and STR ($p$=0.15). While no significant differences were found in DCL, VCL, ALH, or BCF measurements, several interesting trends were identified.

For DCL measurements, ANTI was trending at 4 μm lower ($p$=0.09) than vehicle, while FCCP was trending at 4.3 μm higher than vehicle ($p$=0.07). Average FCCP+OLIGO DCL was 0.9 μm smaller than vehicle but did not differ significantly ($p$=0.9), and DCL with OLIGO treatment was 0.4 μm higher than vehicle but also did not differ significantly ($p$=0.99). For VCL measurements, ANTI was trending with a mean VCL 9.7 μm/s smaller than vehicle ($p$=0.07) and FCCP was trending having a VCL 9.5 μm/s higher than vehicle ($p$=0.08). While no significant differences were identified in ALH measurements, FCCP was trending with a mean ALH 0.24 μm higher than vehicle ($p$=0.07). For BCF measurements, no significant differences were identified relative to vehicle, but ANTI was trending with a mean BCF 2.9 Hz smaller than vehicle ($p$=0.06).

*Correlational analysis*

Vehicle treatment correlational data is displayed in Table 2.2. For the vehicle treatment at t6, no significant correlations were identified between $pO_2$ and any motility parameters, morphology parameters or total sperm numbers. Several significant correlations were observed for $pO_2$ and motility parameters at t30. Specifically, mean $pO_2$ was negatively correlated with local motility(-0.8526, $p$=0.0071, transformed) and positively correlated with DCL (0.7396, $p$=0.0360), DAP (0.7136, $p$=0.0468), and VCL (0.7424, $p$=0.0349). Although not significant, it is worth noting that positive correlations between $pO_2$ and several other motility parameters were trending towards significance, including total motility (0.6368, $p$=0.0895), progressive motility (0.7065, $p$=0.0501), and VAP (0.6984, $p$=0.0540). No significant correlations were found between $pO_2$

and total sperm numbers or morphology. Interestingly, at t6 HS was positively correlated with Local Motile (0.7829, $p$=0.0216; transformed) and negatively correlated with Linear (-0.7127, $p$=0.0472) and BCF (-0.7353, $p$=0.0376), and at t30 MN was negatively correlated with ALH (-0.7170, $p$=0.0453) (data not shown).

**Discussion**

This study aimed to simultaneously evaluate bull sperm mitochondrial function and motility parameters to investigate the role of mitochondrial function in the regulation and maintenance of bovine sperm motility. As expected, bull sperm oxygen consumption was significantly increased by FCCP treatment and decreased with both ANTI and OLIGO treatment. However, significant differences in motility parameters compared to the vehicle treatment were only identified with ANTI treatment, for which many parameters, including total and progressive motility, were reduced. This is particularly interesting because both ANTI and OLIGO effectively eliminated oxygen consumption and did not significantly differ from each other at any timepoints, yet no significant motility deficits were observed with OLIGO treatment. This suggests that the motility deficits observed with ANTI treatment are not attributable to diminished ATP supply, but instead originate from some other mechanism. One possible explanation for this is a disruption in cellular REDOX balance, since ANTI is known to increase ROS production in numerous cell types, including sperm, which may lead to cellular damage and motility deficits[17–19]. Further studies incorporating both ROS assessment and intracellular ATP quantification could aid in elucidating the mechanism underlying the significant motility deficits present with ANTI but not OLIGO treatment.

The significant motility deficits observed in this study with ANTI treatment are in disagreement with studies by Krzyzosiak and colleagues (1999) and Hammerstedt and colleagues (1988) which reported that ETC inhibition with a combined treatment of Antimycin A (4 μM) and rotenone (4 μM; ETC complex I inhibitor) did not significantly impact fresh bull sperm motility [1,20]. Several factors warrant consideration when comparing results from those studies to ours. In addition to not investigating treatment of antimycin as a solitary agent in those studies, the treatment concentrations used in both studies was also four-fold higher than the concentration we found to be optimal (1μM) through titration in development of our specific experimental design.

In contrast, our results are in partial agreement with the more recent study by Magdanz and colleagues (2019), which found higher mitochondrial and metabolic function in the top fraction of swim-up preparation compared to fractions with lower total motility[2]. Notably, Magdanz and colleagues (2019) also used an SP-TALP medium formulation, though their formulation included gentamycin and provided pyruvate as a sole substrate, in contrast to our SP-TALP medium formulation, which excluded antibiotics and included a variety of substrates, including glucose, to provide the sperm cells with the metabolic pathway option for anaerobic production of ATP through glycolysis in the presence of mitochondrial oxidative phosphorylation inhibitors. While our findings also implicate mitochondrial function as a participant in bovine sperm motility regulation, the entirety of our findings do not align completely with those of Magdanz and colleagues (2019). We did not identify a significant positive correlation between total and progressive motility and oxygen consumption, which was expected based on Magdanz and colleagues' (2019) findings. One possible explanation for this discrepancy is that our SP-TALP formulation provided glucose as an alternative substrate, in

contrast to the SP-TALP medium formulation of Magdanz and colleagues (2019), which provided pyruvate as a sole substrate. Additionally, we did observe that both total and progressive motility trended towards significance at t30, suggesting that significance could be determined by increasing the incubation time and sample size. As with any metabolic research, it is important to compare these studies cautiously; discrepancies in findings could be attributable to numerous experimental factors, including differences in medium composition and semen processing. Ultimately, the results from our study and those of Magdanz and colleagues (2019) implicate a role for mitochondrial functionality as a player in bovine sperm motility regulation, and future studies should be carried out to determine the mechanistic aspects of this relationship.

Although no significant differences between FCCP treatment and the vehicle were identified, it was surprising to find trends of FCCP increasing several motility parameters. One possible explanation for this is that FCCP treatment disrupted the cellular NAD balance, indirectly stimulating glycolysis, but further experimentation is necessary to test this hypothesis.

Another potential underlying mechanism for the impact of mitochondrial drug treatments on bovine sperm motility is perturbation of intracellular $Ca^{2+}$ regulation and signaling. Mitochondria of somatic cells are extensively involved in intracellular $Ca^{2+}$ signaling and regulation[21]. There is evidence that inhibition of mitochondrial $Ca^{2+}$ uptake detrimentally impacts capacitation, but not motility, in cryopreserved bovine sperm [22]. However, this mechanism requires further investigation, particularly since published studies regarding mitochondrial $Ca^{2+}$ uptake in sperm fail to provide adequate evidence of validation and concentration selection of the used inhibitors for mitochondrial $Ca^{2+}$ uptake[22,23]. Additionally, in studies of somatic cells, it has become increasingly evident that mitochondrial $Ca^{2+}$ functions are highly dependent on the close anatomic relationship and associated membranes with the

endoplasmic reticulum[24]. Because mature sperm are widely accepted to lack an endoplasmic reticulum[25], this leaves many unanswered questions regarding the basic physiology and function of mammalian sperm mitochondria when compared to somatic cells. Further studies elucidating the functions and mechanisms of basic sperm mitochondrial $Ca^{2+}$ regulation and signaling are necessary. It is possible those studies could shed light on the mechanisms underlying the impact of mitochondrial perturbation on sperm motility. Future studies investigating mitochondrial membrane potential changes correlating with oxygen consumption under mitochondrial effector treatments could provide valuable mechanistic insight; this would be particularly interesting in combination with intracellular $Ca^{2+}$ studies, as mitochondrial membrane potential is known to be the driving force for $Ca^{2+}$ accumulation in somatic mitochondria[21].

Sperm motility is considered an important indicator of sperm quality and fertility in many mammalian species, including bovine, though much of the existing bovine research has been performed with frozen-thawed semen. This is an important consideration because cryopreservation is known to cause cellular damage altering sperm function and metabolism[6]. Farrell and colleagues (1998) found several different combinations of motility parameters highly correlated with fertility in fresh bull semen, and BCF, LIN, and VSL were motility parameters with the highest correlation to fertility[26]. In this study, we found both LIN and VSL were significantly reduced with inhibition of ETC function through ANTI treatment. It would be beneficial to further investigate the relationship between sperm mitochondrial functionality, motility and bull fertility in future studies. Existing literature on bovine sperm mitochondrial function primarily use mitochondrial membrane potential probes, most commonly JC-1, as an assessment of mitochondrial function. However, these probes have several limitations and the capability of providing accurate results, particularly if the correct controls are not applied. In this

study, we demonstrate the effectiveness of a new method for real-time assessment of bovine sperm mitochondrial function, which provides a valuable tool for future research. An additional benefit of this method for sperm assessment is that it is performed using a fluorescence plate reader, making it more accessible to research than alternative methods, which require much more expensive and specialized equipment, such as extracellular flux analyzers.

## Conclusions

A fluorescence-based microplate modality is a repeatable and reliable assessment of mitochondrial oxygen consumption in motile, freely moving bovine sperm. This modality is an exciting new approach to investigate mechanics and metabolism underlying bovine sperm motility. Pharmacological disruption of electron transport chain function significantly effects motility parameters of fresh bovine sperm collected by electroejaculation; notably, motility deficits were observed with ANTI treatment (inhibitor of electron transport chain complex III). No significant motility deficits were observed when OLIGO was used to inhibit ATP synthase, so the motility deficits observed with ANTI may be attributable to cellular mechanisms for motility regulation beyond mitochondrial ETC ATP production, such as ROS generation. Future studies are warranted to further investigate the pathophysiologic mechanism underlying these observations.

## Acknowledgements

The authors thank CFAH for funding support of this study (grant CALV-AH-387). The authors also wish to thank Dr. Pamela Lein and Mr. Donald Bruun, Department of Molecular Biosciences, School of Veterinary Medicine, University of California, Davis CA for technical and methodological assistance for this study.

**Tables and Figures**

| Settings Category | Parameter | Settings |
|---|---|---|
| General | Field of view depth | 20 µm |
| | Pixel to µm ratio | 130 to 100 |
| | Cell identification area | 22 to 60 $\mu m^2$ |
| | Assessment requirements | 5000 cells or 7 fields |
| | Additional particle filtering | None |
| | Light threshold | Min. 180, max. 255 |
| | Points to use in cell path smoothing | 11 |
| Level 1 Cell Classifications | Immotile | AOC < 5 |
| | Local | DSL < 4.5 |
| Level 2 Cell Classifications* | Hyperactive | VCL > 80<br>LIN < 0.65<br>ALH > 6.5 |
| | Linear | STR > 0.5<br>LIN > 0.35 |
| | Nonlinear | STR < 0.5<br>LIN < 0.35 |

**Table 2.1:** ***Technical settings used for SpermVision® (Minitube USA; Boulder, CO).*** CASA system technical settings used for assessment and quantification of motility parameters are displayed. Manufacturer recommended bovine motility settings were used. *Progressive motile selected as cells to check.

| Motility Parameter | Timepoint | | | | | |
|---|---|---|---|---|---|---|
| | T6 | | | T30 | | |
| | Mean ± SD | Correlation with pO2 | p-value | Mean ± SD | Correlation with pO2 | p-value |
| Total Motility | 64.66 ± 15.11 | -0.1000 | 0.8137 | 67.82 ± 11.425 | 0.6368 | 0.0895 |
| Progressive Motility | 57.115 ± 19.87 | -0.1579 | 0.7088 | 59.413 ± 13.20 | 0.7065 | 0.0501 |
| Local Motile[a] | 0.2597 ± 0.1132 | 0.2832 | 0.4967 | 0.2917 ± 0.0435 | -0.8526 | 0.0071* |
| Hyperactive | 5.60 ± 3.70 | -0.1725 | 0.683 | 5.685 ± 1.916 | 0.6831 | 0.0618 |
| Linear | 43.02 ± 20.607 | -0.3006 | 0.4694 | 42.89 ± 12.47 | 0.6894 | 0.0586 |
| Non-Linear[a] | 0.1528 ± 0.0665 | 0.4613 | 0.2499 | | -0.2236 | 0.5945 |
| DCL | 49.75 ± 9.16 | -0.3179 | 0.4429 | 50.30 ± 6.23 | 0.7396 | 0.0360* |
| DAP | 31.22 ± 8.32 | -0.3885 | 0.3416 | 31.094 ± 4.84 | 0.7136 | 0.0468* |
| DSL | 26.44 ± 8.87 | -0.4442 | 0.3056 | 26.34 ± 4.97 | 0.6805 | 0.0633 |

| | | | | | | |
|---|---|---|---|---|---|---|
| VAP | 69.48 ± 18.33 | -0.1213 | 0.292 | 69.335 ± 10.49 | 0.6984 | 0.054 |
| VCL | 110.37 ± 20.41 | -0.3763 | 0.3583 | 111.61 ± 13.03 | 0.7424 | 0.0349* |
| VSL | 58.895 ± 19.56 | -0.4442 | 0.2702 | 58.84 ± 10.91 | 0.6628 | 0.0733 |
| ALH | 3.70 ± 0.42 | -0.1213 | 0.7748 | 3.89 ± 0.245± | 0.1798 | 0.6701 |
| BCF | 30.196 ± 7.09 | -0.3782 | 0.3556 | 29.12 ± 3.04 | 0.6639 | 0.0726 |
| STR | 0.826 ± 0.085 | -0.4612 | 0.25 | 0.84 ± 0.04 | 0.369 | 0.3683 |
| WOB | 0.616 ± 0.072 | -0.4258 | 0.2928 | 0.62 ± 0.05 | 0.2726 | 0.5137 |
| LIN | 0.5157 ± 0.109 | -0.4438 | 0.2707 | 0.52 ± 0.06 | 0.3462 | 0.4009 |
| % Normal Morphology | 89.875 ± 4.086 | 0.5192 | 0.1873 | - | 0.1474 | 0.7277 |
| %MP | 6.25 ± 3.576 | -0.5583 | 0.1504 | - | -0.2645 | 0.5268 |
| %HS | 2.65 ± 1.598 | -0.1531 | 0.7174 | - | -0.1537 | 0.7162 |

| | | | | | | |
|---|---|---|---|---|---|---|
| Total Sperm Numbers | 3148 ± 889.3 | 0.1585 | 0.7077 | - | -0.4039 | 0.3211 |

[a]Transformed transformed Mean ± SD displayed and used for correlational analysis.

[*] $p < 0.05$.

**Table 2.2.** ***Pearson's correlation of $pO_2$ with motility and sperm quality measures.***

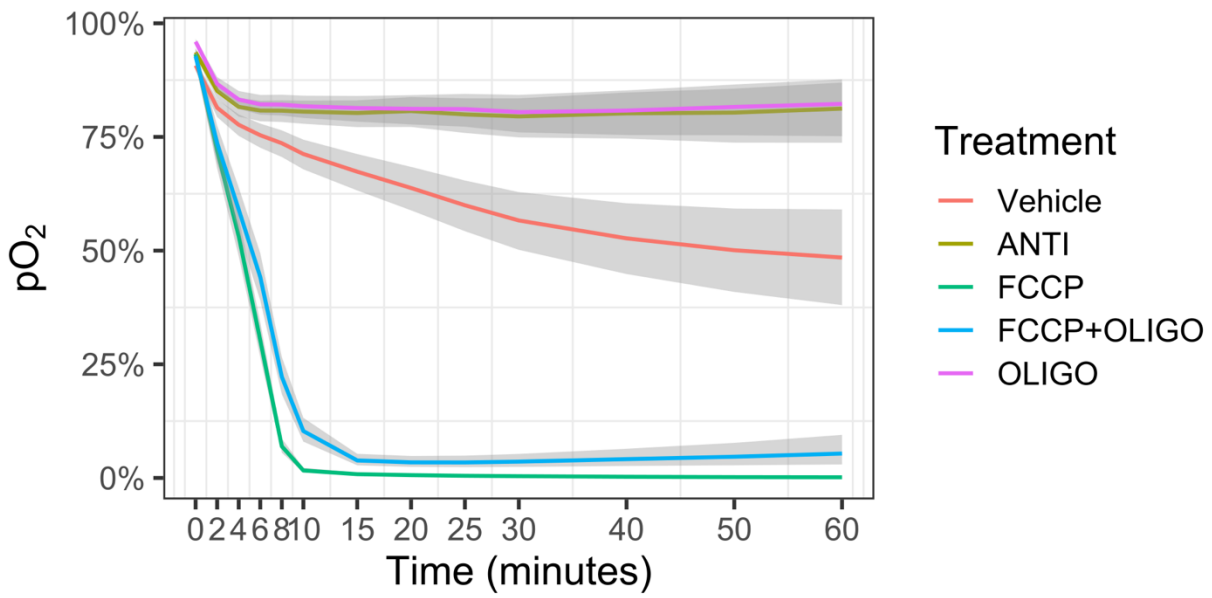


**Fig. 2.1.** ***Average oxygen concentration ($pO_2$) over time in bull sperm across treatment conditions.*** Bull sperm were plated (7M viable/well) into OP96U OxoPlates® with five replicate wells per treatment. Following a 20 min equilibration period at 37°C, treatments of vehicle, ANTI, FCCP, FCCP+OLIGO and OLIGO were applied and repeated fluorescence measurements were taken over 60 min for calculation of well oxygen concentration, as $pO_2$ (% air saturation), according to manufacturer instructions. Bold lines represent the fitted marginal mean pO2 within each treatment condition from mixed effects modeling. Grey shaded areas are 95% confidence intervals. $P<0.05$, N= 260 total observations from 4 bulls.

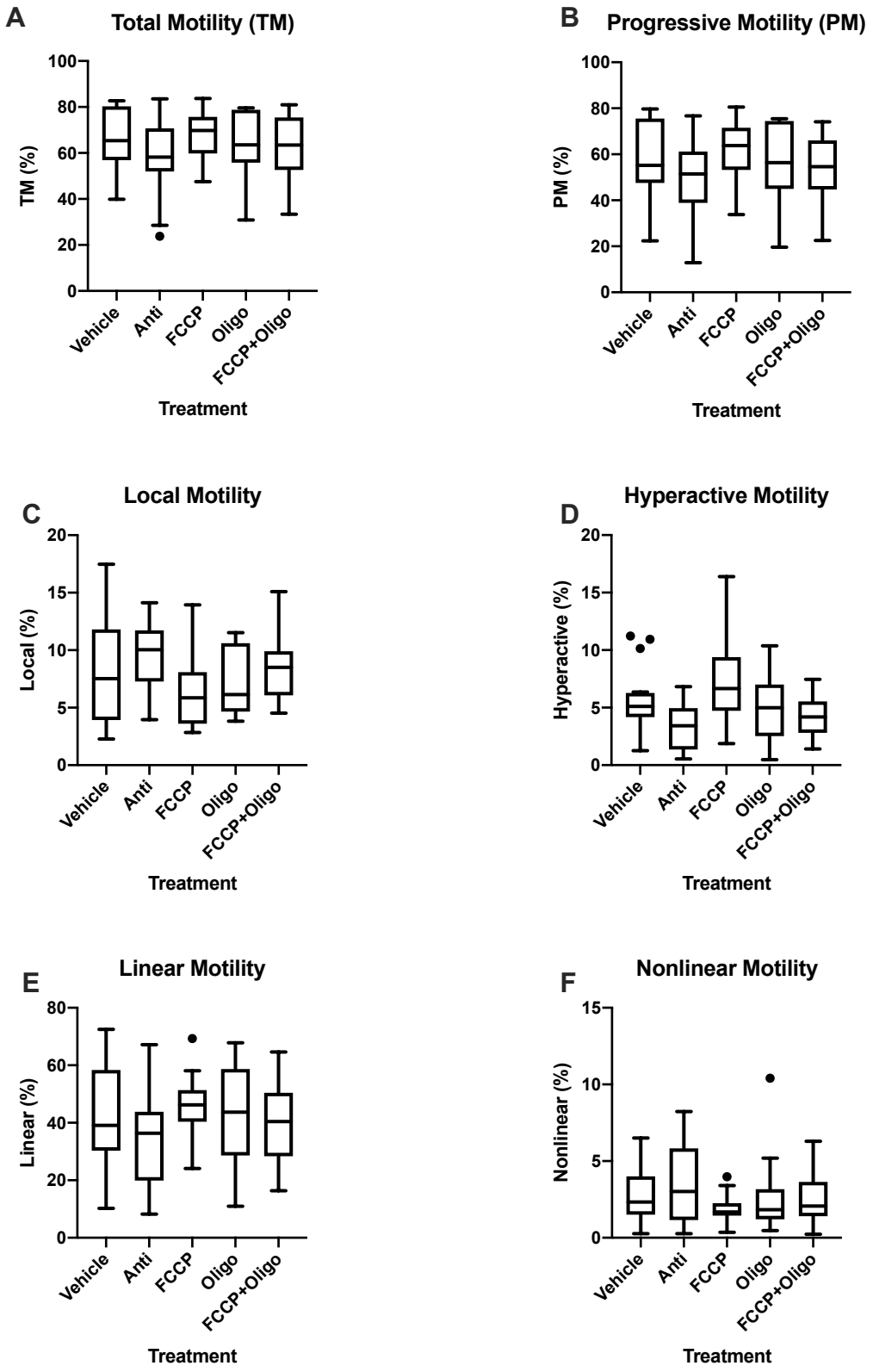
A
Total Motility (TM)
TM (%)
100
80
60
40
20
0
Vehicle
Anti
FCCP
Oligo
FCCP+Oligo
Treatment
B
Progressive Motility (PM)
PM (%)
100
80
60
40
20
0
Vehicle
Anti
FCCP
Oligo
FCCP+Oligo
Treatment
C
Local Motility
Local (%)
20
15
10
5
0
Vehicle
Anti
FCCP
Oligo
FCCP+Oligo
Treatment
D
Hyperactive Motility
Hyperactive (%)
20
15
10
5
0
Vehicle
Anti
FCCP
Oligo
FCCP+Oligo
Treatment
E
Linear Motility
Linear (%)
80
60
40
20
0
Vehicle
Anti
FCCP
Oligo
FCCP+Oligo
Treatment
F
Nonlinear Motility
Nonlinear (%)
15
10
5
0
Vehicle
Anti
FCCP
Oligo
FCCP+Oligo
Treatment

**Fig. 2.2.** ***Summarized motility parameters in the presence of mitochondrial effector treatments.*** Sperm motility parameters were quantified by computer-assisted sperm analysis (CASA) 6 and 30 min (t6 and t30, pooled) post-treatment addition. Tukey box and whisker plots of averaged time points are displayed. (A) Total Motility (TM, %), (B) Progressive motility (PM, %), (C) Local Motility (%), (D) Hyperactive Motility (%), (E) Linear Motility (%), and (F) Nonlinear Motility (%). N=8.

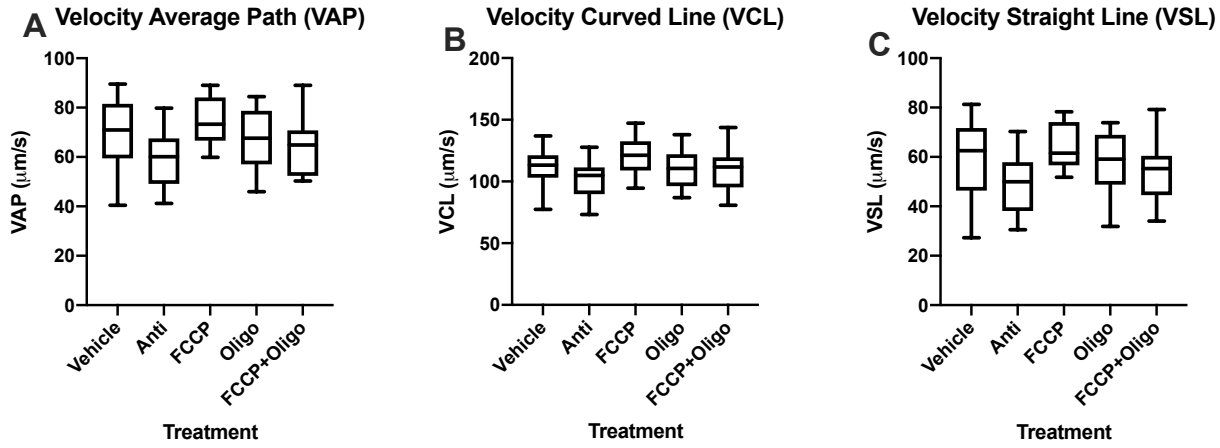


**Fig. 2.3.** ***Velocity measures of motility in the presence of mitochondrial effector treatments*****.** Sperm motility parameters were quantified by computer-assisted sperm analysis (CASA) 6 and 30 min (t6 and t30, pooled) post-treatment addition. Tukey box and whisker plots of averaged time points are displayed. (A) Velocity Average Path (VAP, μm/s), (B) Velocity Curbed Line (VCL, μm/s), and (C) Velocity Straight Line (VSL, μm/s). N=8.

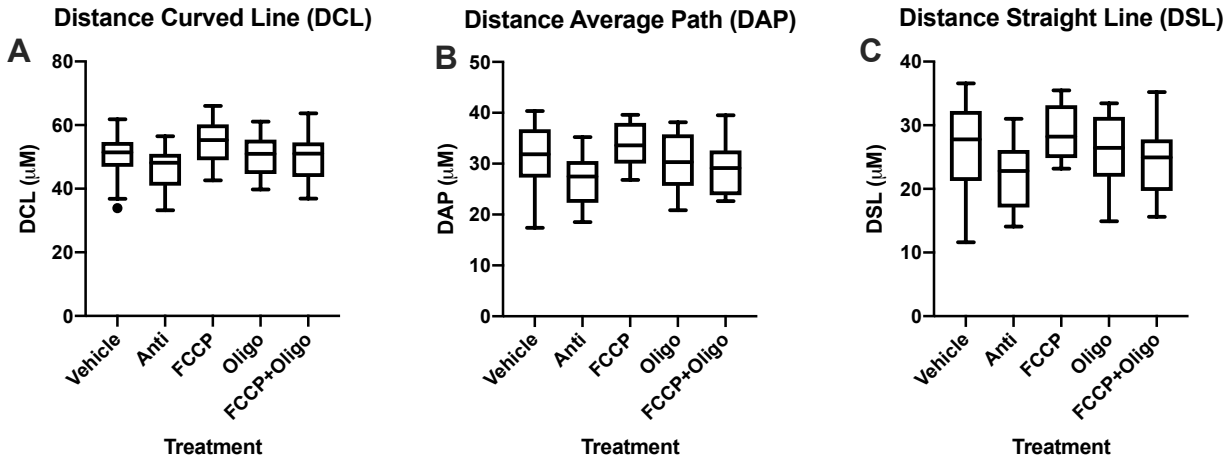


**Fig. 2.4.** ***Distance measures of motility in the presence of mitochondrial effector treatments.*** Sperm motility parameters were quantified by computer-assisted sperm analysis (CASA) 6 and 30 min (t6 and t30, pooled) post-treatment addition. Tukey box and whisker plots of averaged time points are displayed. (A) Distance Curved Line (DCL, μm), (B) Distance Average Path (DAP, μm), (C) Distance Straight Line (DSL, μm). N=8.

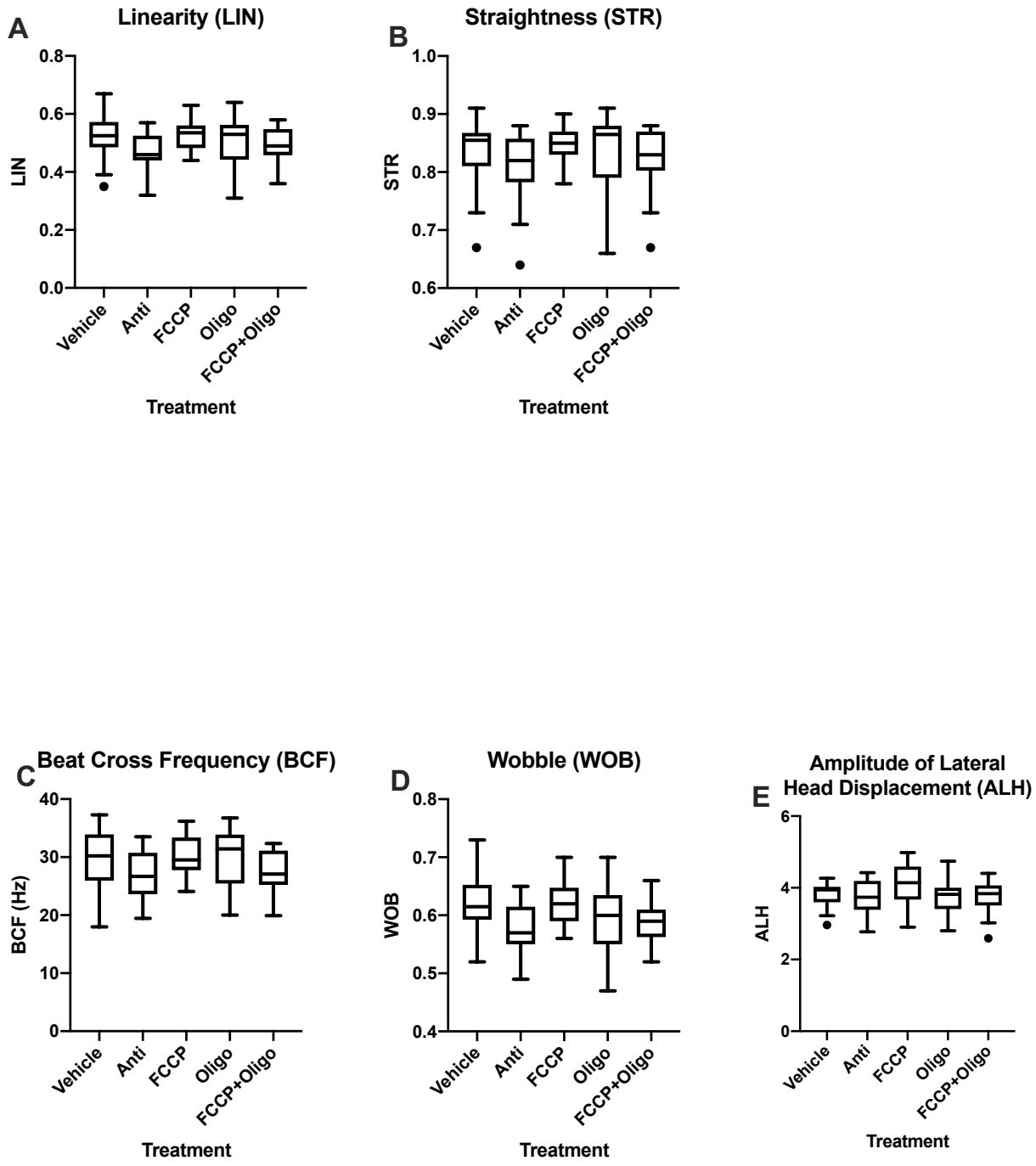


**Fig. 2.5.** ***Linearity measures of motility in the presence of mitochondrial effector treatments.***

Sperm motility parameters were quantified by computer-assisted sperm analysis (CASA) 6 and 30 min (t6 and t30, pooled) post-treatment addition. Tukey box and whisker plots of averaged time points are displayed. (A) Linearity (LIN), (B) Straightness (STR), (C) Beat Cross

Frequency (BCF), (D) Wobble (WOB) and (E) Amplitude of Lateral Head Displacement (ALH). N=8.

**References**


1. Krzyzosiak J, Molan P, Vishwanath R. Measurements of bovine sperm velocities under true anaerobic and aerobic conditions. *Anim Reprod Sci*. 1999;55(3-4):163-173. doi:10.1016/s0378-4320(99)00016-0
2. Magdanz V, Boryshpolets S, Ridzewski C, Eckel B, Reinhardt K. The motility-based swim-up technique separates bull sperm based on differences in metabolic rates and tail length. Kues WA, ed. *PLoS One*. 2019;14(10):e0223576. doi:10.1371/journal.pone.0223576
3. du Plessis S, Agarwal A, Mohanty G, van der Linde M. Oxidative phosphorylation versus glycolysis: what fuel do spermatozoa use? *Asian J Androl*. 2015;17(2):230. doi:10.4103/1008-682X.135123
4. Rich PR, Maréchal A. The mitochondrial respiratory chain. *Essays Biochem*. 2010;47:1-23. doi:10.1042/bse0470001
5. Rizzuto R, De Stefani D, Raffaello A, Mammucari C. Mitochondria as sensors and regulators of calcium signalling. *Nat Rev Mol Cell Biol*. 2012;13(9):566-578. doi:10.1038/nrm3412
6. Darr CR, Cortopassi GA, Datta S, Varner DD, Meyers SA. Mitochondrial oxygen consumption is a unique indicator of stallion spermatozoal health and varies with cryopreservation media. *Theriogenology*. 2016;86(5):1382-1392. doi:10.1016/j.theriogenology.2016.04.082
7. Nascimento JM, Shi LZ, Tam J, Chandsawangbhuwana C, Durrant B, Botvinick EL, Berns MW. Comparison of glycolysis and oxidative phosphorylation as energy sources for mammalian sperm motility, using the combination of fluorescence imaging, laser

tweezers, and real-time automated tracking and trapping. *J Cell Physiol*. 2008;217(3):745-751. doi:10.1002/jcp.21549

8. Hutson SM, Van Dop C, Lardy HA. Mitochondrial metabolism of pyruvate in bovine spermatozoa. *J Biol Chem*. 1977;252(4):1309-1315. http://www.ncbi.nlm.nih.gov/pubmed/838719

9. Bavister BD, Yanagimachi R. The Effects of Sperm Extracts and Energy Sources on the Motility and Acrosome Reaction of Hamster Spermatozoa in vitro. *Biol Reprod*. 1977;16(2):228-237. doi:10.1095/biolreprod16.2.228

10. Parrish JJ, Susko-Parrish JL, First NL. Capacitation of Bovine Sperm by Heparin: Inhibitory Effect of Glucose and Role of Intracellular pH1. *Biol Reprod*. 1989;41(4):683-699. doi:10.1095/biolreprod41.4.683

11. Parrish JJ. Bovine in vitro fertilization: In vitro oocyte maturation and sperm capacitation with heparin. *Theriogenology*. 2014;81(1):67-73. doi:10.1016/j.theriogenology.2013.08.005

12. Cook CC, Kim A, Terao S, Gotoh A, Higuchi M. Consumption of oxygen: A mitochondrial-generated progression signal of advanced cancer. *Cell Death Dis*. 2012;3(1):e258-12. doi:10.1038/cddis.2011.141

13. PreSens Precision Sensing GmbH. *OxoPlates ® Instruction Manual*.; 2016.

14. Divakaruni AS, Paradyse A, Ferrick DA, Murphy AN, Jastroch M. Analysis and interpretation of microplate-based oxygen consumption and pH data. In: *Methods in Enzymology*. Vol 547. 1st ed. Elsevier Inc.; 2014:275-307. doi:10.1016/B978-0-12-801415-8.00016-3

15. Brooks, Mollie E, Kristensen K, Benthem, Koen, J. V, Magnusson A, Berg, Casper W,

Nielsen A, Skaug, Hans J, Mächler M, Bolker, Benjamin M. glmmTMB Balances Speed and Flexibility Among Packages for Zero-inflated Generalized Linear Mixed Modeling. *R J*. 2017;9(2):378. doi:10.32614/RJ-2017-066

16. Bates D, Mächler M, Bolker B, Walker S. Fitting Linear Mixed-Effects Models Using lme4. *J Stat Softw*. 2015;67(1). doi:10.18637/jss.v067.i01

17. Aitken RJ, Jones KT, Robertson SA. Reactive oxygen species and sperm function-in sickness and in health. *J Androl*. 2012;33(6):1096-1106. doi:10.2164/jandrol.112.016535

18. Darr CR, Varner DD, Teague S, Cortopassi GA, Datta S, Meyers SA. Lactate and Pyruvate Are Major Sources of Energy for Stallion Sperm with Dose Effects on Mitochondrial Function, Motility, and ROS Production. *Biol Reprod*. 2016;95(2):34-34. doi:10.1095/biolreprod.116.140707

19. Baumber J, Ball BA, Gravance CG, Medina V, Davies-Morel MCG. The effect of reactive oxygen species on equine sperm motility, viability, acrosomal integrity, mitochondrial membrane potential, and membrane lipid peroxidation. *J Androl*. 2000;21(6):895-902. doi:10.1002/j.1939-4640.2000.tb03420.x

20. Hammerstedt RH, Volonté C, Racker E. Motility, heat, and lactate production in ejaculated bovine sperm. *Arch Biochem Biophys*. 1988;266(1):111-123. doi:10.1016/0003-9861(88)90241-X

21. Bravo-Sagua R, Parra V, López-Crisosto C, Díaz P, Quest AFG, Lavandero S. Calcium transport and signaling in mitochondria. *Compr Physiol*. 2017;7(2):623-634. doi:10.1002/cphy.c160013

22. Rodriguez PC, Satorre MM, Beconi MT. Effect of two intracellular calcium modulators on sperm motility and heparin-induced capacitation in cryopreserved bovine spermatozoa.

*Anim Reprod Sci*. 2012;131(3-4):135-142. doi:10.1016/j.anireprosci.2012.03.015

23. Bravo A, Treulen F, Uribe P, Boguen R, Felmer R, Villegas J V. Effect of mitochondrial calcium uniporter blocking on human spermatozoa. *Andrologia*. 2015;47(6):662-668. doi:10.1111/and.12314

24. Patergnani S, Suski JM, Agnoletto C, Bononi A, Bonora M, De Marchi E, Giorgi C, Marchi S, Missiroli S, Poletti F, Rimessi A, Duszynski J, Wieckowski MR, Pinton P. Calcium signaling around Mitochondria Associated Membranes (MAMs). *Cell Commun Signal*. 2011;9(1):19. doi:10.1186/1478-811X-9-19

25. Varner DD, Johnson L, Green EM. From a sperm's eye view-revisiting our perception of this intriguing cell. *Proc Annu Conv AAEP - Orlando, Florida, 2007*. 2007;53:104-177. http://www.cabdirect.org/abstracts/20083097814.html

26. Farrell PB, Presicce GA, Brockett CC, Foote RH. Quantification of bull sperm characteristics measured by computer-assisted sperm analysis (CASA) and the relationship to fertility. *Theriogenology*. 1998;49(4):871-879. doi:10.1016/s0093-691x(98)00036-3

# Chapter 3: Imaging Flow Cytometry to Characterize the Relationship Between Abnormal Sperm Morphologies and Reactive Oxygen Species (ROS) in Stallion Sperm

Evelyn Bulkeley[1], Anthony C. Santistevan[2], Sheila Teague[3], Dickson Varner[3], Stuart Meyers[1]

[1]Department of Anatomy, Physiology, and Cell Biology, School of Veterinary Medicine, [2] Department of Psychology, College of Letters and Sciences, University of California, Davis, [3]Department of Large Animal Clinical Sciences, College of Veterinary Medicine, Texas A&M University, College Station, TX

**Abstract**

Low levels of intracellular reactive oxygen species (ROS) are essential for normal sperm function and are produced by sperm mitochondria as a byproduct of metabolism, but in excess, ROS can cause catastrophic cellular damage and has been correlated with infertility, poor sperm motility and abnormal morphology in humans[1]. Stallion sperm motility is fueled predominantly by oxidative phosphorylation-produced ATP, requiring high basal rates of mitochondrial function[2,3]. Consequently, whether elevated ROS production by stallion sperm is an indicator of dysfunctional or highly motile cells has been debated by researchers over the last decade. The objective of this study was to evaluate the relationship between various sperm morphologies and ROS production in fresh and cooled stallion semen by employing the novel method of imaging flow cytometry for stallion semen assessment. For evaluation of fresh semen, single ejaculates (n=5) were collected from four resident stallions at the University of California, Davis. For the evaluation of 24-hour cool-stored semen, single ejaculates were collected from stallions at Texas A&M University (n=5) and shipped to the University of California, Davis overnight for evaluation. Ejaculate volume, sperm concentration and motility parameters were recorded. Samples were co-stained for viability and ROS detection with SytoxGreen™ and dihydroethidium (DHE), respectively, and evaluated with the Amnis® ImageStream® system (Luminex Corporation, Austin, TX). Antimycin, an electron transport chain inhibitor that triggers ROS production (1μM), was used as a positive control for DHE, while dead cells (2x snap frozen in liquid nitrogen) served as a positive control for SytoxGreen™. Unstained samples were also evaluated as controls. Imaging flow cytometric analysis was performed with the IDEAS® software (Luminex Corporation, Austin, TX). Evaluated morphologies included abnormal head (AH), abnormal midpiece (AM), abnormal tail (AT), proximal cytoplasmic

droplet (PD), or distal cytoplasmic droplet (DD), and morphologically normal (MN) cells. For fresh semen, an additional abnormality, coiled tail and midpiece (CTM) was assessed; 24-hour cool-stored semen did not contain enough viable CTM cells for analysis. Only cells with obvious, single abnormalities were selected for the first portion of analysis to minimize subjectivity. Mixed effects modelling was used to evaluate the relationship between each morphologic classification and the corresponding DHE fluorescence intensity. Compared to the MN population, ROS production was significantly higher in viable cells with AH, PD and AM ($p< 0.0001$) in both fresh and cooled semen. CTM cells had significantly higher levels of ROS production compared to MN cells in fresh semen ($p<0.0001$). There was no significant difference in ROS levels between MN cells and AT and DD cells in either fresh or cooled semen ($p>0.05$). These results suggest that ROS generation is indicative of abnormal cell morphology and function and confirm that imaging flow cytometry is a valuable tool for the assessment of stallion semen.

## Introduction

During normal mitochondrial metabolism, a small number of electrons leak from electron transport chain (ETC) complexes I and III and react with oxygen, resulting in the formation of reactive oxygen species (ROS)[4,5]. It is well-established that ROS have paradoxical effects on male fertility and sperm function[6,7]. While low levels of ROS are essential for intracellular signaling and initiation of fertilization events, excessive ROS production can overwhelm antioxidant defenses and cause catastrophic oxidative damage to cellular structures and DNA[8,9]. Further, due to a high content of polyunsaturated fatty acids in cellular and mitochondrial membranes, sperm are more sensitive to oxidative stress than most somatic cells[9]. It is not surprising that elevated ROS levels have been linked to decreased sperm quality and increased morphologic abnormalities and are suspected to play a role in over 50% of idiopathic male infertilities[1].

Despite being widely accepted as a negative indicator of sperm health in most species, the implications of increased ROS in stallion sperm have been highly debated[10]. Stallion sperm motility is fueled almost exclusively by mitochondrial-produced ATP, in contrast to other studied species, which primarily use glycolytic pathways to produce ATP[11,12]. Because increased mitochondrial function and ETC electron flow results in increased passive electron leakage, increases in ROS production and oxidative stress accompany increases in mitochondrial activity. In light of this, it has been proposed that stallion sperm generating high levels of ROS are not defective, but actually the highly motile, more robust sperm, and that biomarkers of oxidative stress are a positive indicator of stallion fertility[6,13]. It is worth noting that this conclusion is not consistent with current mitochondrial ROS production theory, which indicates mitochondrial ROS production is greatest when mitochondria have abundant substrate but low respiration and

high membrane potential, indicating that very active mitochondria should have lower ROS production. Additionally, the theory of highly motile, more robust sperm generating high levels of ROS has been challenged by studies in stallion sperm correlating increased ROS with decreased motility, viability, and mitochondrial function[8,9]. Ejaculate ROS levels can be quantified with fluorescence staining and flow cytometry, which makes ROS evaluation a promising prospective addition to diagnostic semen evaluation for stallion infertility if it can be definitively established as a positive or negative biomarker of stallion sperm function. In stallions, a positive correlation has been observed between pregnancy rates and the percent of morphologically normal sperm, and a negative correlation between pregnancy rates and midpiece or tail abnormalities[14,15]. Human sperm ROS production has been positively correlated with abnormal sperm morphology, including abnormal heads, cytoplasmic droplets, midpiece, and tail abnormalities[1,16]. If morphologic abnormalities are correlated with elevated ROS levels in stallion sperm, it will strongly implicate ROS as a negative biomarker of sperm function and fertility in stallions.

In this study, we aimed to determine the relationship between stallion sperm morphology and ROS generation in viable sperm from both fresh and 24-hour cooled semen. This was accomplished using the Amnis® ImageStream® imaging flow cytometer that is capable of simultaneous imaging of multiple fluorophores and brightfield images of single sperm. We hypothesized that increased ROS production will be associated with morphologic abnormalities in living sperm, and that abnormal heads, midpieces, tails, and cytoplasmic droplets have significantly higher ROS production than morphologically normal sperm in both fresh and cooled semen.

## Materials and Methods

*Chemicals and reagents*

All chemicals were purchased from Sigma-Aldrich (Saint Louis, MO, USA) unless otherwise stated. For semen dilution immediately following collection, INRA 96 semen extender (IMV Technologies, Brooklyn Park, MN) was used. For experimental assessment, a modified Biggers, Whitten, and Whittingham (BWW) media was used for semen dilution[2]. This medium consisted of 89.83 mM NaCl, 4.78 mM KCl, 1.19 mM $MgSO_4 \cdot 7H_2O$, 1.19 mM $KH_2PO_4$, 1.7 mM $CaCl_2 \cdot 2H_2O$, 21 mM HEPES buffer, 4 mM sodium bicarbonate, 5.55 mM glucose, 0.25 mM sodium pyruvate, 11%(v/v) DL-Lactic acid syrup, 1% penicillin/streptomycin and 0.1% PVA.

*Semen collection and processing*

All stallions were maintained on a diet of mixed grass hay and grain, with fresh water *ad libitum* and daily exercise according to Institutional Animal Care and Use Committee protocols of the University of California, Davis and Texas A&M University.

For experiment 1, assessment of fresh semen, ejaculates (n=5) were collected using a Missouri model artificial vagina from four light breed stallions at the UC Davis Center for Equine Health and Animal Science Horse Barn according to Institutional Animal Care and Use Committee protocols. An inline nylon micromesh filter (Animal Reproduction Systems, Chino, CA) was used to remove the gel fraction of the ejaculate. Immediately after collection, a NucleoCounter SP-100 (ChemoMetec A/S, Allerød, Denmark) was used to determine the gel-free sperm concentration. The semen was then washed and resuspended with pre-warmed (37°C) BWW media to a concentration of $10x10^6$ cells/mL.

For experiment 2, assessment of 24-hour cooled semen, single ejaculates were collected from stallions (n=5) at Texas A&M University. Samples were extended 1:2 in INRA96, placed in cooled storage, and transported overnight using an Equitainer I (Hamilton BioVet, Ipswich, MA) at 4-8°C to the University of California, Davis for further experimental processing and analysis.

*Computer-assisted sperm analysis (CASA) Motility*

Computer-assisted sperm analysis (CASA) (HTM Ceros, version 12.2g; Hamilton Thorne Biosciences, Beverley, MA, USA) was used to determine sperm motility characteristics. Pre-warmed 4.7µL aliquots of sperm were loaded into a chamber slide (Leja, IMV Technologies, L'Aigle, France) on a slide warmer at 37°C. A minimum of 10 microscopic fields and 500 sperm were analyzed for each sample. Quantified values for total motility (TM, %), progressive motility (PM, %) and mean average path velocity (VAP, µm/s) were recorded.

*Reactive oxygen species (ROS) and viability assessment*

Cellular ROS levels were assessed with dihydroethidium (DHE, Molecular Probes, Eugene, OR, USA), a cell permeant, nuclear probe that fluoresces upon oxidation by superoxide anion ($O_2^{\bullet-}$)[17]. Since dead cells generate high levels of ROS, samples were co-stained with SytoxGreen™ (Molecular Probes, Eugene, OR, USA), which only crosses compromised cell membranes, to detect non-viable cells for gating purposes to remove the non-viable population before subsequent ROS analysis in viable cells only. One mL aliquots of 20 million sperm/mL were incubated with 2µM DHE and 0.3µM SytoxGreen™ for 15 minutes at room temperature in the dark. Antimycin (1µM), an electron transport chain inhibitor that induces mitochondrial ROS

generation, was used as a positive control for ROS production. Single-stain and no-stain controls were also used. Dead cells (snap frozen in liquid nitrogen twice) were used as a positive control for SytoxGreen™.

*Imaging Flow Cytometry Acquisition*

Imaging flow cytometric data was acquired using the Amnis® ImageStream® imaging flow cytometer (Luminex Corporation, Austin, TX) and the INSPIRE® software (Luminex Corporation, Austin, TX), equipped with 405, 488, 658, and 730 nm laser sources with variable, bandwidth-defined powers, and a brightfield light source. The flow core diameter was set to 5μM, samples were loaded, and the flow rate and the image gallery and flow rate were allowed to equilibrate for 1-2 minutes. The 405nm and 642nm lasers were set to 0mW (OFF), and the 488nm laser was set to 200 mW. 785nm laser was only used for side scatter (SSC) and set to 0.74mW. Channel 12 was selected as the SSC channel, and brightfield illumination appeared in channels 1 and 9. The flow error rate was checked prior to acquisition, and events were only recorded if the flow error rate is less than 0.2% per sample. Image files were acquired using the 60× objective. Autofocus and centering were disabled, and manually adjusted between -2 and 2 and -1 and 1, respectively. 20-25,000 events were recorded per sample. After acquisition, the INSPIRE Compensation Wizard was used to collect 500 events from single-stained samples and a compensation matrix was generated for later data analyses.

*Imaging flow cytometry analysis*

Imaging flow cytometry data was analyzed using the IDEAS® software (Luminex Corporation, Austin, TX ). All files were opened with the same compensation matrix and

analysis template. For each sample, all 20-25000 events were opened with the randomized order function for assignment of image gallery order in numbering.

*ImageStream compensation*

The INSPIRE® Compensation Wizard was used for acquisition of 500 events from each of the single-stained, positive control samples. The IDEAS® Compensation Wizard was used to generate a compensation matrix from the collected files. All cross-talk coefficients were manually checked and adjusted to ensure the coefficient error rate was within the manufacturer recommended range.

*Analysis template and image gallery properties*

An analysis template was generated in IDEAS®. First, using the "Analysis Wizard" to select for in-focus, single cells. A representative example of the data processing and analysis workstation for a single ejaculate is provided in Figure 3.1. First, focused cells were selected using three plots and the Gradient RMS, and Contrast features (Fig 3.1A-C). The Contrast and Gradient RMS features are similar: both quantify the sharpness of an image by detecting large pixel value changes, but Gradient RMS is calculated with background subtracted and has different weighting for pixel arrays[18]. Next, single cells were selected for using the Area and Aspect Ratio Intensity features (Fig 3.1D). The Aspect Ratio Intensity feature is calculated by dividing the Minor Axis Intensity by the Major Axis Intensity of the imaged object[18]. The Major Axis Intensity is an intensity weighted measurement of the length of the imaged object, and the Minor Axis Intensity is an intensity weighted measurement of the width of the imaged object, with length and width determined based on dimensions of an ellipse of best fit of the imaged

object, and the Area feature is the microns$^2$ in the designated channels mask[18]. Third, a plot of DHE verses SytoxGreen™ Intensity was used to gate out remaining debris (Fig 3.1E). A new scatter plot was then created with the population of focused, single, debris-free cells, which was used for all viability and DHE gating (Fig 3.1F). The acquired positive control files were used to inform gating.

The image gallery properties were adjusted prior to analysis. Figure 3.3 depicts an example of the image display gallery in IDEAS. Channels were renamed to reflect staining of each specific channel. An example of all four channels, including two brightfield channels (BF1 and BF2) and the DHE and SYTOX channels, is displayed in Figure 3.3. The image gallery view displaying only BF1 and BF2 was created to allow morphologic analysis blinded to viability and ROS. Morphologic populations were then selected using the tagging feature (described below in *Morphology and ROS Assessment*) and the DHE fluorescence intensity of individual cells were exported for data analysis.

*ImageStream Morphology Assessment Validation*

Fresh ejaculates (n=5) were used to validate the use of ImageStream for morphologic assessment of stallion semen. For these samples, morphologic analysis was also performed using a conventional method for morphologic assessment of stallion semen. To validate the ImageStream System for equine sperm morphology assessment, total morphology counts on 100 cells were performed with a Zeiss AxioLab A1 phase-contrast microscope (100x) using 2% buffered formalin and Eosin-nigrosin stain (Morphology stain, Society for Theriogenology, AL). For comparison on the ImageStream system, the image gallery was set to view all focused,

single, debris-free cells and the morphology of the first 100 cells was recorded. The percentage of morphologically normal (MN) cells from both assessment methods was then calculated.

*Morphology and ROS assessment*

Morphology was assessed by both the ImageStream system and IDEAS® and with phase-contrast light microscopy. Morphologic assessment was performed with only brightfield channels of viable cells visible in the image gallery to allow analysis blinded to fluorescence indicating ROS production. Representative images of morphologic normal and abnormal sperm are displayed in Figure 3.2. The following classification parameters were used: morphologically normal (MN; Fig. 3.2A , 3.3A and 3.3B), abnormal head (AH; Fig. 3.2F and 3.3F), abnormal tail (AT; Fig. 3.2C and 3.3D), abnormal midpiece (AM; Fig. 3.2D, 3.2I and 3.3E), proximal cytoplasmic droplet (PD; Fig. 3.2G and 3.3A), and distal cytoplasmic droplet (DD; Fig. 3.2H 3.3G**)**. In fresh semen, cells with both coiled tails and coiled midpieces (CTM; Fig. 3.2B and 3.3C) were also classified. CTM cells were not classified in cooled semen due to lack of viable CTM cells in those samples. Classification of AH included, but was not limited to, pyriform heads, microheads, and nuclear vacuoles. Since acrosome abnormalities cannot be confidently, consistently assessed at 60x without specialized staining, any acrosome abnormalities were classified as AH. Classification of AM included bent midpieces, swollen midpieces, and other midpiece abnormalities. AT included bent tails and coiled tails without midpiece involvement. Once gating was performed and image gallery setup was completed to display the two brightfield images of live cells (SytoxGreen™ negative) only, morphologic analysis was performed. Populations of each sperm morphologic type in question were selected using the IDEAS "tag" feature. The image gallery was scrolled through and the first 30, in-focus, viable cells displaying

each morphology (MN, AH, AT, AM, PD, and DD) were tagged for their given abnormality and saved to a population for later data export and analysis. Analysis was performed on the first thirty cells with each abnormality because exploratory data analysis revealed that 30 was the highest number reliably present for each abnormality across ejaculates, and due to the known high variability/range of fluorescence intensity data, for statistical validity the largest *n* possible for each sample and abnormality was desired. For this portion of the analysis, cells with multiple abnormalities were not included to simplify analysis by eliminating potential confounding effects.

*Statistical Analysis*

Statistical analysis for validation of morphologic evaluation using ImageStream acquisition and the IDEAS analysis software was accomplished using a paired-samples t-test performed in JMP® statistical software (version 14.0.0; SAS Institute Inc., Cary, NC, USA).

Mixed-effects modeling performed in R version 3.6.2 (R Core Team, 2019) was used to investigate the relationship between ROS production (DHE fluorescence intensity) and sperm morphology, with random intercepts given for ejaculates to account for within ejaculate correlation of ROS measurements. A total N= 1,050 cells from five ejaculates taken from 4 stallions were analyzed for fresh semen, and N= 900 cells from five ejaculates from 5 stallions were analyzed for cooled semen. Exploratory analysis revealed marked skewing of DHE intensity, as is typical of fluorescence imaging data, so a Log10 transformation of DHE fluorescence intensity was used for analysis to reduce skewing. We tested for significant differences between Log10 DHE in morphologically normal to all other morphologies and adjusted the p-values for multiple comparisons using Dunnett's method. Dunnett's method is a multiple comparisons procedure developed for comparing a number of conditions to a single

group (in this case, morphologically normal). Hypothesis testing was performed with an alpha = 0.05 level of significance and 95% confidence intervals are shown where appropriate.

## Results

*ImageStream Morphologic Assessment Validation.*

A paired-samples t-test was conducted to compare morphologic assessment of stallion sperm by imaging flow cytometry and conventional microscopy techniques. The percent of morphologically normal cells were compared between morphologic assessment performed by conventional methods to manual morphologic assessment using the ImageStream and IDEAS system. Results indicated no significant difference between morphologic assessment between the two systems ($p$=0.59, *t-ratio*= 0.58, $R$= 0.89).

*Sperm Morphology and ROS generation*

Representative images of brightfield and fluorescence microscopy staining for viability (SytoxGreen™) and ROS production (DHE) for normal and abnormal morphologic types are displayed in Figure 3.3. The linear mixed effects modeling revealed elevated ROS production in viable cells with certain morphologic abnormalities compared to morphologically normal cells in both fresh and cooled semen. The statistical results for the difference in Log10 DHE fluorescence intensity (ROS production) between cells with each assessed morphologic abnormality and MN cells for fresh and cooled semen are displayed in Tables 3.1 and 3.2, respectively. Graphic representation of results from mixed-effects modeling to assess differences in log(DHE Intensity) as a function of sperm morphology for fresh and cooled semen are depicted in Figures 3.4 and 3.5, respectively. Compared to the MN population, ROS production

was significantly higher in viable cells with AH, PD and AM ($p < 0.0001$) in both fresh and cooled semen (Fig. 3.4 and 3.5). For fresh semen, the DHE intensity for AH, PD, and AM populations was 30.31%, 24.94%, and 30.74% higher than that of MN cells, respectively (Fig. 3.4). For cooled semen, the DHE intensity for the AH, PD and AM populations was 21.40%, 19.03% and 20.09% higher than that of MN cells, respectively. No significant differences were identified between the MN population ROS levels and those of the DD ($p > 0.05$) or AT populations ($p > 0.05$) for either fresh or cooled semen. In fresh semen, an additional morphological abnormality, CTM, was evaluated and demonstrated significantly higher ROS production compared to MN cells ($p<0.0001$). CTM cells had a Log10 DHE intensity that was 47.47% higher than that of MN cells. This abnormality was only evaluated in fresh semen due to a lack of CTM cells in the viable population of cooled semen.

**Discussion**

In this study, we utilized a powerful and novel investigative tool, imaging flow cytometry, to investigate the relationship between stallion sperm morphologies and ROS production at the single-cell level. Our data demonstrate the reliability of imaging flow cytometry since sperm identified as MN were equivalent with MN determined using traditional light microscopy. In both fresh and 24-hour cooled stallion semen, we identified cells with certain morphologic abnormalities (AH, AM, and PD), as well as CTM in fresh ejaculates, that have significantly higher ROS production than MN cells. To our knowledge, this is the first study evaluating the relationship between stallion sperm morphology and ROS production at the single-cell level, although there are many published studies that evaluate measures of oxidative stress and sperm quality, including morphologic evaluation, at the ejaculate level[1,16].

Comparisons of results from these studies to previous reports should be performed cautiously due to differences in semen processing, media composition and experimental techniques.

The variation in ROS production observed between stallions in the present study is not unexpected, as both inter-stallion and inter-ejaculate variation in ROS levels have previously been reported, including in cooled semen[19]. Despite the variation in mean ROS level between stallions, the fluorescence intensity among morphologic abnormalities relative to each other was consistent between all five stallions and results demonstrated strong statistical significance (Table 3.1 and Table 3.2).

The results from our study regarding abnormal morphologies and ROS generation have potential implications for stallion fertility. A previous study found the percent morphologically normal sperm was highly correlated with fertility evaluated as per cycle pregnancy rate (PC) and percent pregnant at first cycle (FCP) [20]. Love (2011)[20] also found that increased levels of most sperm morphologic abnormalities (including abnormal and detached heads, proximal and distal droplets, and general midpiece abnormalities, and coiled tails) were associated with a decline in PC and FCP. A study by Morrell and colleagues[21] also identified a positive relationship between normal morphology and pregnancy rate; the same study also assessed oxidative DNA damage using the Sperm Chromatin Structure Assay (SCSA), revealing a negative correlation between DNA fragmentation index (DFI) and pregnancy rate[21]. The results from our study, in support of earlier studies, have several clinical implications for stallion fertility and breeding management.

We provide evidence that certain morphologic abnormalities (AH, PD, AM, and CTM) demonstrate elevated ROS production in viable sperm compared to morphologically normal cells. Because elevated ROS production is known to cause catastrophic sperm cell damage, ejaculates with a large proportion of high ROS abnormalities may be less suitable for cooled

storage. An additional result worth highlighting for clinical relevance was the marked elevation in ROS production observed in fresh CTM cells, although analysis of CTM cells was limited to fresh semen because very few live CTM cells were able to be identified in cooled semen. It is possible that the elevated ROS production in sperm cells with CTM causes premature cell death, which is why so few viable CTM cells were identified in the viable populations of cooled semen, precluding assessment of CTM cells in cooled semen due to lack of statistically significant sample size. Particular avoidance of cooled storage for ejaculates with high levels of CTM morphologic abnormalities may be beneficial due to the elevated ROS production and potential shorter lifespan of these cells compared to both morphologically normal cells and other abnormalities.

Future studies utilizing the ImageStream® imaging flow cytometer for evaluation to further elucidate the pathophysiology accompanying elevated ROS production in morphologically abnormal sperm would be beneficial. Specifically, utilization of fluorescence dyes for concurrent investigation of the cellular antioxidant status, such as thiols, mitochondrial membrane potential, and ROS generation could provide valuable insight to the role of mitochondrial oxidative metabolism in elevated ROS generation in morphologically abnormal sperm. Additionally, utilization of membrane dyes to employ automated morphologic evaluation of imaging flow cytometry data by the IDEAS® software would be useful as it would improve efficiency of data analysis utilizing this system.

In this study, we employed the novel use of imaging flow cytometry for evaluation of the relationship between stallion sperm morphology and ROS generation. We identified significantly higher ROS generation in several abnormal morphologies in both fresh and cooled ejaculates, including cells with AH, AM, and PD. We also identified significantly higher ROS generation in

CTM cells in fresh ejaculates but were unable to evaluate this morphologic abnormality in cooled ejaculates due to lack of viable samples. These findings suggest that excessive oxidative stress contributes to the pathophysiology of morphologic abnormalities, which may contribute to previous findings linking certain morphologic abnormalities to decreased fertility in stallions. Future studies investigating the relationship between morphologic abnormalities, ROS, and measurements such as mitochondrial oxygen consumption or mitochondrial membrane potential, would be useful to investigate the contribution of mitochondrial function to the current findings.

**Acknowledgements**

The authors would like to express appreciation for our collaborators at TAMU, Dr. Dickson Varner and Ms. Sheila Teague. This project was supported by "Students Training in Advanced Research" (STAR) Fellowship award from the UC Davis School of Veterinary Medicine Endowment Funds, the National Institutes of Health (NIH), National Center for Research Resources as a Ruth L. Kirschstein National Research Service Award (NRSA; grant number T32OD010931-11), the UC Davis Center for Equine Health (2017-18) with funds provided by the State of California Satellite Wagering Fund and contributions by private donors.

**Tables and Figures**

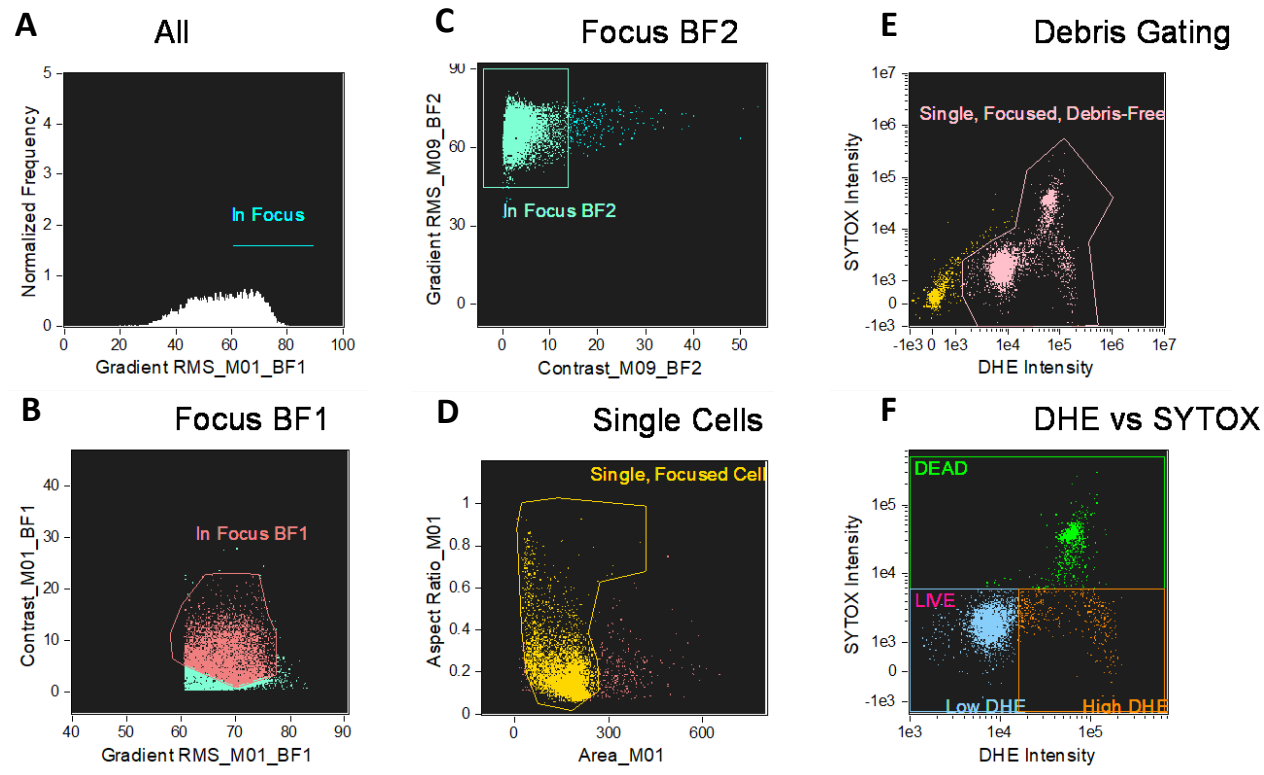


**Figure 3.1**: ***Bivariate plots and gating used to select in focus, single, debris-free cells to evaluate reactive oxygen species (ROS) production.*** An example of the data processing and analysis workstation in the IDEAS software from a single ejaculate is shown (n=1). (A) Gradient RMS versus normalized frequency initial focus gating plot. (B) Gradient RMS versus Contrast for BF1 (channel 01) (C) Contrast versus Gradient RMS of BF2 (channel 9). (D) Area versus Aspect Ratio for BF1 (channel 1). (E) DHE versus SYTOX (SytoxGreen™) intensity scatterplot of Single, Focused cells to gate out debris. (F) DHE versus SYTOX intensity scatterplot of In Focus, Single, Debris-Free cells for viability and high/low DHE gating.

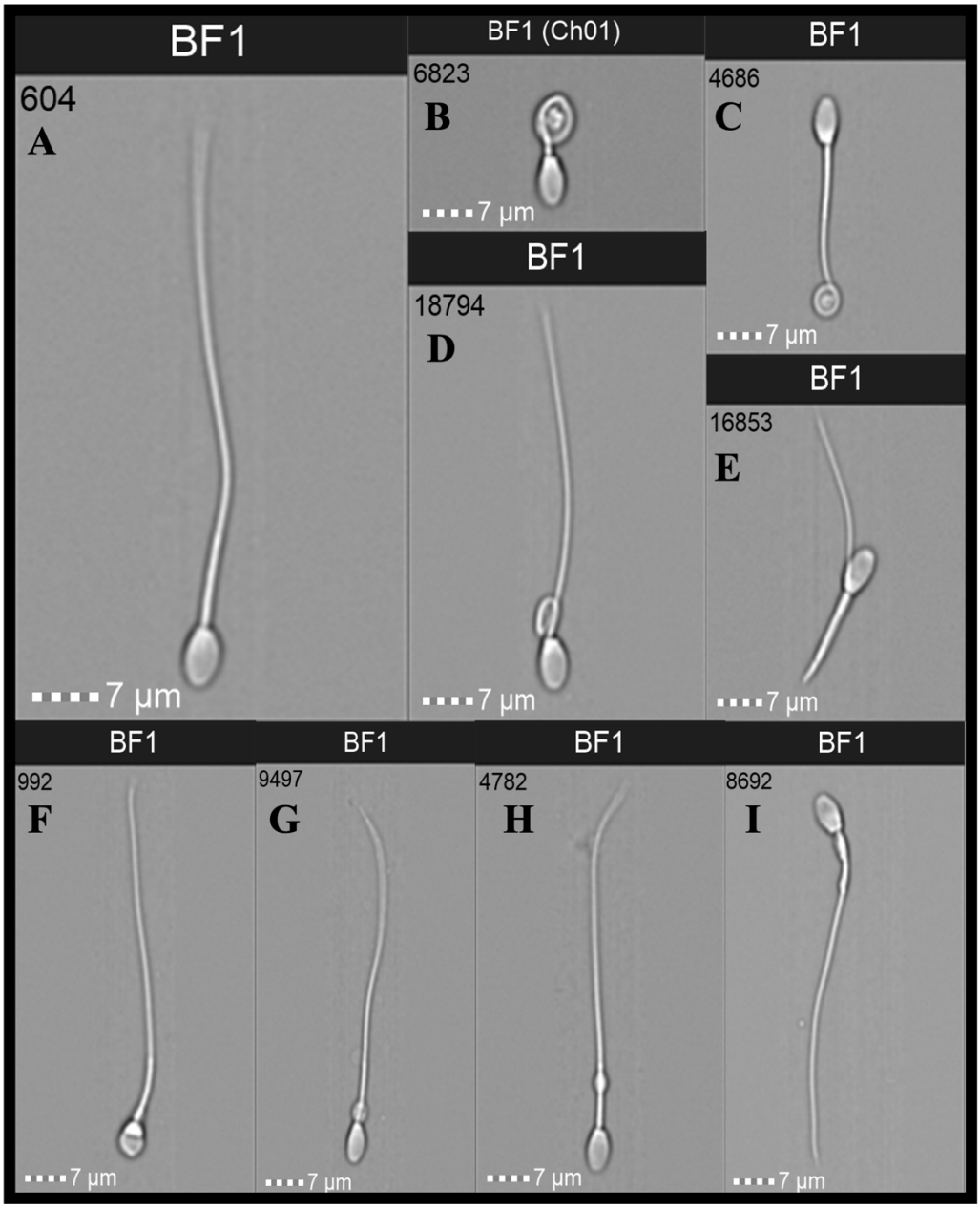


**Figure 3.2.** ***Brightfield images of various sperm morphologies using an imaging flow cytometer.*** Brightfield images of individual sperm cells with different morphologies are displayed. (A) Morphologically normal cell (MN), (B) cell with a coiled tail and midpiece (CTM), (C) cell with an abnormal tail (AT), (D) cell with an abnormal midpiece (AM), (E) cell with an abnormal tail (AT), (F) cell with an abnormal head (AH), (G) cell with a proximal droplet (PD), (H) cell with a distal droplet (DD), and (I) cell with an abnormal midpiece (AM).

These images were acquired using the Amnis ImageStream® X imaging flow cytometer with the 60x objective and the Inspire® acquisition software and analyzed in Ideas® (Amnis Corp.).

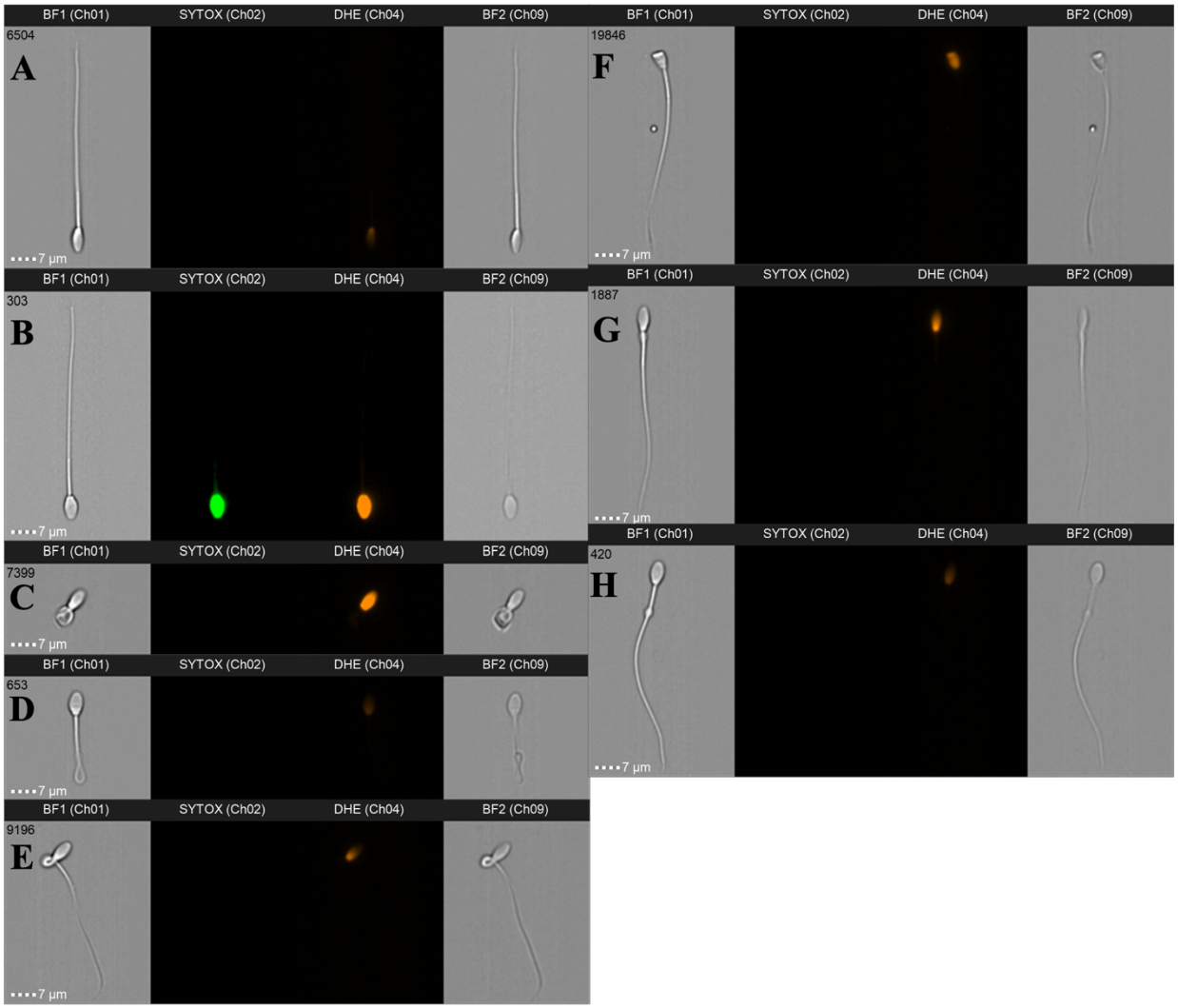


**Figure 3.3**. ***Image Gallery display in the IDEAS software of morphologically normal and abnormal equine sperm.*** A representative image gallery display of a stallion sperm acquired by imaging flow cytometry is shown. These images were acquired using the Amnis ImageStream® X imaging flow cytometer and the Inspire® acquisition software and analyzed in Ideas® (Amnis Corp.). Cells were stained to indicate viability (membrane integrity, SytoxGreen; Ch02) and reactive oxygen species production (Superoxide anion indicator, DHE; Ch04). (A) This is an example of a morphologically normal, viable (SYTOX negative) cell, with low ROS production (DHE fluorescence). (B) This is an example of a morphologically normal, non-viable (SYTOX positive) cell with strong ROS production. Examples of cells with morphologic abnormalities are

shown in (C) a morphologically abnormal, viable cell with a coiled tail and midpiece (CTM), (D) a morphologically abnormal, viable cell with an abnormal tail (AT), (E) a morphologically abnormal, viable cell with an abnormal midpiece (AM), (F) a morphologically abnormal, viable cell with an abnormal head (AH), (G) a morphologically abnormal, viable cell with a proximal droplet (PD), and (H) a morphologically abnormal, viable cell with a distal droplet (DD). For initial blinded morphologic analysis and population tagging, only channels BF1 and BF2 were displayed in the image gallery.

| Morphologic abnormality | Estimate | SE | t-ratio | p-value |
|---|---|---|---|---|
| Abnormal head (AH) | 0.3031 | 0.0242 | 12.528 | <.0001 |
| Proximal droplet (PD) | 0.1903 | 0.0242 | 10.309 | <.0001 |
| Distal droplet (DD) | 0.0437 | 0.0242 | 1.812 | 0.2823 |
| Abnormal midpiece (AM) | 0.3074 | 0.0242 | 12.704 | <.0001 |
| Abnormal tail (AT) | 0.0367 | 0.0242 | 1.517 | 0.4505 |
| Coiled Tail and Midpiece (CTM) | 0.4757 | 0.0242 | 19.660 | <.0001 |

**Table 3.1.** ***Summary statistics of* morphologic analysis of fresh, viable equine sperm**. Displayed results were generated by contrast with the morphologically normal (MN) cell population (df=20) and mixed effects modeling. The 'Estimate' column represents the difference in Log10 DHE intensity (ROS production) between cells with the listed morphologic abnormality and MN cells. The 'estimate' can be multiplied by 100 to express the intensity difference as a percentage. Table 2A contains results from fresh semen analysis, table 2B contains results from cooled semen analysis. N=210.

| Morphologic abnormality | Estimate | SE | t-ratio | p-value |
|---|---|---|---|---|
| Abnormal head (AH) | 0.2140 | 0.0330 | 6.4835 | 1.2098 e-5 |
| Proximal droplet (PD) | 0.1903 | 0.0330 | 5.7664 | 5.7213 e-5 |
| Distal droplet (DD) | 0.0437 | 0.0330 | 1.3231 | 0.54763 |
| Abnormal midpiece (AM) | 0.2009 | 0.0330 | 6.0855 | 2.8443 e-5 |
| Abnormal tail (AT) | 0.0173 | 0.0330 | 0.5255 | 0.94505 |

**Table 3.2.** ***Summary statistics of morphologic analysis of cooled, viable equine sperm***. Displayed results were generated by contrast with the morphologically normal (MN) cell population (df=20) and mixed effects modeling. The 'Estimate' column represents the difference in Log10 DHE intensity (ROS production) between cells with the listed morphologic abnormality and MN cells. The 'estimate' can be multiplied by 100 to express the intensity difference as a percentage. N=180.

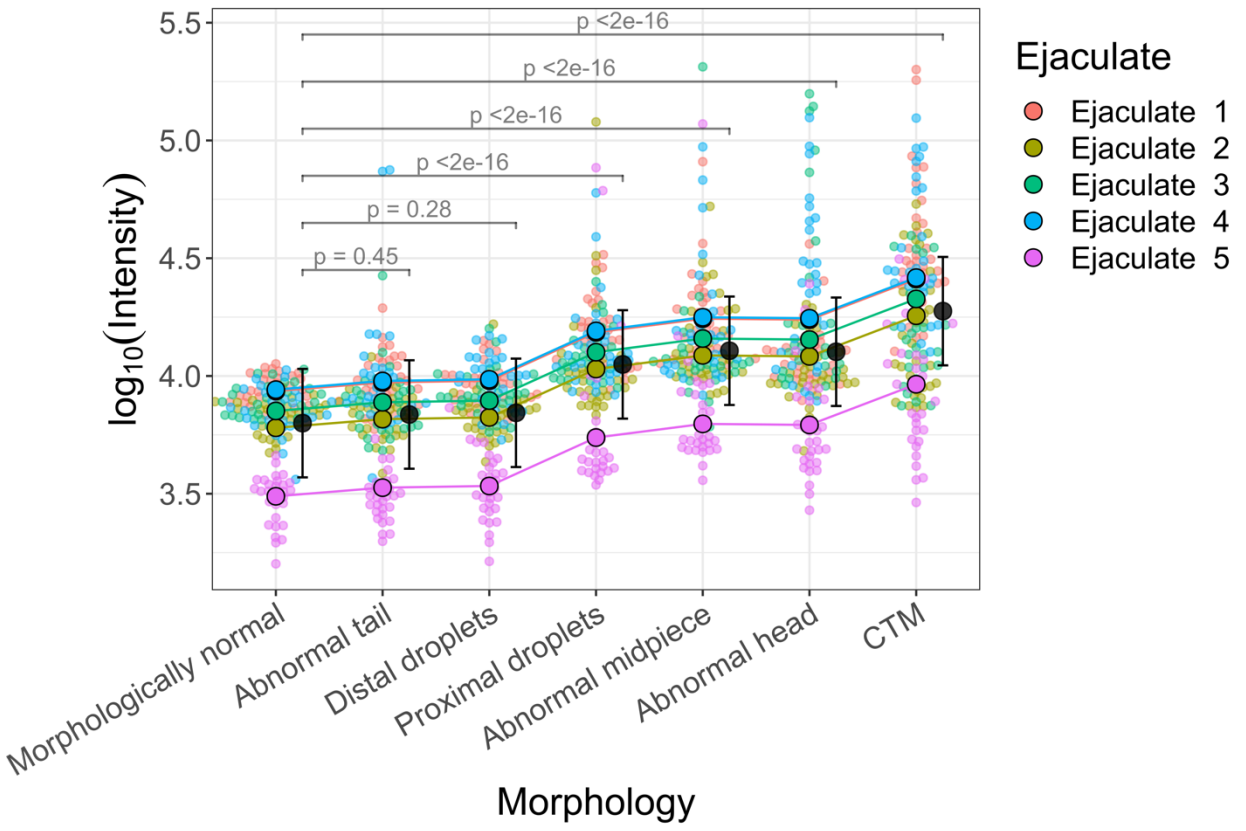


**Figure 3.4.** ***Morphologic analysis of fresh, viable equine sperm***. Mixed-effects models were used to assess differences in log(DHE Intensity) as a function of sperm morphology, accounting for repeated measurements made from each ejaculate. Individual observations plotted and colors represent the ejaculate from which the measurements were made. Points connected by lines are the average intensity for a given ejaculate. Black points are the overall means with 95% confidence intervals. Sperm with proximal droplets, abnormal midpieces, abnormal heads and coiled tail and midpiece (CTM) had significantly higher DHE intensity compared to morphologically normal sperm. N=1050, cells.

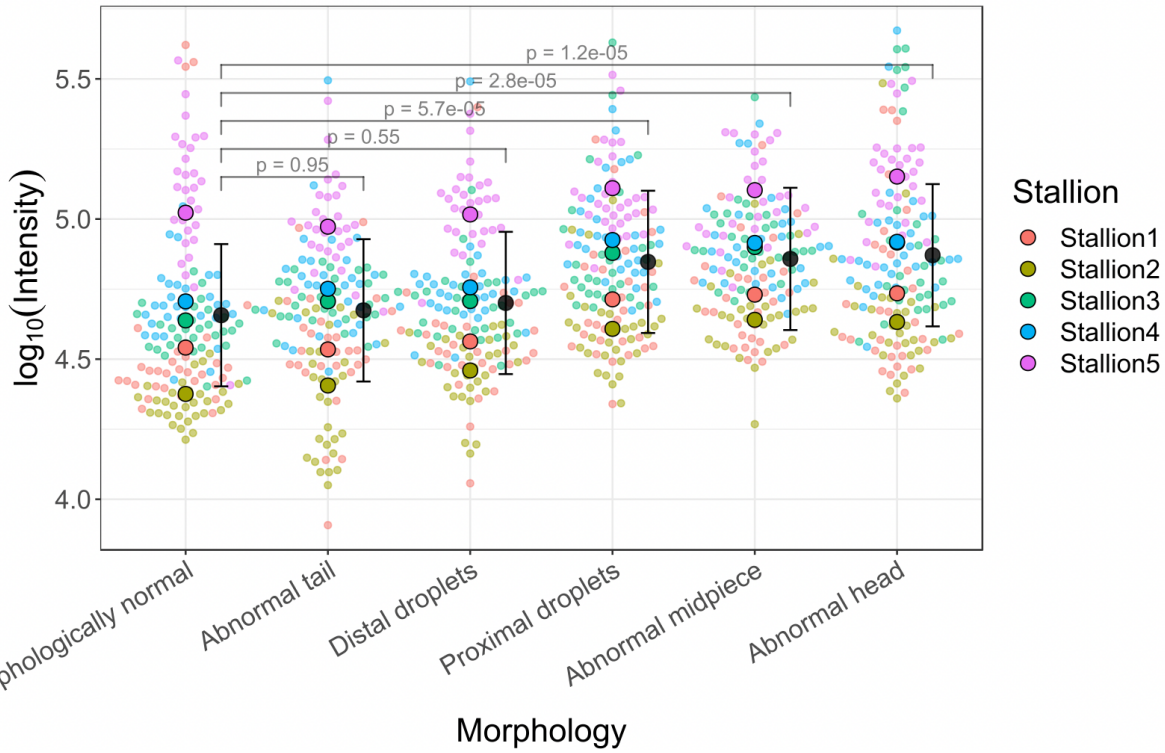


**Figure 3.5**. ***Morphologic analysis of cooled, viable equine sperm***. Mixed-effects models were used to assess differences in log(DHE Intensity) as a function of sperm morphology, accounting for repeated measurements made from each ejaculate. Individual observations plotted and colors represent the ejaculate from which the measurements were made. Points connected by lines are the average intensity for a given ejaculate. Black points are the overall means with 95% confidence intervals. Sperm with proximal droplets, abnormal midpieces, and abnormal heads had significantly higher DHE intensity compared to morphologically normal sperm. N=900, cells.

**References**


1. Aziz N, Saleh RA, Sharma RK, Lewis-Jones I, Esfandiari N, Thomas AJ, Agarwal A. Novel association between sperm reactive oxygen species production, sperm morphological defects, and the sperm deformity index. *Fertil Steril*. 2004;81(2):349-354. doi:10.1016/j.fertnstert.2003.06.026
2. Darr CR, Varner DD, Teague S, Cortopassi GA, Datta S, Meyers SA. Lactate and Pyruvate Are Major Sources of Energy for Stallion Sperm with Dose Effects on Mitochondrial Function, Motility, and ROS Production. *Biol Reprod*. 2016;95(2):34-34. doi:10.1095/biolreprod.116.140707
3. Gibb Z, Lambourne SR, Aitken RJ. The Paradoxical Relationship Between Stallion Fertility and Oxidative Stress. *Biol Reprod*. 2014;91(3):1-10. doi:10.1095/biolreprod.114.118539
4. Koppers AJ, De Iuliis GN, Finnie JM, McLaughlin EA, Aitken RJ. Significance of mitochondrial reactive oxygen species in the generation of oxidative stress in spermatozoa. *J Clin Endocrinol Metab*. 2008;93(8):3199-3207. doi:10.1210/jc.2007-2616
5. Hirst J, King MS, Pryde KR. The production of reactive oxygen species by complex I. *Biochem Soc Trans*. 2008;36(5):976-980. doi:10.1042/BST0360976
6. Gibb Z, Lambourne SR, Aitken RJ. The paradoxical relationship between stallion fertility and oxidative stress. *Biol Reprod*. 2014;91(3):1-10. doi:10.1095/biolreprod.114.118539
7. Guthrie HD, Welch GR. Effects of reactive oxygen species on sperm function. *Theriogenology*. 2012;78(8):1700-1708. doi:10.1016/j.theriogenology.2012.05.002
8. Darr CR, Cortopassi GA, Datta S, Varner DD, Meyers SA. Mitochondrial oxygen consumption is a unique indicator of stallion spermatozoal health and varies with

cryopreservation media. *Theriogenology*. 2016;86(5):1382-1392. doi:10.1016/j.theriogenology.2016.04.082

9. Baumber J, Ball BA, Gravance CG, Medina V, Davies-Morel MCG. The effect of reactive oxygen species on equine sperm motility, viability, acrosomal integrity, mitochondrial membrane potential, and membrane lipid peroxidation. *J Androl*. 2000;21(6):895-902. doi:10.1002/j.1939-4640.2000.tb03420.x
10. Gibb Z, Lambourne SR, Curry BJ, Hall SE, Aitken RJ. Aldehyde dehydrogenase plays a pivotal role in the maintenance of stallion sperm motility. *Biol Reprod*. 2016;94(6):133. doi:10.1095/biolreprod.116.140509
11. Darr C, Martorana K, Scanlan T, Meyers S. The effect of low oxygen during the early phases of sperm freezing in stallions with low progressive motility: Can we improve post-thaw motility of stallion sperm? *J Equine Vet Sci*. 2016;42:44-51. doi:10.1016/j.jevs.2016.03.022
12. Ford WCL. Glycolysis and sperm motility: does a spoonful of sugar help the flagellum go round? *Hum Reprod Update*. 2006;12(3):269-274. doi:10.1093/humupd/dmi053
13. Lei XG, Zhu JH, Cheng WH, Bao Y, Ho YS, Reddi AR, Holmgren A, Arnér ESJ. Paradoxical roles of antioxidant enzymes: basic mechanisms and health implications. *Physiol Rev*. 2016;96(1):307-364. doi:10.1152/physrev.00010.2014
14. Saacke RG. Sperm morphology: Its relevance to compensable and uncompensable traits in semen. *Theriogenology*. 2008;70(3):473-478. doi:10.1016/j.theriogenology.2008.04.012
15. Love CC, Varner DD, Thompson JA. Intra- and inter-stallion variation in sperm morphology and their relationship with fertility. *J Reprod Fertil Suppl*. 2000;(56):93-100. http://www.ncbi.nlm.nih.gov/pubmed/20681120

16. Said TM, Aziz N, Sharma RK, Lewis-Jones I, Thomas AJ, Agarwal A. Novel association between sperm deformity index and oxidative stress-induced DNA damage in infertile male patients. *Asian J Androl*. 2005;7(2):121-126. doi:10.1111/j.1745-7262.2005.00022.x

17. Burnaugh L, Sabeur K, Ball BA. Generation of superoxide anion by equine spermatozoa as detected by dihydroethidium. *Theriogenology*. 2007;67(3):580-589. doi:10.1016/j.theriogenology.2006.07.021

18. Amnis. *IDEAS® Image Data Exploration and Analysis Software User 's Manual 6.0*.; 2013.

19. Johannisson A, Lundgren A, Humblot P, Morrell JM. Naturally and stimulated levels of reactive oxygen species in cooled stallion semen destined for artificial insemination. *Animal*. 2014;8(10):1706-1714. doi:10.1017/S1751731114001499

20. Love CC. Relationship between sperm motility, morphology and the fertility of stallions. *Theriogenology*. 2011;76(3):547-557. doi:10.1016/j.theriogenology.2011.03.007

21. Morrell JM, Johannisson A, Dalin AM, Hammar L, Sandebert T, Rodriguez-Martinez H. Sperm morphology and chromatin integrity in Swedish warmblood stallions and their relationship to pregnancy rates. *Acta Vet Scand*. 2008;50(1):2. doi:10.1186/1751-0147-50-2

# Chapter 4: Assessment of an iPad-based Sperm Motility Analyzer for Determination of Canine Sperm Motility

Evelyn Bulkeley[1], Christine Collins[1], Azarene Foutouhi[1], Kris Gonzales[2], Heather Power[2], Stuart Meyers[1]

Department of Anatomy, Physiology, and Cell Biology, School of Veterinary Medicine, University of California, Davis, CA[1] and Guide Dogs for the Blind, San Rafael, California[2]

Keywords: canine, sperm, motility, CASA, viability, iSperm

**Abstract**

The objective of this study was to evaluate the repeatability and accuracy of canine sperm motility (total and progressive) assessment with a tablet-based Canine iSperm® instrument compared to computer-assisted sperm analysis (CASA). The experiment used fresh and frozen/thawed canine semen samples for comparisons of semen analysis parameters (concentration, total motility, and progressive motility) between a CASA system, iSperm®, and NucleoCounter® SP-100™ (concentration) instruments. Spearman's Rho correlational analysis was used to identify significant associations between motility assessment methods. Significant positive correlations were found between CASA assessment and iSperm® for both progressive and total motility measurements. We also determined the coefficient of variation (CV) for repeatability of sample analysis for iSperm® and CASA for fresh sperm, wherein each sample was assessed 10 times on both devices. For fresh and frozen-thawed samples, concentration assessment by iSperm® showed high variability (CV= 19.9 ± 1.5%). For iSperm® assessment of total and progressive motility, the CV's were 6.3 ± 0.5% and 10.7 ± 0.8%, respectively. The results indicate that the iSperm® application offers an accurate and alternative measurement of motility to traditional CASA analysis, though caution should be taken when assessing concentration due to the high CV observed in this study.

## Introduction

Microscopic assessment of sperm in motion has been used as a clinical and research tool for human and animal reproductive health over the past 340 years. Antoni van Leewenhoek reported microscopic sperm morphology in 1678 for human and dog sperm [1] using an early single-lens microscope [2,3]. In the past 40 years, the advancement of computer-assisted sperm analysis (CASA) has highlighted the ability to objectively assess large populations of motile and immotile sperm and has been summarized in considerable detail [3].

Visual assessments of canine sperm motility are subject to observer bias and for this reason the use of automated or computerized systems have been growing for wider clinical usage. Automated or computerized assessment of sperm motility, a sperm physiological parameter that is necessary for fertilization in vivo, has grown as a standard of practice for human fertility clinics as well as livestock breeding. The animal agriculture industry has recently taken advantage of new low-cost microprocessors and software for on-farm use. Automated sperm motility analysis has not been widely available to canine breeding programs which are largely performed by veterinary and lay breeding personnel and some specialty veterinary practices. CASA has been successfully employed for accurate motility assessment in dogs [4,5]; however, due to high costs and bench-space limitations, few small animal veterinary practitioners have access to CASA systems [6].

On-site semen evaluation has pushed technology developers to produce affordable, objective, and portable systems that can use a tablet-based camera with warming lenses that support real-time animal-side sperm analysis. The objective of this study was to assess the accuracy and reliability of a new and inexpensive tablet-based CASA system for sperm motility evaluation. We evaluated the iSperm® instrument for repeatability and accuracy in assessment of

canine sperm motility. Additionally, we assessed the repeatability of sperm concentration assessment by the iSperm®.

## Materials and Methods

*Chemicals and Reagents.*

The iSperm® sampling chips were obtained from GenePro (Fitchburg, WI). NucleoCounter® SP-100™ cassettes and reagents were purchased from ChemoMetec (Allerød, Denmark). All other chemicals were obtained from Sigma Chemical Co. (St. Louis, MO) unless otherwise stated. A modified Tyrode's medium (TALP) was used for all experiments [7]. This media consisted of 1 mg/mL PVA, 81 mmol/L NaCl, 2.8 mmol/L KCl, 0.2645 mmol/L $KH_2PO_4$, 40 mmol/L HEPES sodium salt, 2 mmol/L $NaHCO_3$, 2 mmol/L $CaCl_2$ (0.1 M solution, Ricca), and 0.4 mmol/L $MgCl_2$ (1 M solution). Media metabolites consisted of 5 mmol/L D-glucose, 1 mmol/L sodium pyruvate, and 0.1862% (v/v; 21.6 mmol/L) DL-Lactic acid syrup and pH was adjusted to 7.4 ± 0.02 and osmolality of 300 ± 10 mOsm/kg.

*Animals*

Fresh semen was collected by manual collection at the Guide Dogs for the Blind (GDB; San Rafael, CA) from dogs (n=5) owned by GDB that resided with a guardian owner in the San Francisco metropolitan area. They were under the medical care of veterinarians and staff at GDB during visits to the GDB campus and all animals were current in vaccinations. The dogs were, fed similar diets, and in good overall health per annual veterinary evaluation at GDB. For cryopreserved semen, ejaculates were collected at the University of California, Davis Veterinary Medicine Teaching Hospital (VMTH) under IACUC-approved guidelines on an out-patient basis

from dogs (n=4) with signed owner consent from Golden Retriever (n=1), Newfoundland (n=1), and Labrador Retriever dogs (n=2) by digital manipulation at UC Davis Veterinary Medicine Teaching Hospital under University of California IACUC-approved guidelines.

*Semen Collection and Processing.*

Fresh Semen. Fresh semen was collected from Labrador (n=3) and Golden Retrievers (n=2) by a veterinarian using a standard manual method and teaser female. Semen was collected into sterile plastic funnels attached to 15 mL conical tubes after the dog achieved erection during the mount. Semen was processed immediately for ejaculate volume and concentration and subjective initial motility evaluation on a phase contrast microscope at 400X magnification was performed at GDB. The samples were then diluted 1:2 (semen to extender ratio) using TALP and transported at ambient temperature by car for the one hour trip to the lab at UC Davis. Upon arrival in the lab, diluted semen samples were assessed for initial concentration using a NucleoCounter® SP-100™ by following the manufacturer's guidelines. Significant decline in sperm motility was not observed following transport in any samples. The semen samples were then diluted and concentrations were re-evaluated by a NucleoCounter® SP-100™ to ensure concentrations were between 30-60 million sperm/mL, the manufacturer recommended concentration range for canine iSperm® assessment. The diluted samples were then placed in an incubator at 37ºC on their sides to prevent sperm compaction at the bottom of the tube, and only removed from the incubator to retrieve a sample to be used for iSperm® and CASA.

Cryopreserved semen. Ejaculates were manually collected on an out-patient basis at the UC Davis VMTH from Golden Retriever (n=1), Newfoundland (n=1), and Labrador Retriever

dogs (n=2). Ejaculate volume was recorded and concentration and viability were quantified using a NucleoCounter® SP-100™ (ChemoMetec, Allerod, Denmark). To estimate sperm motility for freezing, Initial sperm motility parameters were quantified using CASA (SpermVision® SAR system, Minitube USA Inc., Verona, WI, USA). Seminal plasma was separated from sperm cells using Semen Separating Solution (Zoetis Inc, Parsippany-Troy Hills, NJ, USA) in preparation for freezing. Sperm was diluted 2:1 using Canine Freeze Buffer (Zoetis) and adjusted to a final concentration of 150 x $10^6$ sperm/mL using the addition of Zoetis Dilution Buffer® (Zoetis Inc.). Samples were loaded into 0.50 mL straws (Agtech Inc, Manhattan, KS, USA) and carefully sealed with polyvinyl alcohol powder. Cryopreservation was performed using a Planar Kryo 10 Series III controlled rate freezer (Planar Limited, Middlesex, United Kingdom). Straws were cooled to 10°C beginning at room temperature 24°C, using the cooling rate of -0.3 °C / min which was completed in 20 minutes. Straws were cooled over the next 60 minutes at a rate of -0.2°C/ min until reaching 4°C, then -10°C/ min until reaching -15°C, then -17°C/ min until reaching -110°C. Straws were removed from the Planar freezer and immediately plunged in liquid nitrogen (-196 °C). At thawing, the frozen semen straws were removed individually from liquid nitrogen storage tanks and placed into a warm water bath at 37°C for 30 seconds. After 30 seconds, the semen straw was cut on both ends and the contents decanted into a tube. These samples were then checked for their concentration and diluted as described above for fresh samples.

*Sperm Analysis: comparison between iSperm® and SpermVision® SAR (CASA).*

The iSperm® software (Aidmics Biotechnology Co., Ltd, Taipei City 10647, Taiwan) and instrumentation included an iPad Mini® (Apple Inc., Cupertino, CA, USA) plus the proprietary

microscope camera (Aidmics) which were set up according to the guidelines of the iSperm® instruction manual. When conducting all of the trials, a sample of 7.5µl was collected using a micropipette and placed onto the surface of the base chip, then flipped over into the cover chip and pressed for one to two seconds on the countertop, as per the instruction manual. The base chip plus cover chip were then screwed into the microscope attached to the iPad Mini® camera in order to be analyzed. Each semen sample (fresh ejaculate or frozen-thawed straw) was assessed using three separate iSperm® sample chips (eg. in triplicate), and each sample chip was analyzed ten times consecutively in the iSperm® application to allow for later calculation of the coefficient of variation (CV). The same orientation was used throughout the process of measuring the sample ten times in a row with the 'analyze' button being pushed ten times consecutively, providing data acquisition for ten observations. There were no other changes to the sample chip until analysis was completed and a new chip was sampled. The amount of time taken to analyze one sample chip ten times ranged from three to five minutes. The parameters quantified and collected in the iSperm® application included total motility (%), progressive motility (%) and concentration (M/mL).

For CASA, 3.5µl semen samples were loaded into each well of four-chambered Leja slides (Leja Products BV, Luzernestraat 10, The Netherlands). The slides were then placed on a warming plate (37ºC) for five minutes. The slide was then placed on the warmed (37ºC) stage of a Zeiss AxioLab A1 phase-contrast microscope, connected to a PC laptop equipped with SpermVision® SAR software (Minitube USA). Each sample was loaded into three separate chambers for motility assessment by SpermVision® SAR (eg. in triplicate). Per manufacturer recommendations, the CASA system motility analysis was performed for each slide chamber by recording motility parameters of seven different microscopic fields and averaging the seven for

endpoint analysis of the sample. Because the iSperm® manual provided limited information regarding motility parameter settings and due to inherent differences between the iSperm® and SpermVision® software, it was not possible to exactly match the motility settings between the two instruments for comparison. However, to allow the best possible direct comparison between the two modalities, all possible adjustments were made to match motility settings for SpermVision® analysis to the defined iSperm® settings. This was accomplished using the SpermVision® manufacturer-recommended motility settings for canine sperm analysis as a base template. CASA assessment using these modified settings will be referred to as "CASA_iSperm." For additional comparison, all samples were also analyzed using the unmodified manufacturer-recommended settings for canine motility assessment, which will be referred to as "CASA_canine". In summary, two separate CASA analyses were performed on each sample, one using the manufacturer recommended canine SpermVision® settings ("CASA_canine"), and another analysis using SpermVision® settings manually adjusted to best match the settings programmed by iSperm® ("CASA_iSperm"). The parameters of interest that were collected and analyzed by the CASA included total motility (TM, %) and progressive motility (PM, %).

*Data Management and Statistical Analysis.*

Data from each assessment method (iSperm®, CASA_canine, and CASA_iSperm®) was exported to Microsoft Excel. The coefficient of variation (CV), or relative standard deviation (rsd), was calculated [(sd/mean)*100] for each of the iSperm® sample chips for TM, PM, and concentration data. We considered CV's less than 0.15 (15%) to be indicative of nonsignificant differences between replicates. The ten consecutive measurements recorded for each parameter were averaged for all additional analyses. Exploratory and statistical analyses were performed

using JMP® statistical software (version 14.0.0; SAS Institute Inc., Cary, NC, USA). Data distributions were checked for normality with the Shapiro-Wilk test. Nonparametric Spearman's Rho ($r_s$) correlational analysis was then performed to identify significant associations between assessment methods. Comparisons between TM and PM measurements between assessment methods were carried the Wilcoxon method.

**Results**

For fresh and frozen-thawed samples, concentration assessment by iSperm® showed high variability (CV= 19.9 ± 1.5%). The very low sperm motility of the post-thaw samples resulted in a high variation during consecutive motility assessments for CV calculation (Table 1). Consequently, only fresh samples (n=15) were used to evaluate the CV of motility measurements. For iSperm® assessment of total and progressive motility, the CV's were 6.3 ± 0.5% and 10.7 ± 0.8%, respectively.

Spearman's Rho correlational analysis was used to identify significant associations between motility assessment methods because the data were not normally distributed. Strong significant positive correlations were found between all assessment methods for both TM and PM measurements. Specifically, TM measurements were strongly correlated between the iSperm® and both the CASA_iSperm ($r_s$=0.95$p$<0.0001) and the CASA_canine ($r_s$=0.93, $p$<0.0001), as well as between the CASA_iSperm and CASA_canine ($r_s$=0.97, $p$<0.0001) (Fig. 1A). Strong positive correlations were also identified for PM measurements between the iSperm® and both CASA_canine ($r_s$=0.87, $p$=0.0004) and CASA_iSperm ($r_s$=0.87, $p$=0.0004), in addition to between CASA_iSperm and CASA_canine ($r_s$=1.00, $p$<0.0001) (Fig. 1B).

Comparisons between TM values between assessment method revealed no significant differences between the iSperm® and CASA_canine (Z=-0.39 *p*=0.69) or CASA_iSperm (Z=-0.79, *p*=0.43). No significant differences were identified between CASA_iSperm and CASA_canine (Z=0.92, *p*=0.36) (Fig. 2A). Comparisons between PM measurements revealed a slight, although significant difference between iSperm® and CASA_iSperm (Z=-1.97, *p*=0.05), but no significant difference between iSperm® and CASA_canine (Z=-1.90, *p*=0.06). No significant differences were observed in PM measurements between CASA_iSperm and CASA_canine (Z=1.05, *p*=0.29) (Fig. 2B).

**Discussion**

The iSperm® Canine software was created to provide a relatively inexpensive and portable device that can be used for semen analysis as an animal-side test in clinical and field conditions, such as veterinary hospitals, dog shows and competitive sporting events where semen evaluation is commercially performed. The iSperm® was designed to measure sperm concentration and motility parameters (including total and progressive motility)  abnormality, VCL, VAP, VSL, STR, and LIN of a sample, which can then be used to calculate an extended semen dose for breeding. Our goal was to assess the iSperm® Canine application's repeatability by assessing CV values for concentration, total and progressive motility measurements, as well as to validate and assess the accuracy of motility assessment by the iSperm® Canine application through comparison to motility assessment by CASA, the "gold standard" of semen motility assessment.

The commercial CASA instrument used for validation, Sperm Vision® SAR, has been widely used to assess sperm motility and morphology through digitized video recordings of

sperm. This instrument computes their motion tracks which can then be analyzed and then standardized [8]. The iSperm® application utilizes a similar process to calculate sperm concentration and motility by using video recordings through the iPad Mini to calculate the trajectory and concentration of the sperm in the sample but uses different and proprietary algorithms and software for the process. Due to inherent differences in software and minimal details available regarding the iSperm® motility parameter settings (threshold values, etc.), it was not possible to completely match the CASA parameter settings between the two systems (iSperm and CASA). For this reason, we compared motility assessment with the iSperm® Canine application to CASA assessment using both the Sperm Vision® manufacturer-recommended canine settings (CASA_Canine), and a version of those settings modified to best match the pre-programmed settings of the iSperm® Canine application (CASA_iSperm).

Correlational analysis with Spearman's Rho revealed significant strong positive correlations in both TM and PM measurements between all three assessment methods (iSperm® Canine application, CASA_iSperm and CASA_canine). For TM assessment, the correlation was slightly stronger between the iSperm® Canine application and CASA_iSperm than with CASA_canine, but the correlation for PM assessment was comparable between the iSperm® Canine application and both the CASA_iSperm and CASA_canine. Comparison of TM and PM values between analysis methods by the Wilcoxon method overall did not reveal significant differences, with the exception of a slight, although significant, difference in PM values between the iSperm and CASA_iSperm. Overall, these results demonstrate the accuracy of the iSperm® application for measuring the total motility in canine semen. These results also suggest reasonable accuracy of the iSperm® for PM assessment. Although a very slight significant difference was detected between PM values with the CASA_iSperm, no significant differences

were detected in PM values between the iSperm Canine application and the CASA_canine. This, in combination with the high positive correlation seen in PM measurements between the iSperm® canine application and both settings used for CASA assessment, leads us to conclude that iSperm® Canine application also demonstrates reasonably accurate progressive motility assessment.

Dini and colleagues (2019) determined the iSperm® for horses had different results on the ability of iSperm® for concentration of a semen sample [9]. They reported a higher correlation between the iSperm® and the NucleoCounter® SP-100™ and less than 10 % difference when measuring semen samples between 20-100M/ml. In contrast. our results did not identify a high correlation between the two methods of estimating sperm concentration. However, similar to our findings, Dini et al. (2019) showed high correlations between the iSperm® and NucleoCounter® SP-100™ when measuring semen concentrations in samples on the lower side of the iSperm® indicated range. Just as our results identified a strong correlation between CASA and iSperm® for the measurement of progressive motility, Dini et al. (2019) similarly reported a strong positive correlation between iSperm® and Androvision®. This demonstrates the utility and accuracy of the iSperm® for the portable measurement of progressive motility for different species.

Although the motility data from this study did not follow a normal distribution, that was expected, as both high-quality fresh semen and poor-quality frozen semen were evaluated in this study. By analyzing semen with low motility and semen with excellent motility, we were able to observe the maximum ranges of the iSperm® and determine its accuracy for these points. We analyzed very high-quality semen that had high total and progressive motilities from dogs that have been selected as having outstanding fertility and semen quality in the GDB Breeding

Center. Our other semen samples came from out-patient dogs, which had not been bred and selected for high fertility and often had poor fresh semen quality. The initial deficits in semen quality were compounded by the process of cryopreservation, which is known to result in as much as a 50% loss of motility in a single freeze-thaw cycle [10]. Thus, the sperm motilities observed in our experiment were very low in frozen-thawed semen, resulting in the distribution veering from normality.

In this study, we assessed the repeatability of sperm concentration and motility assessment with the iSperm® Canine. Coefficients of Variation (CVs) and this for motility measurements were only assessed for fresh ejaculates due to the high variability inherent to the frozen-thawed samples with very low motility. Total and progressive motility assessment of fresh semen by the iSperm canine application revealed relatively low variability, with CVs of 6.3 and 10.7%, respectively. Pooled observations of fresh and frozen-thawed samples revealed high variability in concentration assessment by iSperm® Canine.

Moraes and coworkers (2019) concluded that the iSperm® Equine application was a valid means for concentration, concentration, total motility, and progressive motility assessment of equine semen. This study found that iSperm Equine assessment of semen concentration did not significantly differ from NucleoCounter or hemocytometer assessment. However, the authors of this study did not investigate the CV for concentration values generated by the iSperm Equine application. In agreement with our findings, Moraes and coworkers (2019) found that the iSperm Equine application provided accurate TM and PM motility assessment when compared to a CASA system[11]. In agreement with the existing literature, our result indicate that the iSperm® could be a very useful and affordable tool for onsite analysis of canine semen, though we

recommend repeated measures for concentration assessment due to the high CV we observed for this parameter.

One last technical observation worth noting is that although the iSperm® is efficient to use when the specimen on the sample chip comes out clean for the sample collector, but the methodology of placing a semen sample with a micropipette on a base chip and pressing it into the cover chip accounts for many technical difficulties. For every "good" sample chip there were about three "bad" sample chips that had bubbles in the sample from pressing the base chip into the cover chip. These bubbles made the sample unusable and was discarded. Thus, many sample chips were wasted from the bubbles created by the design of the sample chips. However, with improvements in the chip design so that bubble formation could be decreased, the iSperm® would become more efficient and 'field-ready'. Certainly, with more technical experience loading chips, technicians can minimize chip wastage.

**Conclusions**

The iPad-based iSperm® Canine application and apparatus is an innovative instrument that can be beneficial for some canine breeding programs. The total motility and progressive motility for fresh and frozen-thawed samples were found to be accurate when compared to a standard CASA system. Concentration measurements when compared to the NucleoCounter® SP-100™ were not well correlated. The iSperm® demonstrated some inefficiencies regarding the setup of analyzing a sample (i.e. the formation of bubbles in sample chips). Not only does the iSperm® provide accurate measures of progressive and total motility that reliably match that of the CASA system, but also supplies the capture of sample images, allowing the user to conduct more objective measures of canine breeding potential in an inexpensive and efficient manner.

**Acknowledgements**

This study was supported by Aidmics Biotechnology Co., Ltd (Taiwan), manufacturer of the iSperm® semen analysis system. They generously provided us with financial and material support of the iSperm® software to conduct this study. However, by contractual agreement there was no personal remuneration for performing this study. The authors also greatly acknowledge the cooperation and participation of Guide Dogs for the Blind for access to dog semen used in this study. We also appreciate the technical support of Ms. Kayla Wigney and Dr. Janice Cain for semen collection.

**Tables and Figures**

| Fresh semen | Concentration | | Total Motility | | Progressive Motility | |
|---|---|---|---|---|---|---|
| | CV | SEM | CV | SEM | CV | SEM |
| | 22.97 | 1.50 | 6.13 | 0.46 | 10.68 | 0.80 |

**Table 1.** ***Coefficients of variation (CV) determinations for iSperm concentration and motility in fresh semen (n=15, p<0.05).***

**Fig. 1A.**

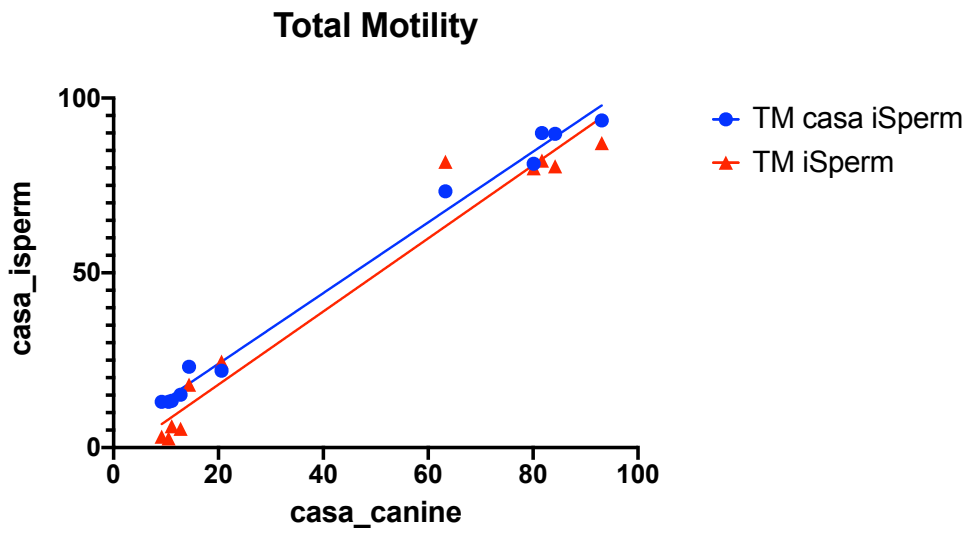


**Fig. 1B.**

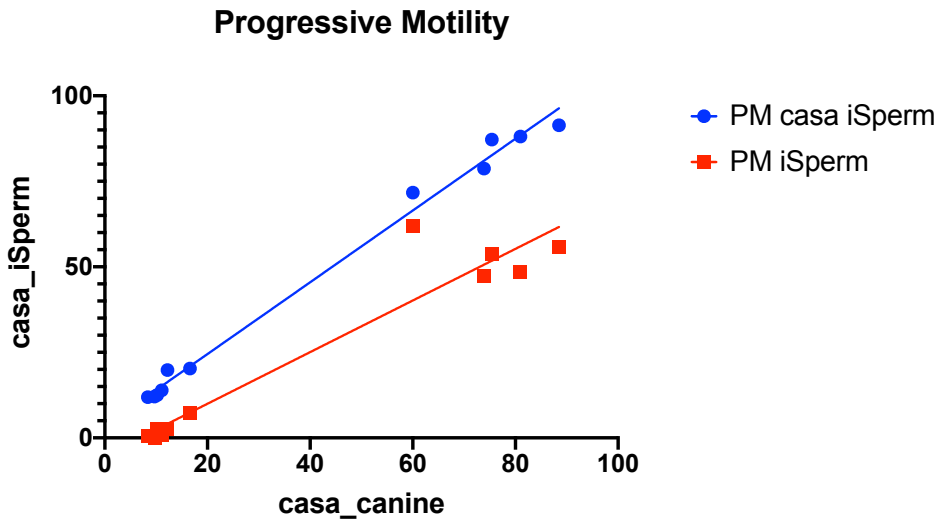


**Figure 1.** ***Comparison of Assessment Methods for Motility Assessment.*** Comparison of motility assessment by conventional CASA systems (casa_canine) and the iSperm system (casa_iSperm) is shown for (A) total motility (TM) and (B) progressive motility (PM) measurements. N=11.

| Semen Type | Concentration | | Total Motility | | Progressive Motility | |
|---|---|---|---|---|---|---|
| | CV | SEM | CV | SEM | CV | SEM |
| Fresh | 22.97 | 1.50 | 6.13 | 0.46 | 10.68 | 0.80 |

**Table 1.** ***Coeffients of Variation CVs determinations for iSperm concentration and motility***.

Data represents fresh semen assessment (N=15).

**Fig. 2A.**

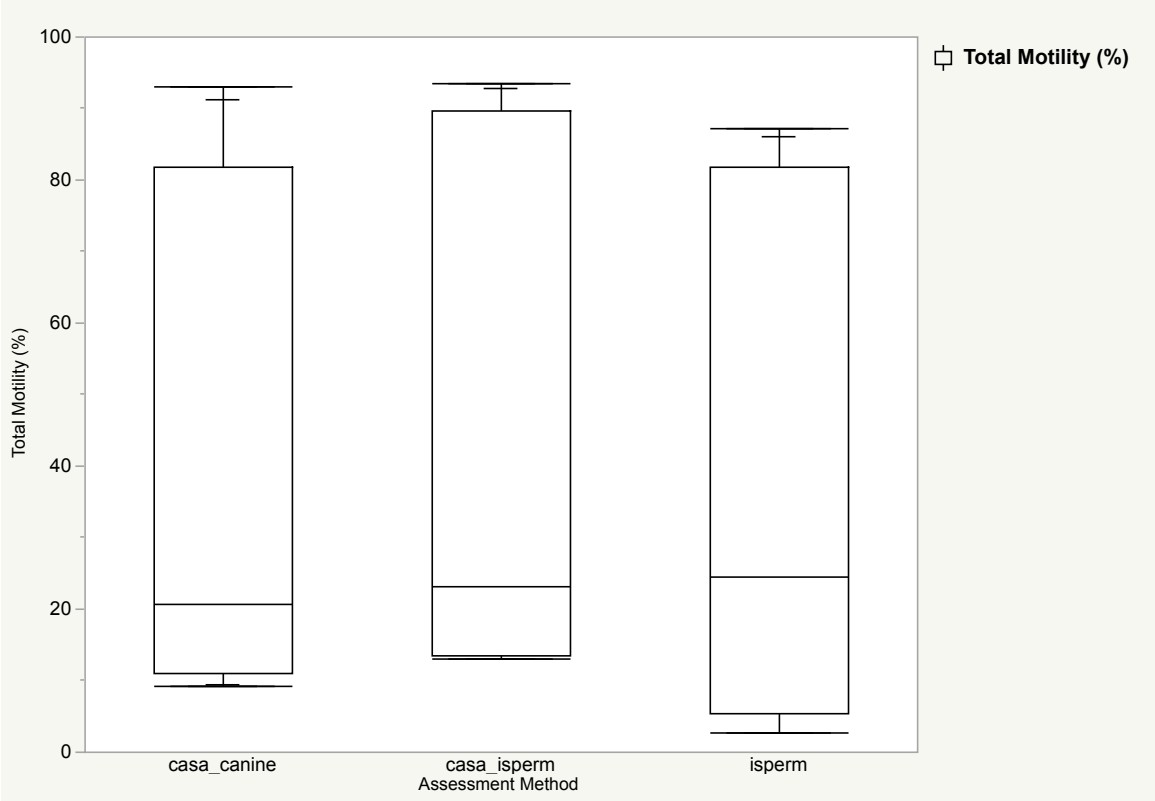
Total Motility (%)
100
80
60
40
20
0
Total Motility (%)
casa_canine
casa_isperm
isperm
Assessment Method

**Fig. 2B.**

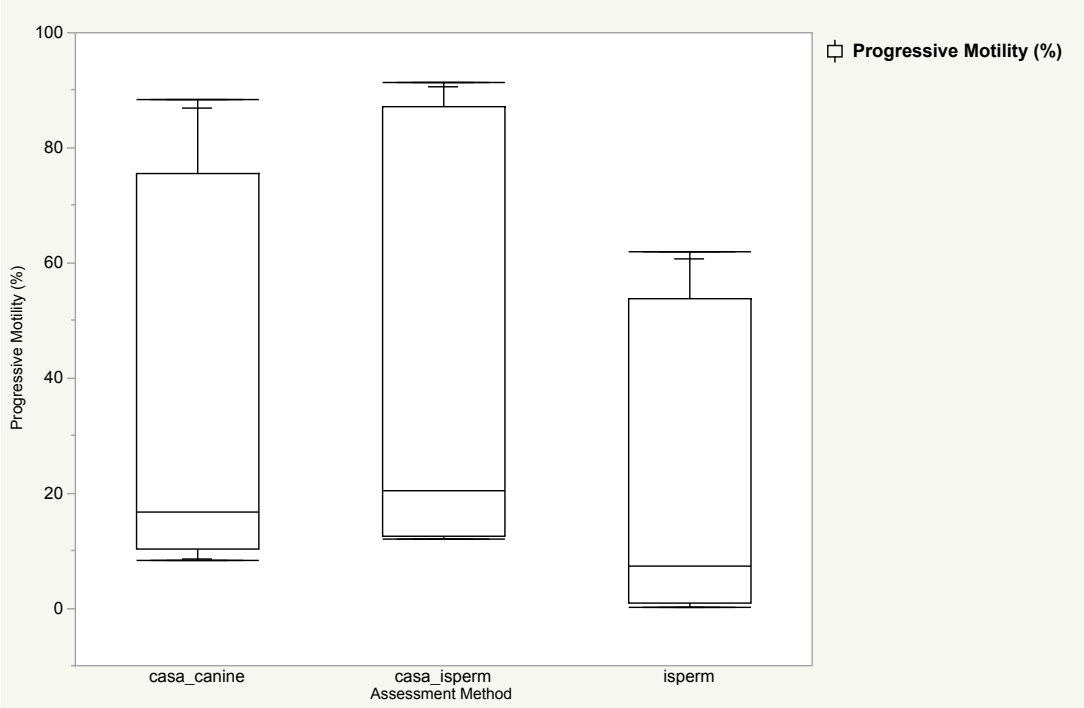
Progressive Motility (%)
100
80
60
40
20
0
Progressive Motility (%)
casa_canine
casa_isperm
isperm
Assessment Method

**Figure 2.** ***Total and Progressive motility measurements by assessment method****.* Quantile box plots demonstrating canine sperm total and progressive motility measurements by assessment method. (A) Total motility (B) Progressive motility. N=11.

**References**


1. Ruestow EG. Images and ideas: Leeuwenhoek's perception of the spermatozoa. *J Hist Biol*. 1983;16(2):185-224. doi:10.1007/BF00124698
2. Amann RP, Katz DF. Andrology Lab Corner*: Reflections on CASA After 25 Years. *J Androl*. 2004;25(3):317-325. doi:10.1002/j.1939-4640.2004.tb02793.x
3. Amann RP, Waberski D. Computer-assisted sperm analysis (CASA): Capabilities and potential developments. *Theriogenology*. 2014;81(1):5-17.e3. doi:10.1016/j.theriogenology.2013.09.004
4. Ellington J, Scarlett J, Meyers-Wallen V, Mohammed HO, Surman V. Computer-assisted sperm analysis of canine spermatozoa motility measurements. *Theriogenology*. 1993;40(4):725-733. doi:10.1016/0093-691X(93)90208-M
5. Walker JS, Winet H, Freund M. A Comparison of Subjective and Objective Sperm Motility Evaluation. *J Androl*. 1982;3(3):184-192. doi:10.1002/j.1939-4640.1982.tb00667.x
6. Root Kustritz MV. The value of canine semen evaluation for practitioners. *Theriogenology*. 2007;68(3):329-337. doi:10.1016/j.theriogenology.2007.04.017
7. Parrish JJ. Bovine in vitro fertilization: In vitro oocyte maturation and sperm capacitation with heparin. *Theriogenology*. 2014;81(1):67-73. doi:10.1016/j.theriogenology.2013.08.005
8. Spiropoulos J. Computerized Semen Analysis (CASA): Effect of Semen Concentration and Chamber Depth on Measurements. *Arch Androl*. 2001;46(1):37-42. doi:10.1080/01485010150211137

9. Dini P, Troch L, Lemahieu I, Deblende P, Daels P. Validation of a portable device (iSperm®) for the assessment of stallion sperm motility and concentration. *Reprod Domest Anim*. 2019;54(8):1113-1120. doi:10.1111/rda.13487

10. Nöthling JO, Shuttleworth R. The effect of straw size, freezing rate and thawing rate upon post-thaw quality of dog semen. *Theriogenology*. 2005;63(5):1469-1480. doi:10.1016/j.theriogenology.2004.07.012

11. Moraes CR, Runcan EE, Blawut B, Coutinho da Silva MA. Technical Note: The use of iSperm technology for on-farm measurement of equine sperm motility and concentration. *Transl Anim Sci*. 2019;3(4):1513-1520. doi:10.1093/tas/txz115

## Dissertation Conclusion

The objective of this dissertation research was to investigate the physiology and pathophysiology of commonly assessed sperm quality parameters, specifically motility and morphology. The aim was to further elucidate the physiologic significance of such parameters and improve both scientific knowledge and clinical knowledge of semen assessment, and in turn male fertility. This was accomplished in a series of four chapters. In Chapter 1, I provided a review of the literature regarding mammalian sperm quality and oxidative metabolism. This review also highlighted knowledge gaps regarding the physiologic significance of commonly assessed sperm quality parameters, such as sperm motility and morphology. The subsequent chapters aimed to reduce those knowledge gaps with the long-term goals of improving knowledge of sperm physiology and the pathophysiology underlying sperm quality parameters that are commonly assessed in a clinical setting.

In Chapter 2, the objective was to investigate the relationship between mitochondrial function and motility in bull sperm. This was accomplished by concurrently monitoring mitochondrial oxygen consumption and motility parameters in the presence of mitochondrial effector drug treatments. Results revealed significant reductions in motility parameters, including total and progressive motility, with antimycin (inhibitor of ETC complex III) treatment. These results suggest that bovine sperm motility is impacted by mitochondrial functionality, contrary to historical findings[1] and in agreement with a more recent report in the literature[2]. Interestingly, no significant difference in motility parameters was observed with oligomycin (inhibitor of ATP Synthase) or FCCP (mitochondrial uncoupler) treatment, suggesting that mitochondrial ATP generation is not critical for maintenance of bovine sperm motility. I hypothesize that the motility deficits observed with antimycin treatment are attributable to cellular mechanisms for

motility regulation beyond mitochondrial ATP production, such as reactive oxygen species (ROS) production, as antimycin treatment is known to trigger mitochondrial ROS generation.

In Chapter 3, we aimed to determine the relationship between stallion sperm morphology and ROS generation in both fresh and 24-hour cooled semen. This was accomplished by employing the novel use of imaging flow cytometry for concurrent evaluation of morphologic abnormalities and cellular ROS generation on an individual cell level. Compared to morphologically normal sperm, ROS production was significantly higher in sperm with abnormal heads, proximal droplets and abnormal midpieces in both fresh and cooled semen. Sperm with both coiled tails and midpieces had significantly higher levels of ROS production compared to morphologically normal sperm in fresh semen; there were very few viable sperm with this morphologic abnormality in cooled semen, preventing statistical assessment of this morphologic abnormality in cooled semen. The association found between morphologic abnormalities and elevated ROS generation does not appear exclusive to stallions. Studies have also linked sperm head defects and oxidative DNA damage have been linked to infertility in humans[3]. Similarly, reactive oxygen species production has been linked to infertility and subfertility in humans and has also been associative with sperm morphologic defects and an elevated sperm deformity index[4,5]. Additionally, abnormal head morphology and oxidative DNA damage have also been negatively correlated with fertility in bulls[6]. The use of high-throughput imaging flow cytometry to investigate the relationship between morphologic abnormalities and ROS generation on an individual cell level, as performed on stallion semen in Chapter 3, would be beneficial to confirm the findings in other mammalian species reported in the literature.

In Chapter 4, we evaluated the repeatability and accuracy of the tablet-based Canine iSperm® instrument compared to computer-assisted sperm analysis (CASA) for assessment of

motility (total and progressive) in fresh and frozen-thawed canine sperm. Correlational analysis revealed significant positive correlations between CASA and iSperm® assessment for both fresh and frozen-thawed samples. These results indicate the iSperm® system offers an accurate clinic-based alternative to CASA for measurement of canine sperm motility. Because traditional CASA systems are very costly, this economic alternative offers the potential to allow for more accurate motility assessment by veterinary clinicians. This could allow for more data collection and larger sample sizes for future population studies in canine sperm quality and fertility, which would be invaluable to future research efforts to expand knowledge of canine sperm physiology. Further, application of a tablet-based system for sperm motility analysis of other mammalian species could improve access to semen analysis for clinicians and expand data collection for researchers.

Nearly 50% of infertility cases are attributed to male factor, and up to 40% of male infertility cases remain idiopathic[7]. In recent decades, human semen quality has been declining world-wide at an alarming rate[8], with a meta-regression analysis by Levine and coworkers revealing that male sperm counts in the western world halved from 1973 to 2011[9], sparking attention from the mainstream media and igniting public concern. Additionally, an age-related decline in fertility is well-established in men[10,11]. Declines in sperm mitochondrial function with aging are likely due to abnormalities in spermatogenesis and factors intrinsic to the aging testicular environment[12–14]. The majority of studies focused on effects of aging human male fertility utilize rodent models[15–18], which have significant limitations due to interspecies differences and short lifespan. There is a need for alternative, non-rodent animal models for more accurate investigation of male fertility pathophysiology and interventions to correct declines in male sperm quality and fertility.

Previous work in our laboratory identified age-related decreases in mitochondrial oxygen consumption (MITOX), which is highly correlated with motility parameters, as well as increased production of reactive oxygen species (ROS) in cryopreserved stallion sperm[19]. This comports with the Free Radical Theory of Aging[20] in which mitochondrial dysfunction, particularly in high-energy tissues[21–23], is accompanied by increases in ROS production, which has also been linked to age-related declines in human sperm quality and fertility[24]. In this dissertation, we identified a significantly higher ROS generation in sperm with abnormal stallion sperm morphology, such as abnormal heads, abnormal midpieces, and proximal droplets, and similar relationships have been identified in human sperm[5]. The stallion is a potential large animal model for study of male reproductive aging. Other species also have potential benefits as animal models of male reproductive aging, with the dog being a strong candidate due to extended lifespan compared to rodent models and the fact that dogs live in the same environment as their human owners, so they are exposed to similar environmental conditions, including toxins, that may impact fertility and sperm quality. However, there are few studies regarding canine fertility and sperm mitochondrial function[25], and more research is needed to determine whether canine and human sperm are physiologically similar enough for dogs to act as a good scientific model. Affordable equipment for reliable data acquisition on sperm quality, such as the iSperm® system validated in Chapter 4 of this dissertation, will improve sample sizes and available data pertaining to canine fertility.

Futures studies employing a multi-species, multi-technique comparative approach to further investigate the findings of this dissertation research on sperm pathophysiology and sperm quality would be beneficial for advancement of the field. For example, a study employing the imaging flow cytometry and oxygen consumption monitoring techniques, established and

utilized in this dissertation, to simultaneously investigate motility, morphology and mitochondrial function in sperm from multiple species would provide invaluable knowledge in sperm physiology and pathophysiology. This could be accomplished by performing simultaneous acquisition of mitochondrial oxygen consumption data and motility analysis, as described in Chapter 2, and also using imaging flow cytometry to assess morphology and ROS generation, as described in Chapter 3, in the same specimens. The strength of this experiment could be further improved by utilizing a mitochondrial membrane potential fluorescence indicator die to have an assessment of mitochondrial function on an individual cell level for associations with ROS and sperm morphology. Logistically, this experiment would be challenging due to a need for a large research team to simultaneously run multiple experimental modalities, but feasibility could be improved by employing fixable fluorescent stains for imaging flow cytometry studies to allow them to be performed at a later date. For example, a relatively new ROS probe, CellRox Deep Red® (Life Technologies, NY, USA) has been validated for use in equine sperm[26]. Additionally, studies incorporating evaluation of intracellular calcium ($Ca^{2+}$) regulation would be beneficial as intracellular $Ca^{2+}$ is known to be important in both sperm[27,28] and mitochondrial physiology[29,30]. Further study of the role of sperm mitochondria and $Ca^{2+}$ regulation would also benefit knowledge advancement of cellular physiology in general, due to some key differences in organelle composition between sperm and somatic cells.

Mitochondrial function is known to be largely effected by mitochondrial $Ca^{2+}$ uptake through the mitochondrial $Ca^{2+}$ uniporter (MCU)[31]. Many of the $Ca^{2+}$-regulated mitochondrial functions, including substrate oxidation and ROS production, are largely dependent on the close anatomical and functional relationship between mitochondria and endoplasmic reticulum (ER) membranes (mitochondrial associated membranes; MAMs)[32]; however, because mature sperm

lack an intact ER, there is a critical knowledge gap regarding the role of $Ca^{2+}$ in modulating sperm mitochondrial functions. Despite fundamental difference in cellular anatomy, surprisingly few studies investigating the relationship between mitochondrial function, $Ca^{2+}$, and motility regulation have been performed in sperm[33,34]. Further research elucidating the roles of mitochondrial function and intracellular $Ca^{2+}$ ($Ca^{2+}_i$) dynamics on sperm function and motility regulation is needed. Additionally, interactions between mitochondrial metabolism and $Ca^{2+}_i$ have been implicated in age-related diseases[35], with recent research implicating age-related changes at MAMs[36]. Similar alterations mitochondrial metabolism and $Ca^{2+}_i$ may also play a role in age-related declines in sperm quality and male fertility.

The multispecies work in this dissertation reports findings in sperm quality, physiology and bioenergetics. The results of this work directly contribute to current clinical knowledge and improve the diagnostic power of commonly employed sperm quality measures by elucidating underlying pathophysiology of sperm morphologic abnormalities and sperm motility. Further, the findings from this dissertation research informs future research efforts, with potential applications in advancement and improvement of mammalian male fertility, sperm preservation techniques, species conservation efforts and mitochondrial physiology.

**References**


1. Krzyzosiak J, Molan P, Vishwanath R. Measurements of bovine sperm velocities under true anaerobic and aerobic conditions. *Anim Reprod Sci*. 1999;55(3-4):163-173. doi:10.1016/s0378-4320(99)00016-0
2. Magdanz V, Boryshpolets S, Ridzewski C, Eckel B, Reinhardt K. The motility-based swim-up technique separates bull sperm based on differences in metabolic rates and tail length. Kues WA, ed. *PLoS One*. 2019;14(10):e0223576. doi:10.1371/journal.pone.0223576
3. Elshal MF, El-Sayed IH, Elsaied MA, El-Masry SA, Kumosani TA. Sperm head defects and disturbances in spermatozoal chromatin and DNA integrities in idiopathic infertile subjects: Association with cigarette smoking. *Clin Biochem*. 2009;42(7-8):589-594. doi:10.1016/j.clinbiochem.2008.11.012
4. Said TM, Aziz N, Sharma RK, Lewis-Jones I, Thomas AJ, Agarwal A. Novel association between sperm deformity index and oxidative stress-induced DNA damage in infertile male patients. *Asian J Androl*. 2005;7(2):121-126. doi:10.1111/j.1745-7262.2005.00022.x
5. Aziz N, Saleh RA, Sharma RK, Lewis-Jones I, Esfandiari N, Thomas AJ, Agarwal A. Novel association between sperm reactive oxygen species production, sperm morphological defects, and the sperm deformity index. *Fertil Steril*. 2004;81(2):349-354. doi:10.1016/j.fertnstert.2003.06.026
6. Sailer BL, Tost LK, Evenson DP. Bull sperm head morphometry related to abnormal chromatin structure and fertility. *Cytometry*. 1996;24(2):167-173. doi:10.1002/(SICI)1097-0320(19960601)24:2<167::AID-CYTO9>3.0.CO;2-G
7. Kadioglu A, Ortac M. The role of sperm DNA testing on male infertility. *Transl Androl*

*Urol*. 2017;(4):1-4. doi:10.21037/tau.2017.03.82

8. Pereira M de L, Oliveira H, Fonseca HMAC, Costa FG, Santos C. The Role of Cytometry for Male Fertility Assessment in Toxicology. In: Schmid I, ed. *Flow Cytometry - Select Topics*. InTech; 2016. doi:10.5772/62965
9. Levine H, Jørgensen N, Martino-Andrade A, Mendiola J, Weksler-Derri D, Mindlis I, Pinotti R, Swan SH. Temporal trends in sperm count: a systematic review and meta-regression analysis. *Hum Reprod Update*. 2017;(September):1-14. doi:10.1093/humupd/dmx022
10. Johnson SL, Dunleavy J, Gemmell NJ, Nakagawa S. Consistent age-dependent declines in human semen quality: A systematic review and meta-analysis. *Ageing Res Rev*. 2015;19:22-33. doi:10.1016/j.arr.2014.10.007
11. Stewart AF, Kim ED. Fertility Concerns for the Aging Male. *Urology*. 2011;78(3):496-499. doi:10.1016/j.urology.2011.06.010
12. Chen H, Hardy MP, Huhtaniemi I, Zirkin BR. Age-related decreased Leydig cell testosterone production in the brown Norway rat. *J Androl*. 1994;15(6):551-557. doi:https://doi.org/10.1002/j.1939-4640.1994.tb00498.x
13. Chen H, Huhtaniemi I, Zirkin BR. Depletion and repopulation of Leydig cells in the testes of aging Brown Norway rats. *Endocrinology*. 1996;137(8):3447-3452. doi:10.1210/en.137.8.3447
14. Wang X, Shen CL, Dyson MT, Eimerl S, Orly J, Hutson JC, Stocco DM. Cyclooxygenase-2 Regulation of the Age-Related Decline in Testosterone Biosynthesis. *Endocrinology*. 2005;146(10):4202-4208. doi:10.1210/en.2005-0298
15. Midzak AS, Chen H, Papadopoulos V, Zirkin BR. Leydig cell aging and the mechanisms

of reduced testosterone synthesis. *Mol Cell Endocrinol*. 2009;299(1):23-31. doi:10.1016/j.mce.2008.07.016

16. Chen H, Jin S, Guo J, Kombairaju P, Biswal S. Knockout of the transcription factor Nrf2 : Effects on testosterone production by aging mouse Leydig cells. *Mol Cell Endocrinol*. 2015;409:113-120. doi:10.1016/j.mce.2015.03.013
17. Zirkin BR, Chen H, Papadopoulos V. Leydig Cell Development and Aging in the Brown Norway Rat. In: *Conn's Handbook of Models for Human Aging*. Second Edi. Elsevier; 2018:853-862. doi:10.1016/B978-0-12-811353-0.00062-2
18. Huang D, Wei W, Xie F, Zhu X, Zheng L, Lv Z. Steroidogenesis decline accompanied with reduced antioxidation and endoplasmic reticulum stress in mice testes during ageing. *Andrologia*. 2018;50(1):e12816. doi:10.1111/and.12816
19. Christa R Darr, Luis E Moraes, Tawny N Scanlan, Julie Skaife, Paul R. Loomis, Gino A. Coropassi SAM. Sperm mitochondrial function is affected by stallion age and predicts post-thaw motility. *J Chem Inf Model*. 2013;53(9):1689-1699. doi:10.1017/CBO9781107415324.004
20. Harman D. Aging: a theory based on free radical and radiation chemistry. *J Gerontol*. Published online 1956. doi:10.1093/geronj/11.3.298
21. Janssens JP, Pache JC, Nicod LP. Physiological changes in respiratory function associated with ageing. *Eur Respir J*. 1999;13(1):197-205. doi:10.1034/j.1399-3003.1999.13a36.x
22. Li C, White SH, Warren LK, Wohlgemuth SE. Skeletal muscle from aged American Quarter Horses shows impairments in mitochondrial biogenesis and expression of autophagy markers. *Exp Gerontol*. 2018;102(December 2017):19-27. doi:10.1016/j.exger.2017.11.022

23. Harper ME, Monemdjou S, Ramsey JJ, Weindruch R. Age-related increase in mitochondrial proton leak and decrease in ATP turnover reactions in mouse hepatocytes. *Am J Physiol*. 1998;275(2 Pt 1):E197-206. http://www.ncbi.nlm.nih.gov/pubmed/9688619

24. Bisht S, Faiq M, Tolahunase M, Dada R. Oxidative stress and male infertility. *Nat Rev Urol*. 2017;14(8):470-485. doi:10.1038/nrurol.2017.69

25. Fuente-Lara A de la, Hesser A, Christensen B, Gonzales K, Meyers S. Effects from aging on semen quality of fresh and cryopreserved semen in Labrador Retrievers. *Theriogenology*. 2019;132:164-171. doi:10.1016/j.theriogenology.2019.04.013

26. Lançoni R, Arruda RP De, Bianchi M, Alves R, Oliveira LZ. Validation of the CellRox Deep Red ® fluorescent probe to oxidative stress assessment in equine spermatozoa. 2017;0:437-441. doi:10.21451/1984-3143-AR842

27. Darszon A, Nishigaki T, Beltran C, Treviño CL. Calcium Channels in the Development, Maturation, and Function of Spermatozoa. *Physiol Rev*. 2011;91(4):1305-1355. doi:10.1152/physrev.00028.2010

28. Lishko P V, Mannowetz N. CatSper: a unique calcium channel of the sperm flagellum. *Curr Opin Physiol*. 2018;2:109-113. doi:10.1016/j.cophys.2018.02.004

29. Rizzuto R, De Stefani D, Raffaello A, Mammucari C. Mitochondria as sensors and regulators of calcium signalling. *Nat Rev Mol Cell Biol*. 2012;13(9):566-578. doi:10.1038/nrm3412

30. Mammucari C, Raffaello A, Vecellio Reane D, Gherardi G, de Mario A, Rizzuto R. Mitochondrial calcium uptake in organ physiology: from molecular mechanism to animal models. *Pflugers Arch Eur J Physiol*. 2018;(Imm). doi:10.1007/s00424-018-2123-2

31. Kirichok Y, Krapivinsky G, Clapham DE. The mitochondrial calcium uniporter is a highly

selective ion channel. *Nat Cell Biol*. 2004;427(6972):360-364. http://www.nature.com/doifinder/10.1038/nature02246%5Cnpapers2://publication/doi/10.1038/nature02246

32. Patergnani S, Suski JM, Agnoletto C, Bononi A, Bonora M, De Marchi E, Giorgi C, Marchi S, Missiroli S, Poletti F, Rimessi A, Duszynski J, Wieckowski MR, Pinton P. Calcium signaling around Mitochondria Associated Membranes (MAMs). *Cell Commun Signal*. 2011;9(1):19. doi:10.1186/1478-811X-9-19

33. Bravo A, Treulen F, Uribe P, Boguen R, Felmer R, Villegas J V. Effect of mitochondrial calcium uniporter blocking on human spermatozoa. *Andrologia*. 2015;47(6):662-668. doi:10.1111/and.12314

34. Ho HC, Suarez SS. Characterization of the Intracellular Calcium Store at the Base of the Sperm Flagellum That Regulates Hyperactivated Motility1. *Biol Reprod*. 2003;68(5):1590-1596. doi:10.1095/biolreprod.102.011320

35. Gibson GE, Thakkar A. Interactions of Mitochondria/Metabolism and Calcium Regulation in Alzheimer's Disease: A Calcinist Point of View. *Neurochem Res*. 2017;42(6):1636-1648. doi:10.1007/s11064-017-2182-3

36. Janikiewicz J, Szymański J, Malinska D, Patalas-Krawczyk P, Michalska B, Duszyński J, Giorgi C, Bonora M, Dobrzyn A, Wieckowski MR. Mitochondria-associated membranes in aging and senescence: structure, function, and dynamics. *Cell Death Dis*. 2018;9(3):332. doi:10.1038/s41419-017-0105-5